



8-2011

A Feasibility Study for Using Commercial Off The Shelf (COTS) Hardware for Meeting NASA's Need for a Commercial Orbital Transportation Services (COTS) to the International Space Station - [COTS]²

Chad Lee Davis

University of Tennessee - Knoxville, cdavis20@utk.edu

Follow this and additional works at: https://trace.tennessee.edu/utk_gradthes



Part of the [Aerodynamics and Fluid Mechanics Commons](#), [Other Aerospace Engineering Commons](#), and the [Space Vehicles Commons](#)

Recommended Citation

Davis, Chad Lee, "A Feasibility Study for Using Commercial Off The Shelf (COTS) Hardware for Meeting NASA's Need for a Commercial Orbital Transportation Services (COTS) to the International Space Station - [COTS]²." Master's Thesis, University of Tennessee, 2011.
https://trace.tennessee.edu/utk_gradthes/965

This Thesis is brought to you for free and open access by the Graduate School at TRACE: Tennessee Research and Creative Exchange. It has been accepted for inclusion in Masters Theses by an authorized administrator of TRACE: Tennessee Research and Creative Exchange. For more information, please contact trace@utk.edu.

To the Graduate Council:

I am submitting herewith a thesis written by Chad Lee Davis entitled "A Feasibility Study for Using Commercial Off The Shelf (COTS) Hardware for Meeting NASA's Need for a Commercial Orbital Transportation Services (COTS) to the International Space Station - [COTS]²." I have examined the final electronic copy of this thesis for form and content and recommend that it be accepted in partial fulfillment of the requirements for the degree of Master of Science, with a major in Aerospace Engineering.

James Evans Lyne, Major Professor

We have read this thesis and recommend its acceptance:

Masood Parang, Robert E. Bond

Accepted for the Council:

Carolyn R. Hodges

Vice Provost and Dean of the Graduate School

(Original signatures are on file with official student records.)

To the Graduate Council:

I am submitting herewith a thesis written by Chad Lee Davis entitled “A Feasibility Study for Using Commercial Off The Shelf (COTS) Hardware for Meeting NASA’s Need for a Commercial Orbital Transportation Services (COTS) to the International Space Station [COTS]².” I have examined the final electronic copy of this thesis for form and content and recommend that it be accepted in partial fulfillment of the requirements for the degree of Master of Science, with a major in Aerospace Engineering.

James Evans Lyne
Major Professor

We have read this thesis
and recommend its acceptance:

Masood Parang

Robert E. Bond

Accepted for the Council:

Carolyn R. Hodges
Vice Provost and
Dean of the Graduate School

(Original signatures are on file with official student records.)

**A Feasibility Study for Using Commercial Off The
Shelf (COTS) Hardware for Meeting NASA's Need for
a Commercial Orbital Transportation Service (COTS)
to the International Space Station
[COTS]²**

A Thesis Presented for the
Master of Science
Degree
The University of Tennessee, Knoxville

Chad Lee Davis
August 2011

Copyright © 2011 by Chad Lee Davis
All rights reserved.

DEDICATION

To my wife

Annie Davis

and my parents

Lee Roy & Eileen Davis

ACKNOWLEDGEMENTS

First I would like to thank my loving wife who has supported me through this long and demanding endeavor. I would also like to thank my children; Jacob, Tyler, Alyson and Zachary for the many hours they have given up with me, to allow me to finish this degree program. I can only hope that my desire for knowledge can one day inspire them to study hard in their respective career fields. While having a family, working full-time and being in the Air National Guard has really tested my skills of time management and self discipline. I would also like to thank my parents for their never ending support for their only son and by teaching me to always finish what you start, no matter how long it might take.

There are various people I'd like to say thank you to from Orbital Sciences Corp. and NASA who have answered questions in many areas of the aerospace disciplines and provided technical support during my research and thesis development. I would like to thank my graduate advisor and friend, Dr. Evans Lyne who has encouraged and allowed me to build a degree program in the areas that most interested me in the aerospace field. I appreciate his availability via cell at various hours of the day and night. I'd like to thank my faculty committee members, Dr. Robert Bond and Dr. Masood Parang for agreeing to be on my committee and also the University of Tennessee's Mechanical, Aerospace and Biomedical Engineering Department.

ABSTRACT

The space vehicle system concept (i.e. resupply vehicle) described is based on the new direction that President George W. Bush announced on January 14, 2004 for NASA's Human Exploration, which has the space shuttle retiring in 2011 following the completion of the International Space Station (ISS). This leads to a problem for the ISS community regarding the capability of meeting a sixty metric-ton cargo shortfall in resupply and the ability of returning large payloads, experiment racks and any other items too large to fit into a crew only type spacecraft like the Orion or Soyuz. NASA and the ISS partners have realized these future problems and started developing various systems for resupply to ISS, but none offer the capability for large up or down mass close to that of the shuttle. Without this capability, the primary purpose behind the ISS science mission is defeated and the ability to keep the station functioning properly is at risk with limited payload delivery (i.e. replacement hardware size and mass). There is a solution to this problem and a majority of the solution has already been designed, built, and flight tested. Another portion has been studied heavily by a team at NASA for use in a slightly different mission. Following the retirement of the space shuttle fleet and the loss of heavy up and down mass capability, the only solution to the problem is to design a new spacecraft. However, the budget and new direction for NASA will not allow for a costly new payload carrying spacecraft. The solution is to use existing commercial off the shelf (COTS) hardware to minimize the costs of developing a totally new system. This paper will discuss the technical feasibility of this conceptual configuration.

TABLE OF CONTENTS

Chapter	Page
CHAPTER 1	1
Introduction.....	1
Section 1-1 Mission Background.....	1
Section 1-1.1 Russia’s Progress.....	3
Section 1-1.2 ESA’s Automated Transfer Vehicle (ATV)	5
Section 1-1.3 JAXA’s H-II Transfer Vehicle (HTV)	6
Section 1-1.4 NASA’s Commercial Orbital Transportation Services (COTS) .	7
Section 1-2 Objectives	10
CHAPTER 2	13
Proposed Vehicle Configuration.....	13
Section 2-1 Resupply Vehicle System	13
Section 2-1.1 Multi Purpose Logistics Module (MPLM).....	13
Section 2-1.2 Intern Control Module (ICM).....	16
Section 2-1.3 Ellipsled	18
Section 2-1.4 Landing Recovery System.....	21
Section 2-1.5 STS-to-EELV Adaptor Structure.....	25
Section 2-1.6 Expendable Launch Vehicles (ELVs)	26
Section 2-2 Phases of Flight Configuration	27
Section 2-2.1 Launch Configuration.....	27
Section 2-2.2 On-Orbit Configuration	30

Section 2-2.3	Reentry Configuration	32
Section 2-2.4	Overall Concept of Operations	33
Section 2-3.	Additional Missions	35
Section 2-3.1	ISS Module Assembly	35
Section 2-3.2	GEO & Lunar Cargo Returns	35
Section 2-3.3	Human Returns	36
CHAPTER 3	37
Methodology for Aerodynamic Analysis and Results	37
Section 3-1	Pro-Engineer Modeling.....	37
Section 3-1.1	Component Modeling and Configuration Layout.....	37
Section 3-1.2	Mass Properties.....	39
Section 3-2	Aerodynamic Analysis.....	41
Section 3-2.1	Missile DATCOM	42
Section 3-2.2	Stability.....	44
CHAPTER 4	50
Methodology for Trajectory Analysis and Results	50
Section 4-1	Program to Optimize Simulated Trajectories	50
Section 4-1.1	Input Deck	52
Section 4-2	Reentry Simulations.....	53
Section 4-2.1	Low Earth Orbit Reentry	53
Section 4-2.2	Geosynchronous Earth Orbit Reentry.....	53
Section 4-2.3	Lunar Return Reentry	54
Section 4-3	Entry Corridor.....	54

Section 4-3.1	Undershoot Boundary	55
Section 4-3.2	Overshoot Boundary	56
Section 4-3.3	Entry Trajectory.....	56
Section 4-3.4	Entry Corridor Width.....	57
Section 4-4	Heating Rate Analysis.....	60
Section 4-4.1	Convective Heating Rates.....	61
Section 4-4.2	Total Heating Rates	63
Section 4-4.3	Integrated Heating Loads.....	64
Section 4-5	Dynamic Pressures.....	65
Section 4-5.1	Ascent	65
Section 4-5.2	Reentry.....	66
Section 4-6	Deceleration Limit	67
Section 4-6.1	Ballistic Coefficient.....	68
CHAPTER 5	70
Conclusions and Recommendations	70
Section 5-1	Conclusion	70
Section 5-2	Recommendations for Future Work.....	72
LIST OF REFERENCES	74
APPENDIX	78
A1 - POST input decks	79
A2 - Missile DatCom input decks	85
A3 - Aerodynamic data from Missile DatCom	88
A4 - Parachute Calculation Details	94

A5 – Trajectories used in Analysis	97
VITA.....	98

LIST OF TABLES

Table	Page
Table 1 ICM Features / Capabilities	17
Table 2 System Comparison	21
Table 3 Evolved Expendable Launch Vehicle (EELV) Capabilities	27
Table 4 Maximum Vehicle Configuration	39
Table 5 [COTS]² Resupply Vehicle Mass Breakout	40
Table 6 Body Geometry Input Calculated Values per Configuration	43
Table 7 Trim Angle of Attack	49
Table 8 Typical Applications of POST	52
Table 9 Summary of Entry Corridor Analysis	60
Table 10 Candidate TPS Materials	62
Table 11 ISS Logistics Vehicle Delivery Capability	71

LIST OF FIGURES

Figure	Page
Figure 1 Progress	4
Figure 2 ATV	5
Figure 3 HTV	6
Figure 4 Dragon	9
Figure 5 Cygnus Unpressurized and Pressurized Configurations	10
Figure 6 System Configuration Breakdown	13
Figure 7 Multi Purpose Logistics Module (MPLM)	15
Figure 8 MPLM (ISS Logistics with Discovery)	15
Figure 9 ICM (in system level EMI testing at NRL)	18
Figure 10 Ellipsled Evolution	20
Figure 11 LAP Parachute Deployed for Drop Test	22
Figure 12 STS-to-EELV Adaptor Structure	26
Figure 13 Initial Launch Configuration	29
Figure 14 Non-ICM Launch Configuration	30
Figure 15 On-Orbit Configuration	31
Figure 16 Reentry Configuration	32
Figure 17 Mission CONOP	34
Figure 18 Delta IV Configuration ($r_n = 0.5\text{m}$)	38
Figure 19 Atlas V Configuration ($r_n = 0.8\text{m}$)	38
Figure 20 Generic Configuration ($r_n = 2.7\text{m}$)	39
Figure 21 Resupply Vehicle Center of Gravity	41
Figure 22 Body Geometry Inputs	43
Figure 23 Ellipsled Stability Analysis Assumptions	45
Figure 24 Force and Moment Coefficients for Generic Configuration	46
Figure 25 Force and Moment Coefficients for Delta IV Configuration	47

Figure 26 Force and Moment Coefficients for Atlas V Configuration	48
Figure 27 Reentry Corridor	55
Figure 28 Entry Trajectory from LEO	57
Figure 29 Entry Corridors per Vehicle Configurations	58
Figure 30 Entry Corridor Width per Vehicle Configuration	59
Figure 31 (Max Undershoot) Stagnation Point Results per Vehicle Configurations	62
Figure 32 Stagnation Point Convective Heating Rate per Vehicle Configurations	63
Figure 33 Integrated Heat Load per Vehicle Configurations	64
Figure 34 Launch Vehicle's Dynamic Pressure Ascent Profiles	66
Figure 35 Dynamic Pressure during Reentry per Configurations	67
Figure 36 Deceleration vs Altitude per Vehicle Configuration	68

LIST OF SYMBOLS AND ABBREVIATIONS

AOA	Angle of attack (degrees)
ATV	Automated Transfer Vehicle
C_D	Coefficient of drag
C_{D_0}	Drag coefficient (canopy area S_0)
C_L	Coefficient of lift
cg	Center-of-Gravity
CONOPS	Concept of Operations
COTS	Commercial Off The Shelf / Commercial Orbital Transportation Service
D_0	Constructed parachute diameter
DART	Demonstration of Autonomous Rendezvous Technology
EELV	Evolved expendable launch vehicle
ELC	ExPRESS Logistics Carrier
ELV	Expendable Launch Vehicle
ExPRESS	Expedite the Processing of Experiments to the Space Station
ESA	European Space Agency
g	Gravitational acceleration
GEO	Geosynchronous earth orbit
HTV	H-II Transfer Vehicle
i	Inclination (degrees)
Isp	Specific impulse (sec)
ISPR	International Standard Payload Racks
ISS	International Space Station

JAXA	Japanese Aerospace Exploration Agency
JEM	Japanese Experiment Module
K-1	Rocketplane Kistler RLV
L/D	Lift to drag ratio
L_{ref}	Reference length
l_s	Length of Suspension Line
LAP	Launch Assist Platform
LEO	Low earth orbit
LRS	Landing Recovery System
LSC	Landing System Controller
m/s	meters per second
MPLM	Multi Purposes Logistics Module
MRC	Mean Reference Center
NASA	National Aeronautics and Space Administration
NEO	Near Earth Object
NRL	Naval Research Laboratory
OML	Outer Mold Line
POST	Program to Optimize Simulated Trajectories
Pro-E	Pro-Engineer
r_n	Nose radius
ROD	Rate of Descent
RCS	Reaction Control System
RLV	Reusable Launch Vehicle

S_O	Nominal surface area of canopy
S_{ref}	Reference area (i.e. maximum cross section area for this study)
STS	Space Transportation System (i.e. Space Shuttle)
TPS	Thermal protection system
TRL	Technical Readiness Level

CHAPTER 1

INTRODUCTION

Section 1-1 **Mission Background**

The payload resupply vehicle concept described in this study is based on the new direction that President George W. Bush announced on January 14, 2004 for NASA's Human Exploration, which has the space shuttle fleet retiring in 2011 following the completion of the ISS. This leads to a problem for the ISS community regarding the capability of meeting a sixty metric-ton cargo shortfall in resupply and an inability to return large payloads, experiment racks and any other items too large to fit into a crew only type spacecraft like the Orion or Soyuz. NASA and the ISS partners have realized these future problems and started developing various systems for resupply to ISS, but none offer the capability for large up or down mass close to that of the shuttle. Without this capability, the primary purpose behind the ISS science mission is compromised and the ability to keep the station functioning properly is at risk with limited payload delivery. There is a solution to this problem and a majority of the solution has already been designed, built, and flight tested.

So following the retirement of the Space Transportation System (STS), also known as the Space Shuttle, and the loss of its heavy up and down mass capability, the only solution to the problem is to design a new spacecraft. However, the budget and

new direction for NASA will not allow for a costly new payload carrying vehicle. The solution is to use existing commercial off the shelf (COTS) hardware to minimize the costs of developing a totally new system. This can be done by using the logistics modules (MPLM) which was designed to fly in the space shuttle cargo bay, but instead launch it using an Evolved Expendable Launch Vehicle (EELV). This then would require building an aeroshell structure called an ellipsled to be used as the EELV launch shroud; a portion of this shroud could also double as a reentry vehicle that would return the logistics module with the down mass safely to Earth. The system would be maneuvered in orbit by the Naval Research Laboratory (NRL) developed Interim Control Module (ICM) propulsion system (initially designed as the backup propulsion system for the ISS). While in orbit, the technology developed by Orbital Sciences for the DART (Demonstration of Autonomous Rendezvous Technology) program could be used to provide autonomous rendezvous and proximity operations with the ISS. The ISS can then use its remote manipulator arm to berth the vehicle to the station, to help minimize the complexity of a totally autonomous docking system.

The overall concept is simple, use an EELV to launch the logistics module and ICM incased in a modified shroud. This modified shroud will later be used as an ellipsled following the separation of the unneeded portion of the shroud during ascent to orbit. The logistics module remains securely attached to the ellipsled along with the ICM for on-orbit ops while using an autonomous rendezvous system for approach and berthing to the ISS. Once the logistics resupply activities are complete, the ICM

maneuvers the vehicle away from the ISS and performs a deorbit burn. The ICM separates to stay in orbit for future missions and the resupply vehicle begins its reentry trajectory to the surface.

Currently the US has an up and down payload capability only with the space shuttle but a booked manifest through retirement, then nothing there after. The Russians, Europeans and Japanese resupply ships are the primary vehicles currently capable of performing resupply to the ISS; unfortunately they all have a limited payload delivery mass. ESA's automated transfer vehicle is planned to be used twice a year and has the largest payload delivery capability of the three, but still no down mass return. NASA's Commercial Orbital Transportation Services (COTS) program vehicles are both in the process of developing and testing expendable ISS resupply vehicles, but only one of them currently has the capability to return payload from the station. As a research facility, this is a problem. Also there is no guarantee that the vehicles currently under development for the COTS program will not be cancelled before they are operational, which will put an even greater strain on the ISS ability to perform research and sustain minimum operational capability.

Section 1-1.1 Russia's Progress

The Progress is a Russian expendable resupply freighter spacecraft. The unmanned spacecraft is classified as a manned system, since it docks to a manned space station. The Progress was derived from the Soyuz spacecraft and is launched from a Soyuz expendable launch vehicle. It is currently used to resupply

the ISS, but was originally used to supply Soviet space stations like Salyut 6 and Mir. There are typically three to four flights to the ISS per year. Each spacecraft remains docked until shortly before the new one or a Soyuz manned capsule (which uses the same docking ports designed for fuel transfer) arrives. Then it is filled with waste, disconnected, deorbited and destroyed in the atmosphere.

Since the initial Progress spacecraft was designed, there have been upgrades to the system (improvements based on the Soyuz T and TM designs) and currently the Progress M and Progress M1 are used for the ISS. The Progress M has a launch weight of 7,130 kg, which delivers 2,600 kg of cargo. Cargo can be split into 1,500 kg of dry cargo and 1,540 kg liquid cargo weight. The dry cargo compartment volume is 7.6 m³ and has a diameter of 2.2 m. The Progress M1 is basically the same except for the fact it can carry more propellant but less total cargo. The total launch weight is 7,150 kg, with a cargo capacity of 2,230 kg. The cargo can be split into 1,800 kg dry cargo and 1,950 kg of propellant.



Figure 1 Progress M [21]

Section 1-1.2 *ESA's Automated Transfer Vehicle (ATV)*

The ATV is an expendable, robotic resupply spacecraft developed by ESA. ATVs are designed to supply the ISS with water, propellant, air, payload and experiments. ATVs are intended to be launched every 17 months in order to resupply the ISS. The ATVs are also capable of re-boosting the ISS for station orbital maintenance.

Each ATV weighs 20.7 tons at launch and has a cargo capacity of 8,000 kg. this 8,000 kg consist of 1,500 to 5,500 kg of dry cargo (i.e. resupply goods, scientific payload, etc), up to 840 kg of water, up to 100 kg of one or two gases (i.e. air, oxygen, nitrogen) and up to 4,700 kg of propellant for station re-boost and refueling. The ATVs dock with the ISS for six months and upon completion of a mission is led to a controlled burn-up reentry in the atmosphere after undocking from the ISS.



Figure 2 ATV [22]

Section 1-1.3 JAXA's H-II Transfer Vehicle (HTV)

The HTV is a robotic resupply spacecraft intended to resupply the Kibo JEM and the ISS, if required. JAXA has been developing the design since the 1990's and had a successful first flight in fall of 2009. The HTV is a simpler design which is berthed to the ISS verses performing an autonomous docking like the ATV and Progress spacecraft. The berthing process means the ISS uses its robotic arm to reach out and capture the HTV and finally reorients it relative to the docking port on the station. The HTV is actually two different segments which can be attached together. One segment is pressurized with a 6,000 kg capacity, which can carry eight ISPR (International Standard Payload Racks) in total and 300 kg of water. The second segment is unpressurized. The HTV can remain docked to the ISS for approximately 30 days.

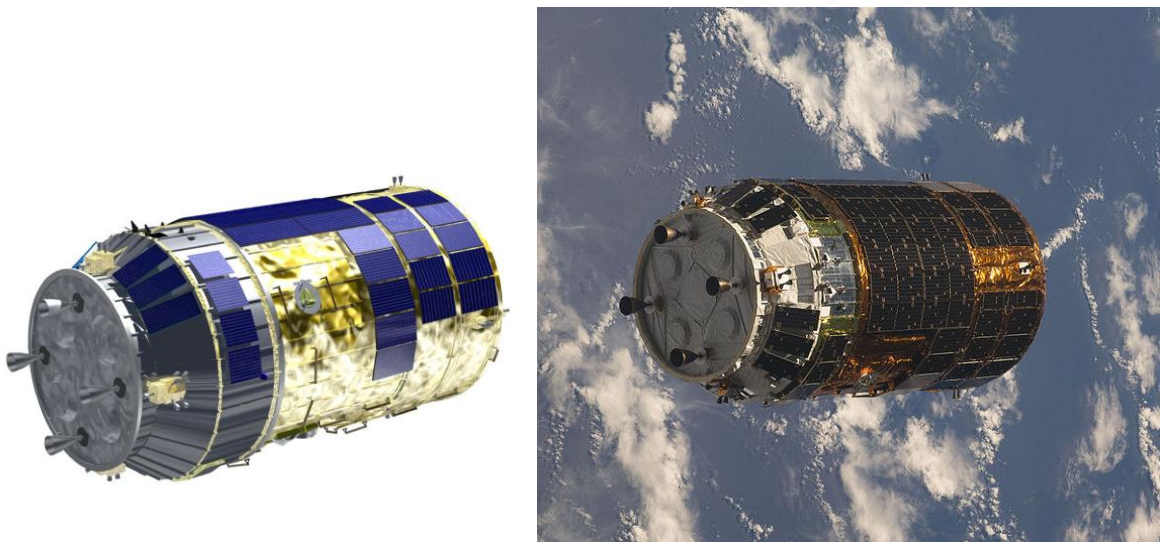


Figure 3 HTV [23]

Section 1-1.4 *NASA's Commercial Orbital Transportation Services (COTS)*

The Commercial Crew/Cargo Program Office at JSC manages the Commercial Orbital Transportation Services (COTS) projects. COTS is an effort by NASA to stimulate, and then take advantage of, a robust commercial market for spaceflight services. Currently NASA has selected two companies to partner with to develop and demonstrate commercial orbital transportation services. The success of these partners could open new markets and pave the way for contracts to launch and deliver cargo and possibly crew to the International Space Station. Once a capability is demonstrated, the Agency plans to purchase these services competitively. Currently Space Exploration Technologies (SpaceX) and Orbital Sciences Corporation have been selected to perform Phase 1 of the COTS contract.

In Phase 1, companies will demonstrate one or more of four capabilities: external, unpressurized cargo delivery and disposal; internal, pressurized cargo delivery and disposal; internal, pressurized cargo delivery and return; and an option for crew transportation. NASA plans to purchase cargo resupply services competitively in Phase 2. This will allow NASA to focus on more of the goals that are appropriate for government, such as exploring the moon, Mars and beyond.

Section 1-1.4.1 SpaceX – Dragon

The Dragon spacecraft is made up of a pressurized capsule and unpressurized trunk used for Earth to LEO transportation of pressurized cargo, unpressurized cargo and eventually crew members. The program was started by SpaceX in 2005 with its first successful demo flight in fall 2010. The Dragon is comprised of three main elements: the nose cone, which protects the pressure vessel and docking adaptor during ascent; the pressurized section, which houses the pressurized cargo and/or crew; and the service section, which contains the avionics, RCS, recovery systems and other support infrastructure. In addition an unpressurized truck is included, which provides for the storage of unpressurized cargo and supports spacecraft's solar arrays and thermal radiators.

The Dragon is fully autonomous rendezvous and docking with manual override capability in a crewed configuration. The pressurized section is 14 m³ which allows greater than 2,500 kg capacity up and down cargo capability. The Dragon is a two-fault tolerant avionics system. The capsule uses a lifting re-entry for landing precision, low g-levels and performs a water landing under parachute for an ocean recovery.



Figure 4 Dragon [24]

Section 1-1.4.2 Orbital Sciences - Cygnus

The Cygnus consists of a common service module and interchangeable pressurized and unpressurized cargo modules. The service module incorporates avionics systems from Orbital's Dawn interplanetary spacecraft plus propulsion and power systems from the STAR GEO communications satellites. The pressurized cargo module is based on the MPLM and is berthed to the ISS to simplify the system. The pressurized volume is 18.7 m³ and has a 2,000 kg total payload delivery mass. The unpressurized cargo module will be used to carry large external cargo units (based on ELC (ExPRESS Logistics Carrier)). The cargo volume is 18.1 m³ and has a 2,000 kg total payload delivery capability (cargo configuration dependant).

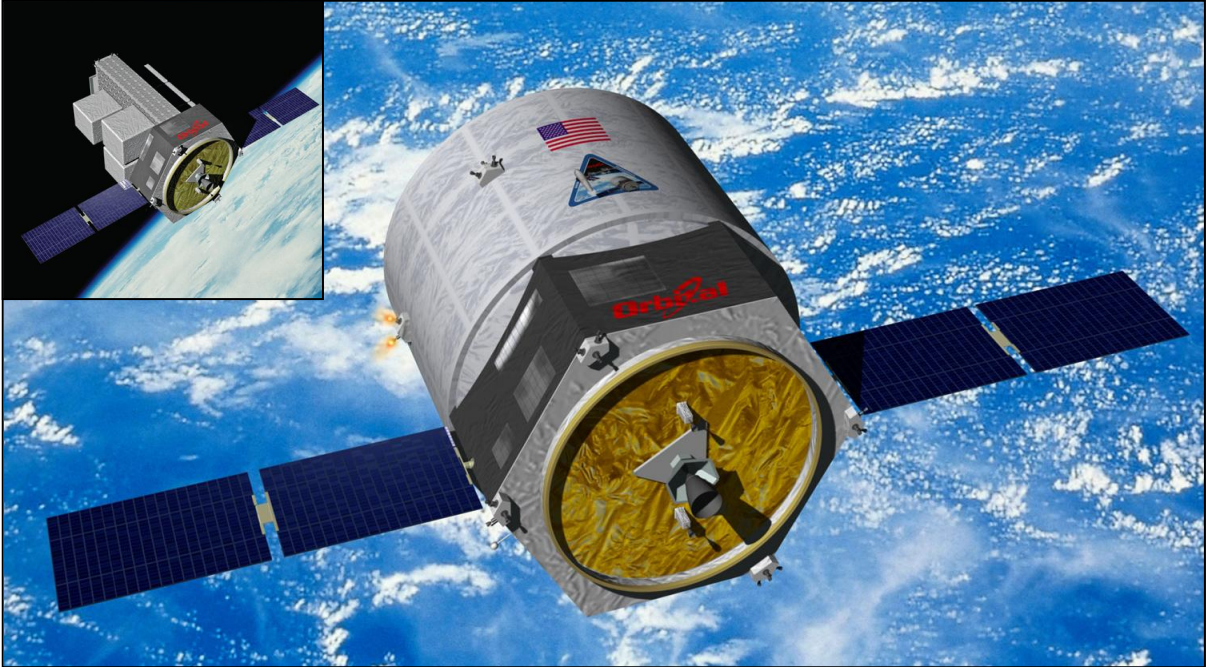


Figure 5 Cygnus Unpressurized and Pressurized Configurations [25]

Section 1-2 Objectives

The scope of this work is to develop a partially reusable ISS resupply vehicle concept that is capable of performing both up/down payload delivery to ISS and return to earth, while utilizing a large majority of flight proven COTS hardware.

These will include a system configuration breakdown, which will identify reusable or expendable hardware and whether the hardware is new or COTS. It will define the vehicle's concept of operations (CONOPs) from launch through landing and focus on the reentry & recovery systems and analysis of the reentry vehicle configuration.

The major tasks to be accomplished during the development of this thesis are as follows:

- Define overall concept vehicle configuration (i.e. primary structures, subsystems and subsystem functionality).
- Define mission operational flow for reentry concept vehicle (CONOP).
- Define the concept of utilizing a portion of the launch vehicle's fairing as a reentry aeroshell and jettisoning the remainder during nominal ascent
- Perform trade studies on the three currently existing heavy lift vehicles that offer the 5 meter fairing variant.
 - Use ProE to build models of the two EELV fairing configurations to help generate the needed ellipsled geometric data
 - Use generic Mars mission ellipsled aerodynamics data as a cross reference to data collected from aero code.
 - Use Missile DATCOM to determine the aerodynamic characteristics (i.e. coefficients) for the two EELV fairings and one generic configuration (scaled down version of the Mars mission ellipsled):
 - Generic
 - Delta 4
 - Atlas 5

- Perform reentry analysis for concept reentry vehicle.
 - Calculate convective heating rates, dynamic pressures and deceleration for L/D over a range of entry speeds corresponding to return from LEO, GEO and the moon.
- Perform parachute sizing and deployment altitude to meet touchdown criteria.

CHAPTER 2

PROPOSED VEHICLE CONFIGURATION

Section 2-1 Resupply Vehicle System

The [COTS]² concept utilizes the following hardware to create a vehicle system that can resupply the ISS and has the potential to meet future follow-on missions. The system is made up of commercial off the shelf hardware developed for other space flight applications and there is some new technology that needs to be matured beyond the design and prototype phases:

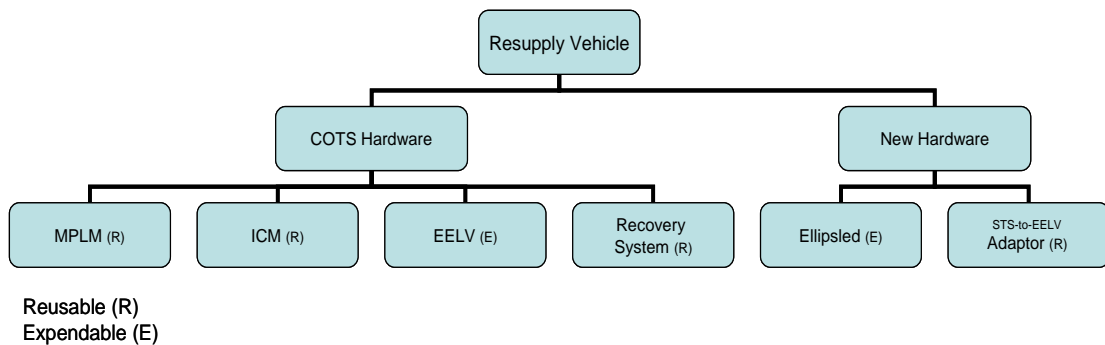


Figure 6 System Configuration Breakdown

Section 2-1.1 Multi Purpose Logistics Module (MPLM)

The MPLM is flight proven space hardware that is currently compatible with ISS operations. Three were built by ESA and currently fly in the space shuttle. The module has two main functions:

- As a carrier it has to fly to the ISS 25 times over 10 years.
- As a manned module it must be able to operate in orbit and guarantee protection from meteorites, environmental control, active and passive thermal control, atmospheric control and conditioning, fire detection and extinguishing, distribution of electrical power, commands and data handling.

The MPLM is able to carry 16 international payload racks and of the 16 racks the module can carry, five can be furnished with power, data and fluid to support a refrigerator freezer. Sufficient volume is provided within the MPLM for two crew members to work simultaneously. One of the more complex tasks that will be performed within an MPLM is the removal of entire payload (ISPR) or systems racks for installation in the ISS or the installation of various resupply storage racks (used to carry materials) for return to Earth. In order to function as an ISS module, the MPLM has some life support, fire detection and suppression, electrical distribution, and Data Management System capabilities. The MPLM has a maximum up and down mass capability of approximately 9,100 kg (10 tons of cargo). The MPLM is 6.4 m in length, 3.57 m in width and has an empty mass of 4,082 kg.

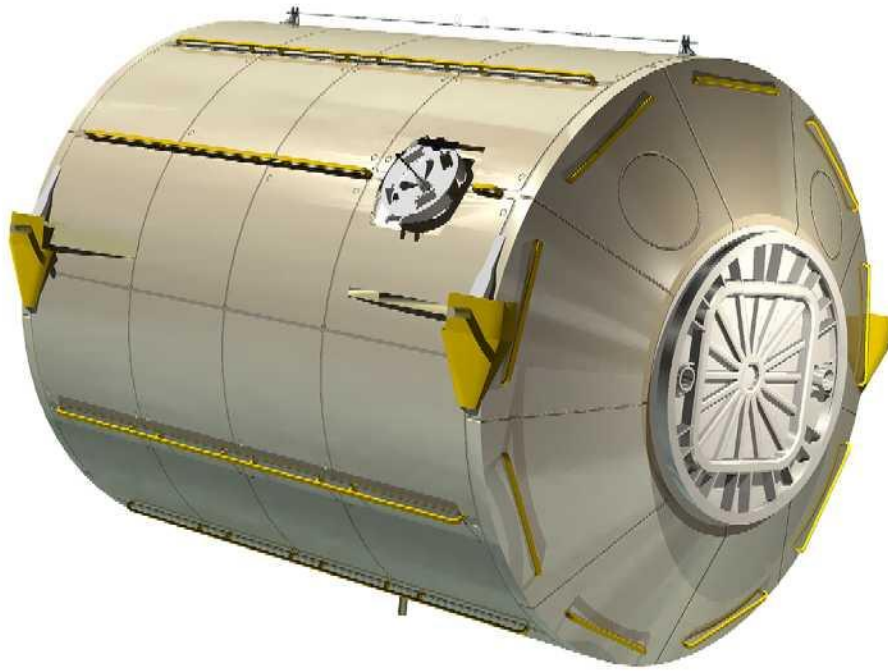


Figure 7 Multi Purpose Logistics Module (MPLM) [17]



Figure 8 MPLM (ISS Logistics with Discovery) [17]

Section 2-1.2 *Interm Control Module (ICM)*

NASA requested that Naval Research Laboratory (NRL) study the feasibility of adapting an existing, heritage spaceflight system to provide low-cost, contingency propulsion operations for the ISS in the event the Russian Service Module was delivered late. From its inception, the ICM was a contingency option for attitude control and reboost of the ISS which would allow NASA to maintain the on-orbit construction schedule. The ICM is based on a satellite dispenser designed and built by NRL.

The ICM is compatible with the ISS close proximity operations and should meet all manned rated requirements, since initially designed for use on the ISS and to be flown in the shuttle. Table 1 shows the ICM propulsion module's key features and capabilities.

Table 1 ICM Features / Capabilities [28]

Requirements	ICM Capability
Autonomous Operations	Compliant with ISS
Fuel	11,700 lbs bi-propellant
Power	Fully self contained at 600W end-of-life capability
	Requires no power from another source
Attitude Determination and Control	Fully self contained
	Star cameras, sun sensor, magnetometer and IMUs
	Thrusters
Launch Compatibility	STS, Delta IV, Atlas V
Redundancy	Single fault tolerant for catastrophic failure
	Dual fault tolerance for some systems
Computer Processing	R3000/11 MIPS, FDIR in HW/SW
Safety Compliance	Completed Phase II Shuttle Safety Reviews
	Includes field and fueling procedures
Docking Aids	Currently requires use of ISS remote arm
	Future could require no docking aids, with use of DART technology

As ISS assembly continued to progress and the international partners were able to meet their hardware delivery dates, the ICM was released by NASA. The ICM is currently in storage at NRL's Payload Processing Facility in Washington, D.C. The vehicle is capable of launch on either the Space Shuttle or an EELV class of expendable booster.

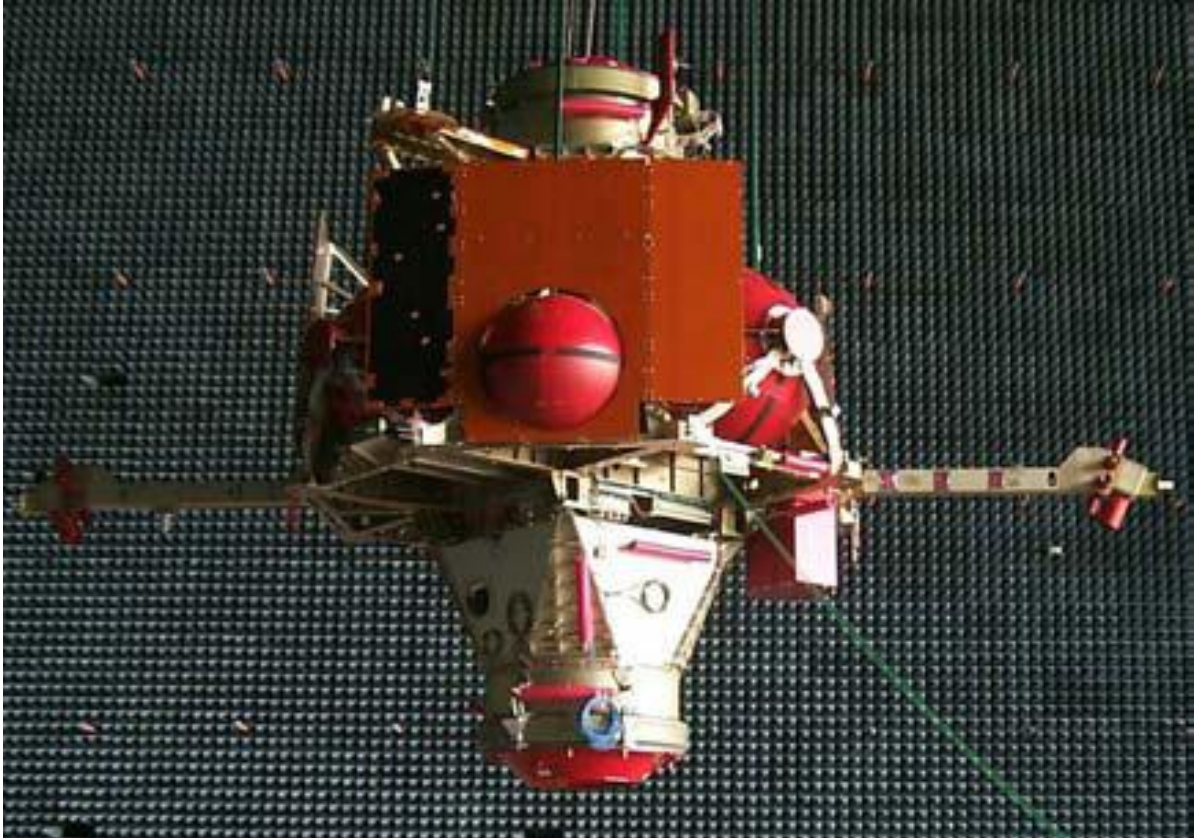


Figure 9 ICM (in system level EMI testing at NRL) [29]

Section 2-1.3 *Ellipsled*

An ellipsled is a biconic shaped aeroshell used for aerobraking and/or aerocapture during atmospheric entry. The term ellipsled comes from the characteristic shape of the aeroshell, which also provides aerodynamic lift. For the purposes of this study, the ellipsled will be used to aerobrake for entry, descent and landing of the down mass payloads. The ellipsled configurations described in this study are modified versions of the launch vehicle's payload fairing. The key factor is the ellipsled maintains the same outer mold line (OML) as the original launch vehicle's fairing so there are no additional analysis or redesigns required on the EELV's overall

aerodynamic characteristics. The only changes are with the actual internal structure to strengthen the ellipsled portion of the fairing, the separation lines for the fairing and the TPS.

Example of an Atlas V Fairing – EllipSled System

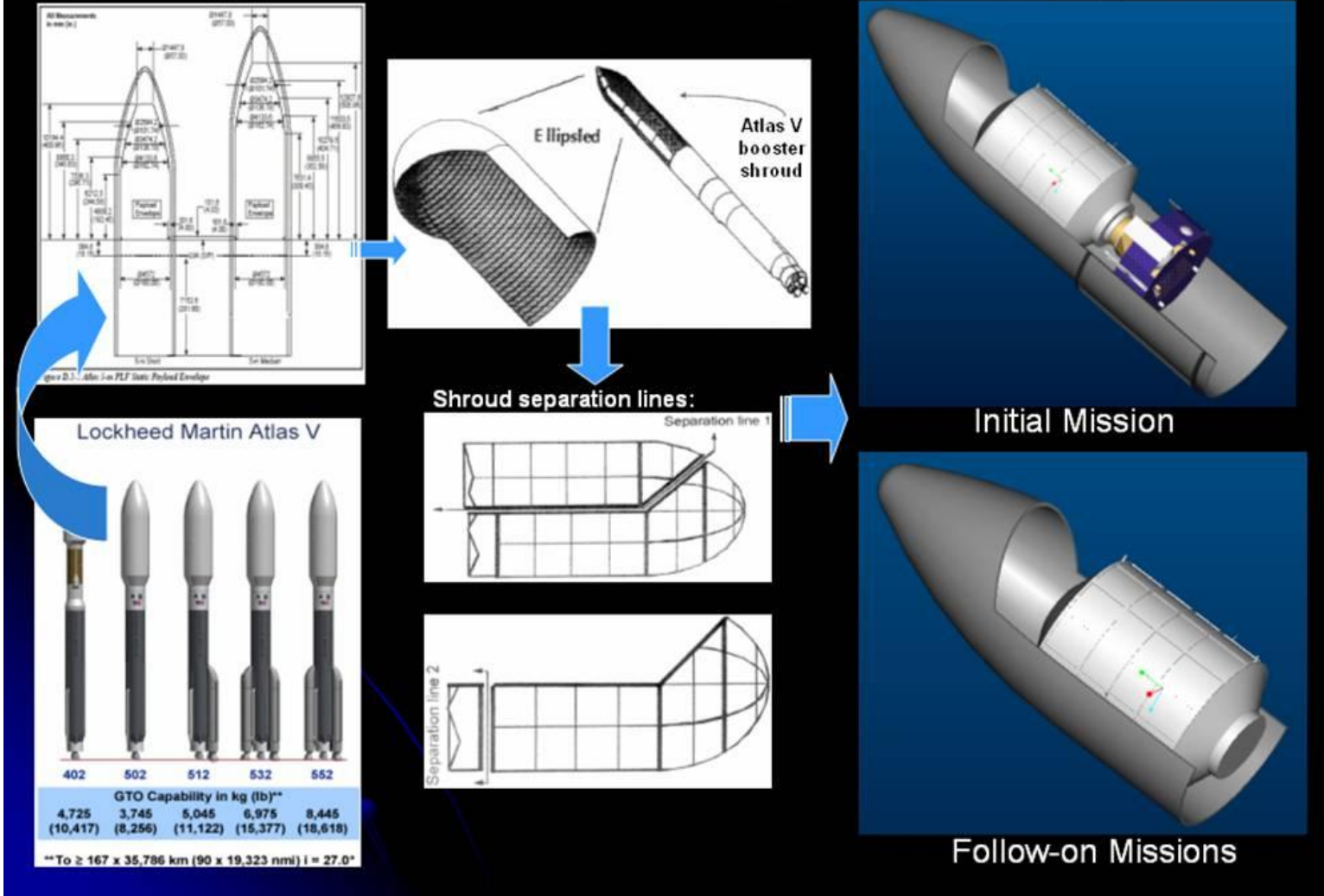


Figure 10 Ellipsled Evolution [5,18,29]

Section 2-1.4 Landing Recovery System

The proposed Landing Recovery System (LRS) would be the parachute system technology borrowed from the Rocketplane Kistler (formally Kistler Aerospace) Company for their K-1 Reusable Launch Vehicle. This is the same type parachute system to be used on the K-1 first stage booster, called the Launch Assist Platform (LAP). Irvin Aerospace was the developer of the landing system for the K-1 Launch Vehicle. Joint development of the K-1 landing system has included completion of several qualification flight tests and production of the first flight parachutes. Based on the similarities between the LAP and [COTS]² resupply vehicles' masses, vehicle overall sizes (reference Table 2) and shape the LRS would meet the immediate needs of the proposed resupply vehicle concept described in this study. This is especially true since the system is a parachute recovery that would allow the resupply vehicle to remain in a relatively horizontal orientation following reentry and post parachute deployment through touchdown.

Table 2 System Comparison

System	Mass (kg)	Length (m)	Diameter (m)
LAP	20,500	18.3	6.7
COTS²	18,500	14.0	~5.0

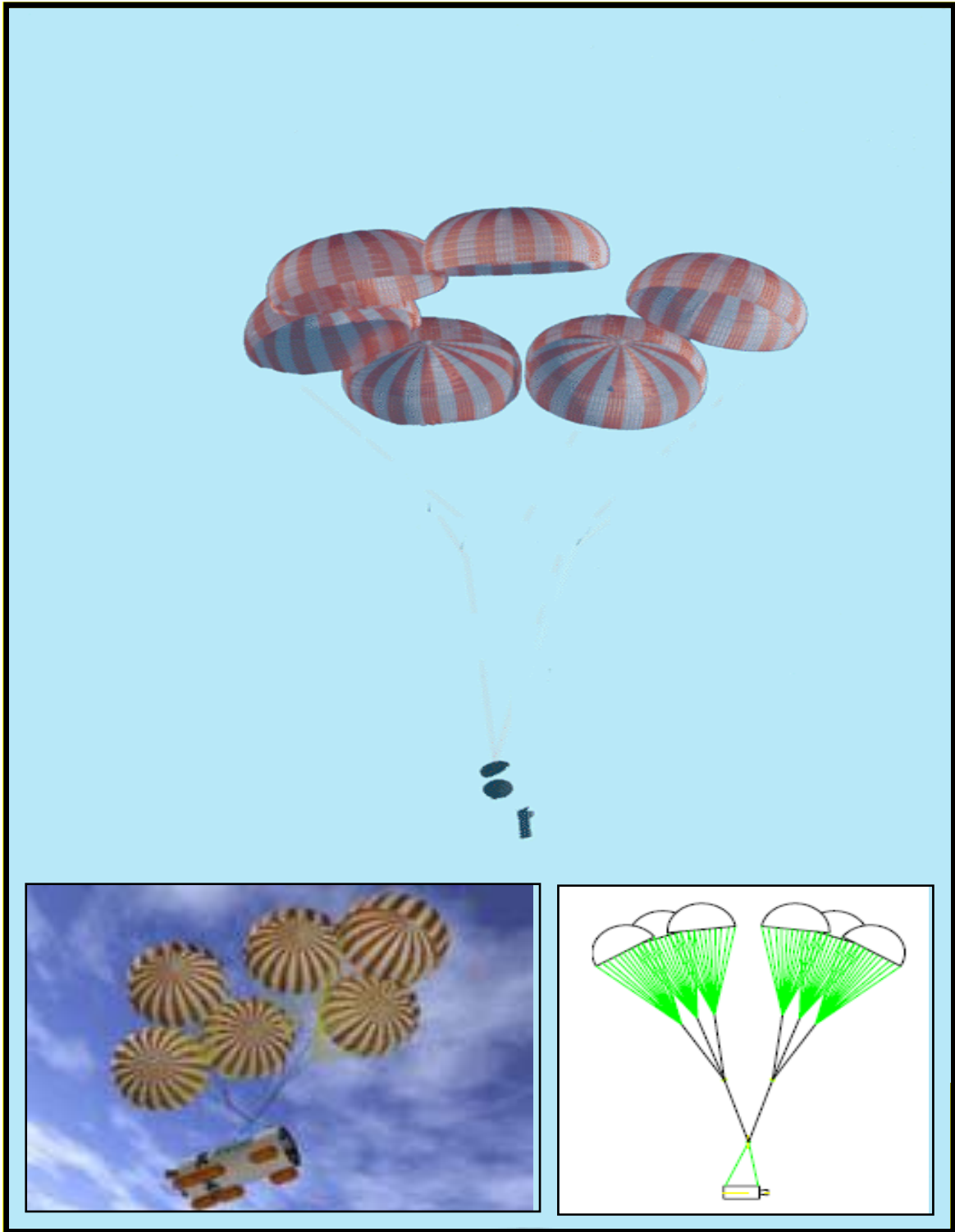


Figure 11 LAP Parachute Deployed for Drop Test [9,20]

The parachute system planned for both vehicles provides deceleration to an acceptable final Rate of Descent (ROD). A trade completed early in the K-1 conceptual definition helped define a correlation between the ROD and the parachute system's mass. Since the [COTS]² resupply vehicle is approximately 2,000 kg less than the LAP, then the 6.7 m/s ROD should be more than acceptable for the deceleration and touch down of the [COTS]² vehicle.

LAP Parachute Deployed Figure 11 provides a schematic for the parachute deployed and shows vehicle's final descent orientation. Due to its cg location, the LAP uses static stability engines first following stage separation and completion of its fly-back maneuver until final deployment of the main parachutes. However the [COTS]² resupply vehicle's static stability is in a relatively horizontal orientation (excluding AOA), by configuration design. The [COTS]² vehicle would use its own drag to decelerate to subsonic velocity at around 7,620 meters (25,000 feet). Based on the K-1 recovery system the initial parachute system deployment condition is approximately 51.8 m/s. This occurs at an altitude of approximately 6,096 meters (20,000 feet), when commanded by the avionics. Two mortars fire to deploy the two 12.2 meters parachute diameter (D₀) conical ribbon drogues. [9] "The drogues are sized and reefed such that either drogue will provide sufficient deceleration for main canopy deployment (at reduced safety factors), thus providing slightly higher reliability than for a single drogue." [9] Following a fixed time delay, the drogue parachutes are released through pyro cutters, allowing the drogues to deploy the six main canopies. The mains are rigged in two clusters of three parachutes. [9]

Reference appendix section A4 to better understand the details associated with the drogue and main parachute nomenclature and design calculation details. [13]

Section 2-1.4.1 Drogue Parachutes

The 20° Conical Ribbon drogue planform was selected. “A Kevlar-nylon hybrid design for the reusable drogue is based on successful reuse of the Space Shuttle Orbiter parabrake. Using nylon horizontal and vertical ribbons plus a nylon heat tack radial on the drag producing surface will both allow efficient manufacture and reduce material cost. Mini-radial style horizontal ribbon spacing control will be applied versus vertical tapes to assure both drag optimization and a strong geometric porosity gradient toward the skirt region for stability and drag enhancement. The structural grid will include Kevlar outer radials and suspension lines. Radial continuation over-the-vent will provide continuity and weight reduction.” [9,13]

Section 2-1.4.2 Main Parachutes

“The main parachute follows the trend in high drag efficiency Ringsail planforms successfully employed on two prior programs. The F-111 Crew Escape Module recovery parachute improvement program was the first to apply the use of (1) mid-range permeability fabric in the central gore height, (2) modified Ringsail planform: quarter spherical with zero fullness at the 60° R/2 tangent point, and (3) linear Ringsail panel leading edge fullness ramp up toward the skirt.” [9] These improvements led to the development of the EELV recovery main parachute D_O of 41.5 meters. This D_O produced a cluster drag coefficient of 0.97. At 48.2 meters

D₀, the K-1 design will prove highest in drag efficiency of all canopies in the class and be more than sufficient for the [COTS]² vehicle. [9,13]

Section 2-1.5 *STS-to-EELV Adaptor Structure*

The STS-to-EELV adaptor structure is a critical piece of the [COTS]² overall vehicle system which allows the MPLM to be mounted in the vertical orientation for launch on an EELV. The STS-to-EELV adaptor allows the MPLM to be bolted using its existing attachment points (as used in the shuttle's cargo bay) and then be attached to the EELV payload interface point. This avoids major structural redesign of the MPLM's mechanical interfaces. It also services as the resupply vehicle's core structure to secure the ellipsled (i.e. non-jettison shroud portion) to the MPLM. The adaptor must be minimized in total mass, while maximized for strength in its design. Once flight proven (with the MPLM), the adaptor could be used on any cargo designed for launch on a space shuttle. Figure 12 shows a cut away view of the [COTS]² resupply vehicle on an EELV.

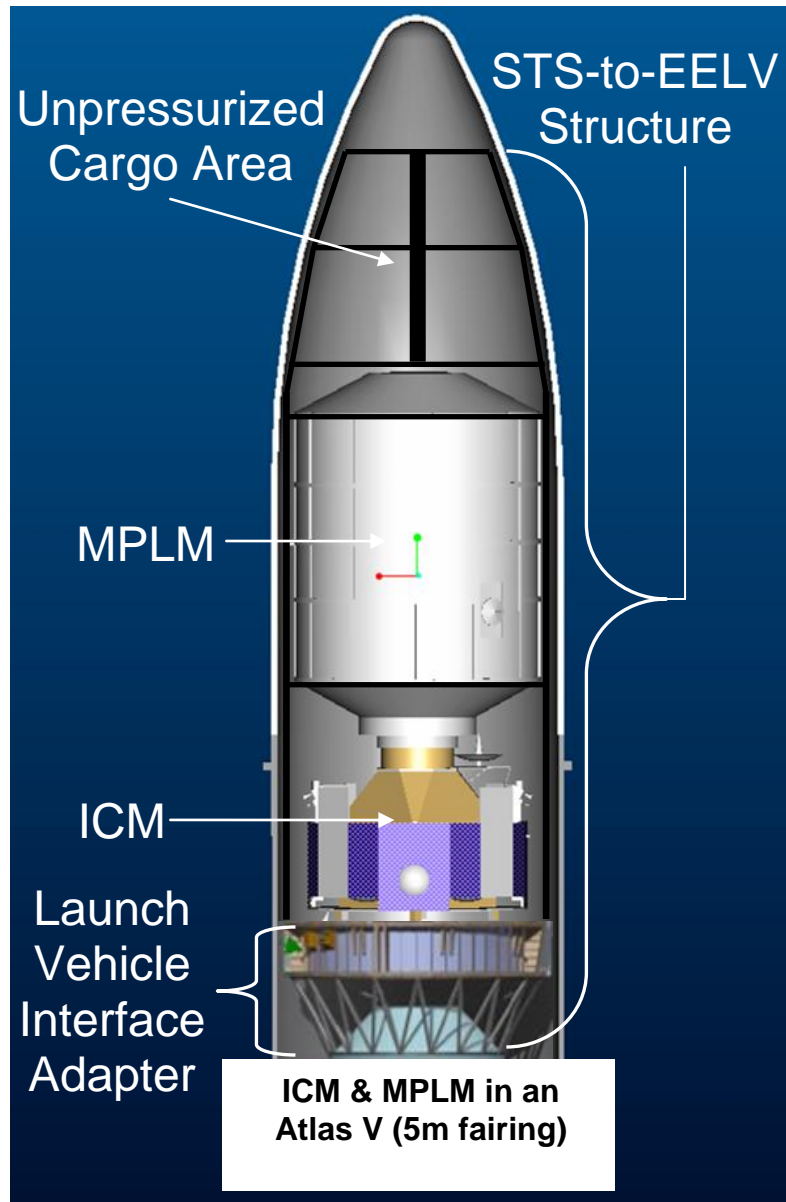


Figure 12 STS-to-EELV Adaptor Structure

Section 2-1.6 Expendable Launch Vehicles (ELVs)

The current fleet of heavy lift ELVs that can meet the large lift capacity required for the proposed resupply vehicles are described in the table below. Typically only the Delta IV and Atlas V are referred to as an EELV, but to avoid any confusion

regarding launch vehicles referenced in this study, the Ariane 5 will also be referred to as an EELV.

Table 3 Evolved Expendable Launch Vehicle (EELV) Capabilities

EELV	Payload Mass (kg)	Diameter (m)
Ariane 5	21,000	5.40
Atlas V - Heavy	29,400	5.43
Delta IV - Heavy	22,977	5.13
*Delta IV - Heavy	~30,000	5.13

*Delta IV with RS-68A engines

The company that designs the fairing used on the Ariane 5 also builds the fairing for the Atlas V EELV. After review of the Outer Mold Line (OML) of these two fairings, it was determined that for the purposes of this study, they have the same basic aerodynamic shape and characteristics. Thus, this study will only look at the difference between the Delta IV and Atlas V fairing configurations during the reentry analysis section.

Section 2-2 Phases of Flight Configuration

The following sections describe the various system configurations and associated hardware needed to perform that phase of flight.

Section 2-2.1 Launch Configuration

The following two sections (2-2.1.1 and 2-2.1.2) show the launch configuration for the system. The difference between the two configurations depends on a few

variants. The first is whether or not it is the initial launch, which requires launch of the ICM for orbital maneuverability of the resupply vehicle and also if the resupply vehicle exceeds the maximum launch capability of a medium class EELV. The ICM would be launched with a full fuel load and the MPLM would reduce its cargo mass to meet the launch performance capabilities of the EELV. Since the ICM is non-reusable and stays in orbit until reaching its min fuel level, it is more cost effective to maximize its on-orbit performance and maneuverability by insuring a full fuel load.

Section 2-2.1.1 Initial Launch Configuration

This example is of the Atlas V Heavy vehicle configuration, but would be similar for the Delta IV Heavy. This configuration would maximize the ICM mass (i.e. fuel load) and adjust the pressurized and unpressurized cargo mass as required to meet the Heavy EELV lift capability. A fully loaded [COTS]² resupply vehicle with a fully fueled ICM is 31,161 kg, so there would have to be a reduction in payload to meet the lifting capacities of the Delta IV-H at 22,977 kg and Atlas V-H at 29,400 kg.

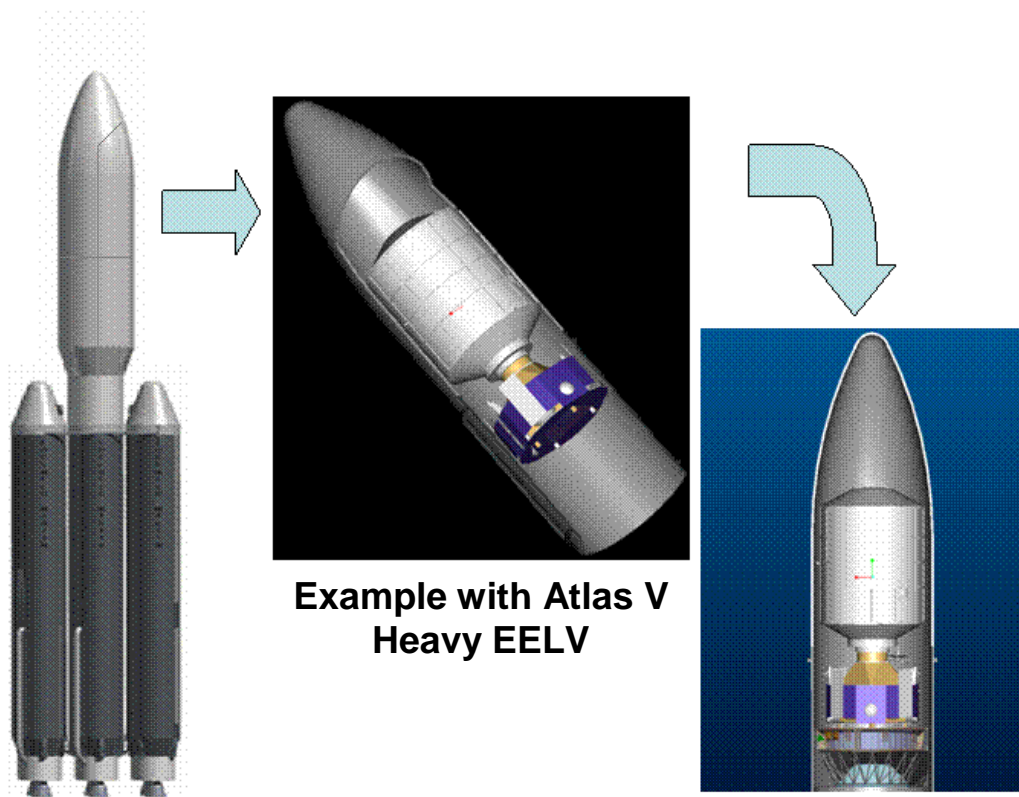


Figure 13 Initial Launch Configuration [18]

Section 2-2.1.2 Follow-on Launch Configurations

This example is of the Atlas 5 Medium vehicle configuration, but would be similar for the Delta IV class of medium EELV. This configuration would maximize the pressurized and unpressurized cargo delivery mass, since there would be no ICM. The primary driver is the Medium EELV lift capability. A fully loaded [COTS]² resupply vehicle without an ICM is 22,991 kg, so there would have to be a reduction in payload to meet the lifting capacities of the Delta IV-M(5,4) at 13,360 kg and Atlas V-551 at 18,500 kg.

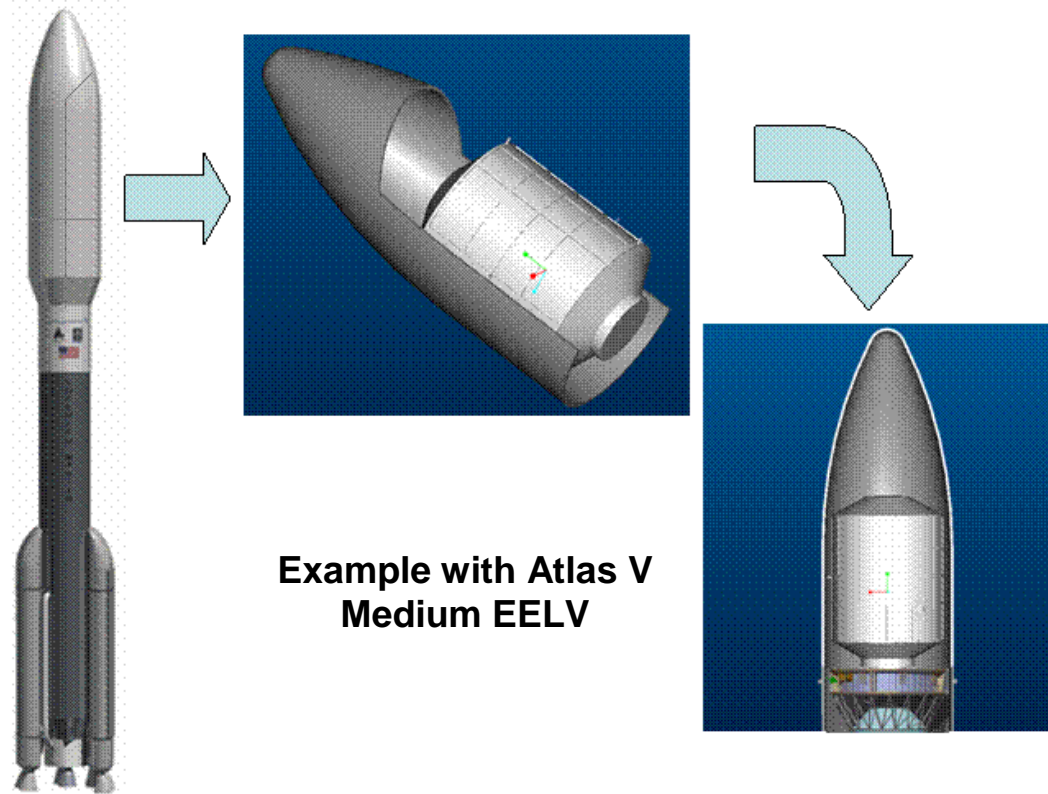


Figure 14 Non-ICM Launch Configuration [18]

Section 2-2.2 *On-Orbit Configuration*

The on-orbit configuration consists of the ellipsled (reentry aeroshell and structure), the MPLM, both pressurized/unpressurized cargo and all the subsystems that make up the resupply vehicle, all docked with the ICM. This configuration will use the ICM to maneuver toward the ISS for rendezvous until it is at an acceptable distance within the approach corridor. The ISS will then use its remote manipulator arm to capture the resupply vehicle for berthing to the station. Once the resupply vehicle is captured, the ICM will separate from the resupply vehicle to allow the MPLM docking port accessibility for berthing to station. Once berthed, the ISS crew will have

access to internal supplies and also unpressurized supplies attached to the exterior cargo carrier structure. The station's remote manipulator arm has the ability to move across the exterior of the ISS to support various external operations. The ICM can then be captured with the arm and berthed to a different docking port on the station, which will allow for ISS reboost capabilities to support required station keeping.

During its time docked to station, the MPLM section can be used as additional station area (i.e. storage, experiments or evening temporary crew quarters). When it is time for return to Earth, all items needing return can be transferred over to the resupply vehicle, to include completed experiment/payload racks, station or crew hardware needing repair, etc.

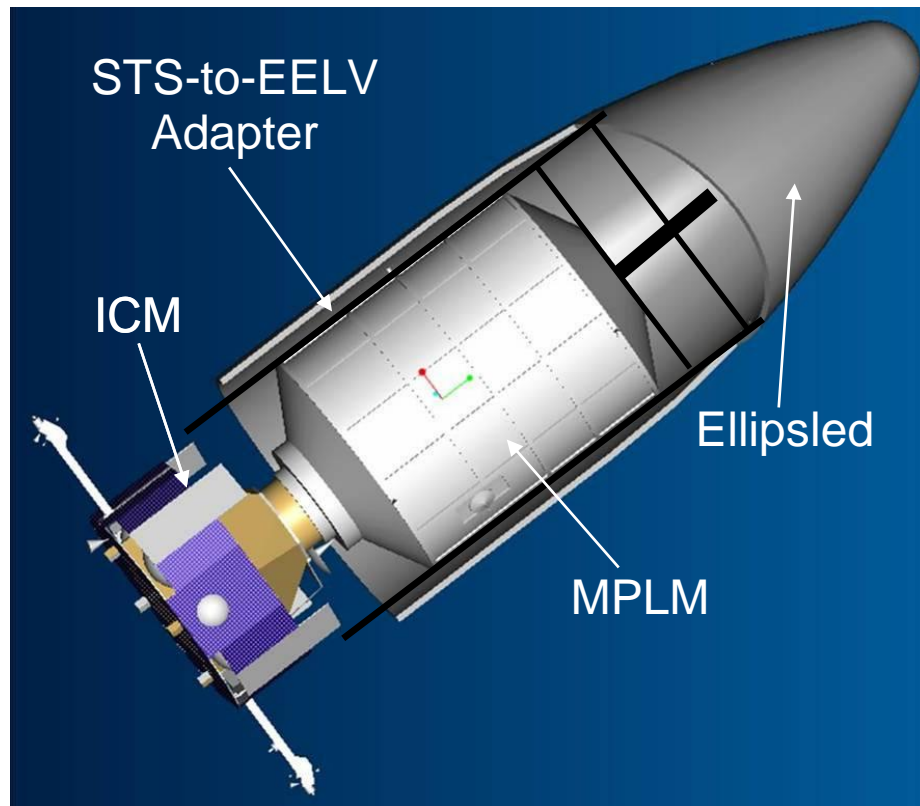


Figure 15 On-Orbit Configuration

Section 2-2.3 *Reentry Configuration*

The reentry configuration is the resupply vehicle once the ICM has performed a de-orbit burn, separated and started the vehicle on its reentry trajectory. The de-orbit configuration consists of the ellipsled (reentry aeroshell and structure), the MPLM, both pressurized/unpressurized cargo and all the subsystems that make up the resupply vehicle. The reentry configuration uses its own RCS to maintain the desired orientation from entry interface through the initiation of the LRS. A loaded [COTS]² resupply vehicle that is stable for reentry is 18,491 kg, which is driven by the placement of the return cargo and the reentry vehicle's cg.

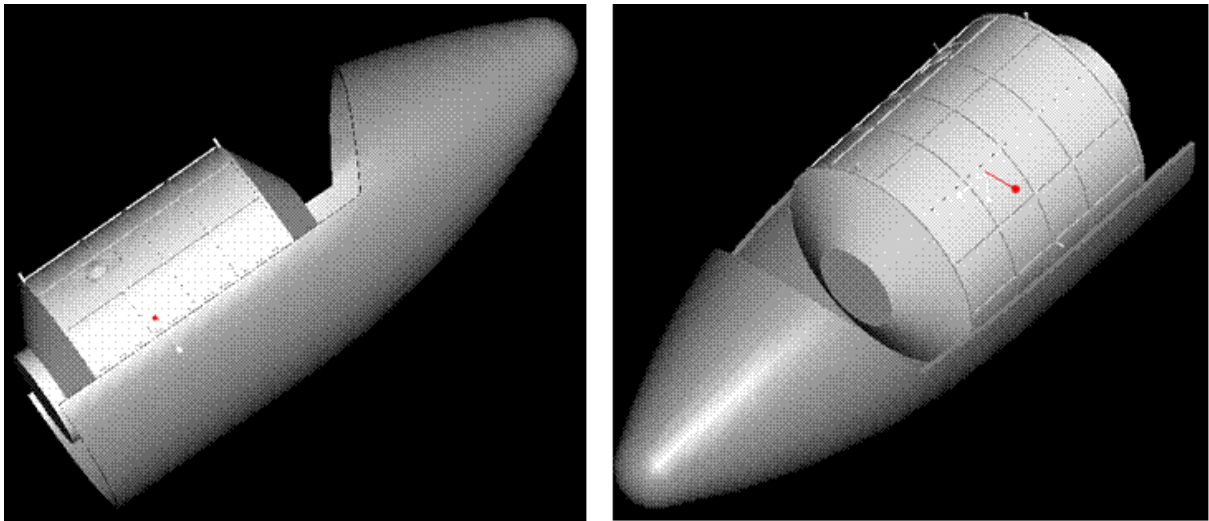


Figure 16 Reentry Configuration

Section 2-2.4 Overall Concept of Operations

Figure 17 shows the overall mission concept of operations (CONOP) for the [COTS]² resupply vehicle system. The CONOP helps define the various phases of flight and interaction between the resupply vehicle and the ICM and ISS. Following LRS activation and touchdown, the internal structure (all reusable hardware), MPLM, STS-to-EELV adapter structure, RLS, RCS and unpressurized payload container system are all recovered for reuse on the next resupply vehicle. The ellipsled is the only portion of the resupply vehicle that is not useable.

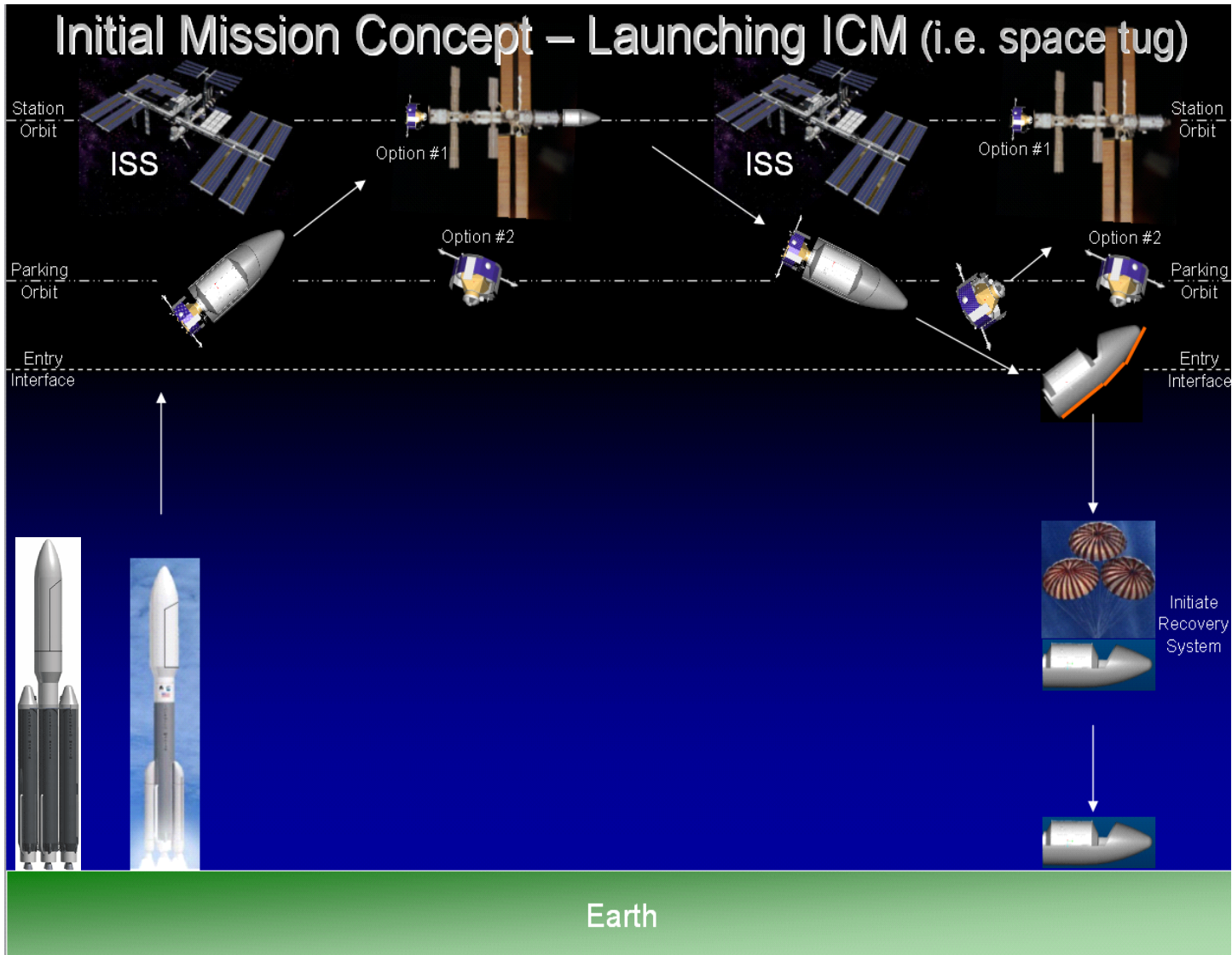


Figure 17 Mission CONOP

Section 2-3. Additional Missions

Section 2-3.1 ISS Module Assembly

The [COTS]² resupply vehicle core elements, the MPLM and STS-to-EELV Adaptor, are based off the existing five point STS interfaces. This means any of remaining ISS components that were initially designed to be flown on the space shuttle should also be capable of integration into the [COTS]² resupply vehicle system, minus the MLPM and still launched to the ISS. The STS-to-EELV adaptor structure, which is essentially the backbone of the [COTS]² resupply vehicle, makes this possible since it is design to pick up the interface loads though the same five attachment points and distribute the load into the EELV interface plane.

Section 2-3.2 GEO & Lunar Cargo Returns

The [COTS]² resupply vehicle could be used as a payload return vehicle. For GEO missions, the MPLM could be removed and a type of cargo bay installed to allow external payloads to be loaded in the vehicle. With the integration of some type of robotic arm system, the vehicle could be used to rendezvous, capture and loading of GEO satellites or even GEO belt space debris into the cargo bay for return to Earth. For lunar missions, the [COTS]² resupply vehicle could be used to return large payloads from lunar orbit to help support a lunar base or lunar mining operations. The MPLM could be loaded with lunar base equipment needing repair, experiments or even containers of mined Helium-3 for return to earth. If those items could not be transferred from the ascent vehicle to the [COTS]² vehicle's MPLM, then the cargo

bay version could be used for larger items unable or not requiring pressurization storage in the MPLM.

An additional advantage to the GEO and lunar return missions would provide the opportunity to test and verify the advanced aerobraking and aerocapture concepts at a large scale level.

Section 2-3.3 Human Returns

Once the [COTS]² ellipsled vehicle configuration has been tested and proven with cargo returns from ISS and the moon, could help lead to a human spacecraft version. Since these vehicles would be returning at higher velocities from a GEO or lunar orbit, this would help scientists increase the Technical Readiness Level (TRL) for future manned missions to Mars and Near Earth Objects (NEO) while reducing the risk for first time application.

CHAPTER 3

METHODOLOGY FOR AERODYNAMIC ANALYSIS AND RESULTS

The following sections describe the methodology used for generating the aerodynamic data and performing the analysis for the three reentry vehicle configurations. There were two main software packages used; Pro-Engineer for solid modeling and Missile Datcom for aerodynamic analysis.

Section 3-1 Pro-Engineer Modeling

Pro-Engineer (Pro-E) is a parametric, integrated 3D CAD/CAM/CAE solution created by Parametric Technology Corporation (PTC). It is a parametric, feature-based, associative solid modeling software in use today. The application runs on Microsoft Windows, Linux and UNIX platforms, and provides solid modeling, assembly modeling and drafting, finite element analysis, and tooling functionality for engineers.

[30]

Section 3-1.1 Component Modeling and Configuration Layout

The ICM, MPLM, Delta IV and Atlas V fairings and the generic ellipsled were all modeled using Pro-E. The models were used for system integration analysis, configuration layout and internal packaging trade studies of the main components. It was also used to determine resupply vehicle center of gravity (cg) for the system components and various reentry vehicle assemblies.

The following figures show the OML for the three ellipsled configurations:

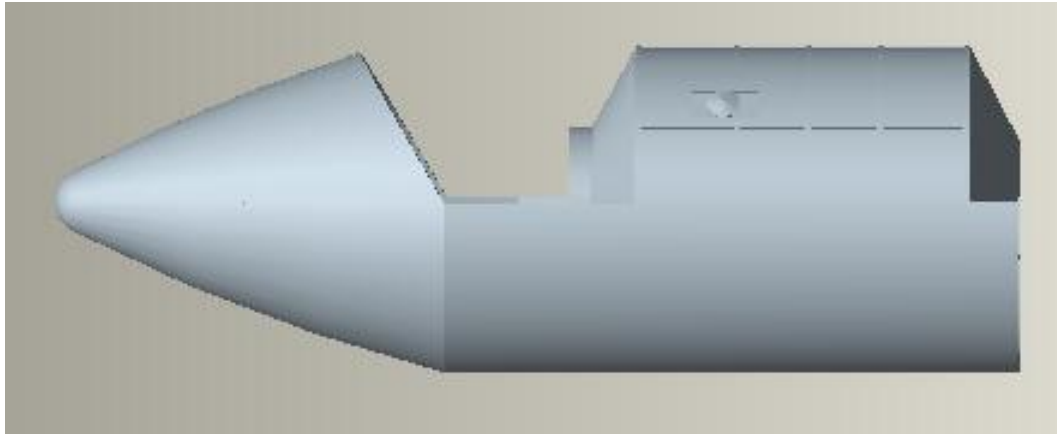


Figure 18 Delta IV Configuration ($r_n = 0.5m$)

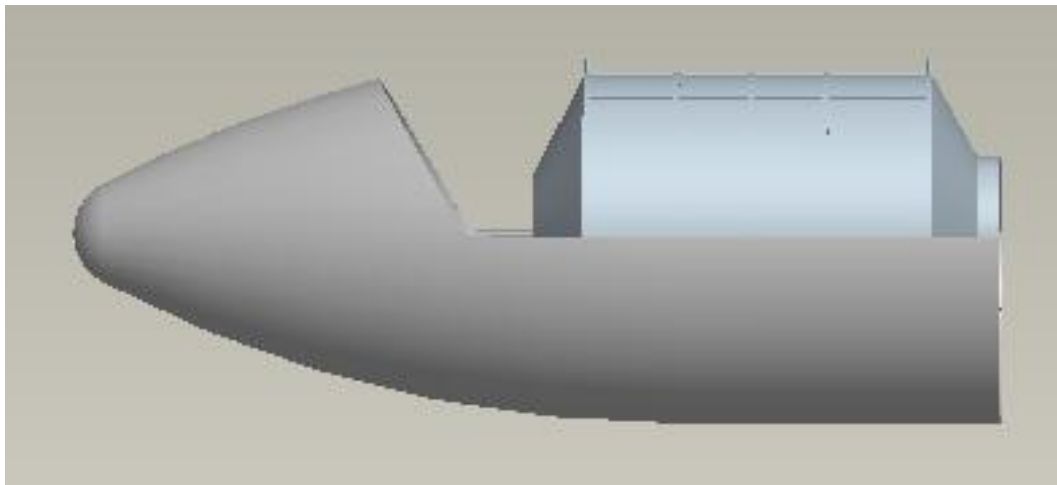


Figure 19 Atlas V Configuration ($r_n = 0.8m$)

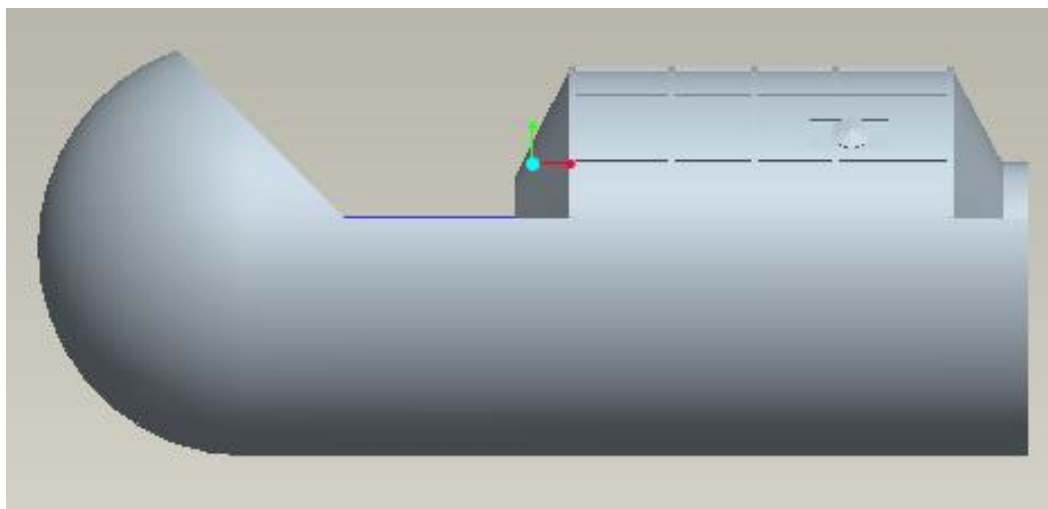


Figure 20 Generic Configuration ($r_n = 2.7\text{m}$)

Section 3-1.2 Mass Properties

The vehicle configuration has the following maximum mass, depending on which configuration is being referenced. The driver for the allowable mass at launch is the maximum lifting capabilities of the EELV selected.

Table 4 Maximum Vehicle Configuration

Resupply Vehicle Description	Maximum Mass (kg)
Total vehicle mass with ICM	31,161
Total vehicle mass without ICM	22,991
Total reentry vehicle mass	18,491

The mass for the resupply vehicle was broken into its major components to perform the cg calculations. The following is a table of the components used in this study:

Table 5 [COTS]² Resupply Vehicle Mass Breakout

Component Description	Mass (kg)	Notes/Remarks
MPLM (empty)	4,080	
Pressurized payload	9,000	MPLM max payload capability
Aeroshell (ellipsled)	3,800	Based off percentage of fairing mass, plus structural strengthening factor
Unpressurized payload	2,500	Based off the ICC used in shuttle
STS-to-EELV adapter	1,600	
RCS	966	Scaled from the NASA Mars Ellipsled [5]
LRS	1,045	System provides 6.7 m/s ROD [9]
ICM (dry)	3,000	
Propellant (ICM)	5,170	Provides delta-v of ~1,472 (m/s)

The cg calculation was performed by taking the component masses and moment arms per the predefined origin (X_0) and using the summation of moments equation to solve for the X_{cg} . Due to the vehicle's symmetric configuration, it was assumed that the Y_{cg} is located on the vehicle's center line. The Z_{cg} was found using the modeling software package, Pro-E.

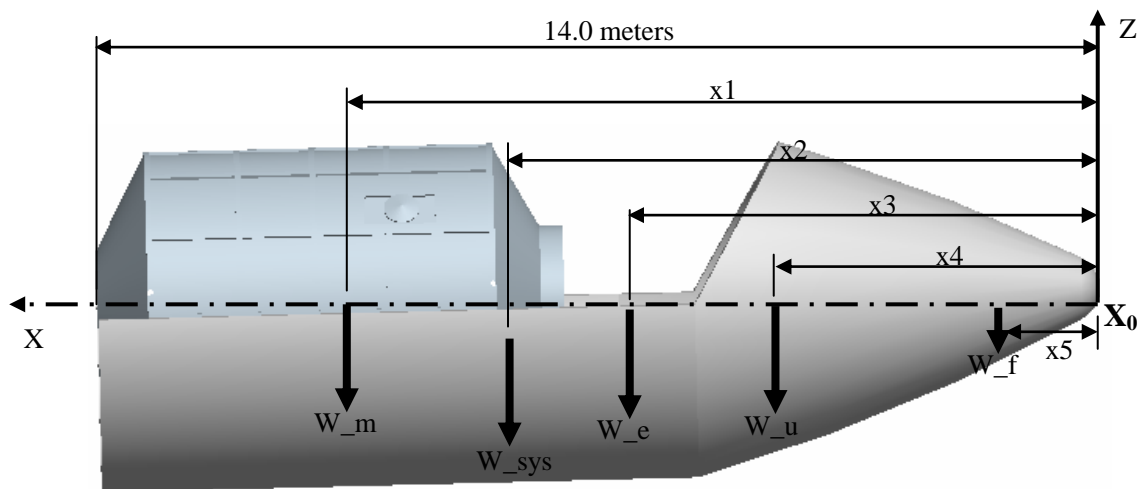


Figure 21 Resupply Vehicle Center of Gravity

$$\sum \frac{W_{sys}(x_2)}{W} = X_{cg}$$

$$X_{cg} = \frac{W_m(x_1) + W_e(x_3) + W_u(x_4) + W_f(x_5) + W_p(x_6)}{W_c}$$

where: W_m = mass of MPLM and pressurized payload

W_e = mass of ellipsled aeroshell and STS-to-EELV structural adaptor

W_u = mass of unpressurized payload

W_f = mass of RCS propellant

W_p = mass of LRS

W_c = mass of [COTS]² vehicle

Section 3-2 Aerodynamic Analysis

The aerodynamic analysis performed on the reentry configuration of the resupply vehicle utilized a preliminary analysis tool that is typically utilized for aerodynamics on missile configuration designs. The details of the aerodynamic analysis code and the additional stability analysis are described in the following sections.

Section 3-2.1 *Missile DATCOM*

In missile preliminary design it is necessary to quickly and economically estimate the aerodynamics of a wide variety of missile configuration designs. Since the ultimate shape and aerodynamic performance are so dependent upon the subsystems utilized, such as payload size, propulsion system selection and launch mechanism, the designer must be capable of evaluating a wide variety of configurations accurately. The fundamental purpose of Missile DATCOM is to provide an aerodynamic design tool which has the predictive accuracy suitable for preliminary design, and the capability for the user to easily substitute methods to fit specific applications.

The computer code is capable of addressing a wide variety of conventional missile designs. Per Missile DATCOM User's Guide, a conventional missile is one which is comprised of the following:

- An axisymmetric or elliptically-shaped body.
- One to four fin sets located along the body between the nose and base. Each fin set can be comprised of one to eight identical panels attached around the body at a common longitudinal position. Each fin may be deflected independently, as an all moving panel or as a fixed panel with a plain trailing edge flap.
- An airbreathing propulsion system.

To minimize the quantity of input data required, commonly used values for many inputs are assumed as defaults. However, all program defaults can be overridden by the user in order to more accurately model the configuration of interest. [11] The input deck controls allow the user to specify parameters for the configuration to include vehicle geometry, aerodynamics and vehicle cg.

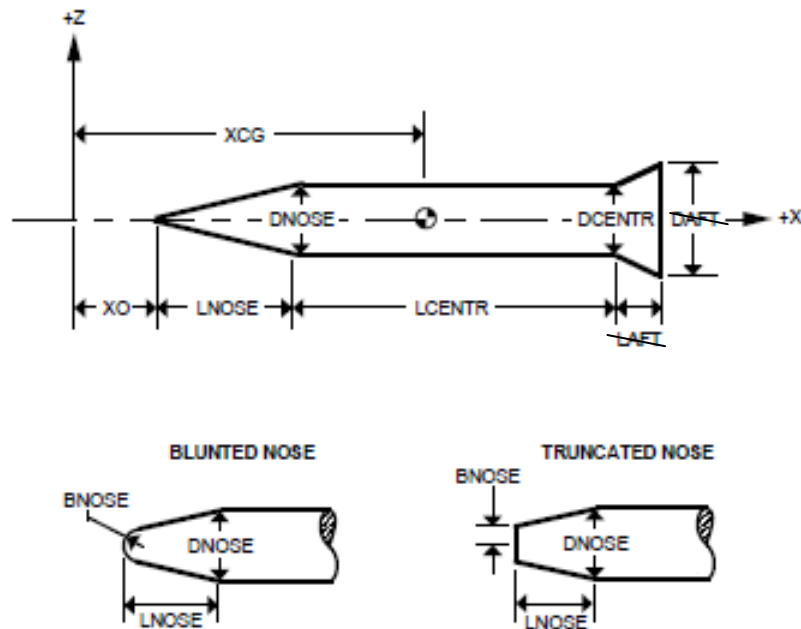


Figure 22 Body Geometry Inputs [11]

Table 6 Body Geometry Input Calculated Values per Configuration

Vehicles	DCENTER	LCENTER	DNOSE	LNOSE	BNOSE	Xcg	Zcg
Generic	212.6	445.881	212.6	105.3	106.3	270.08	-35
Delta IV	202.008	301.097	202.008	250.084	19.685	270.08	-35
Atlas V	213.602	215.433	213.602	335.748	31.496	270.08	-35

*all units in inches

Section 3-2.2 Stability

Flight quality standards are specific to the particular type of aerodynamic vehicle.

For a non-powered vehicle, the flight quality standards are associated with the mass and inertial properties and with the aerodynamic properties. These can be defined by three important criteria: [16]

- The velocity criterion, associated with weight and drag
- The maneuverability criterion, associated with weight and lift
- The controllability criterion, associated with rolling, yawing, pitching moments and inertia tensor

The coefficient of moment, axial force coefficient and normal force coefficient were placed into a summation of moments equation:

$$0 = \sum C_{M_{cg}} = C_M + C_N \frac{y_{cg} - y}{d} + C_A \frac{x_{cg} - x}{d}$$

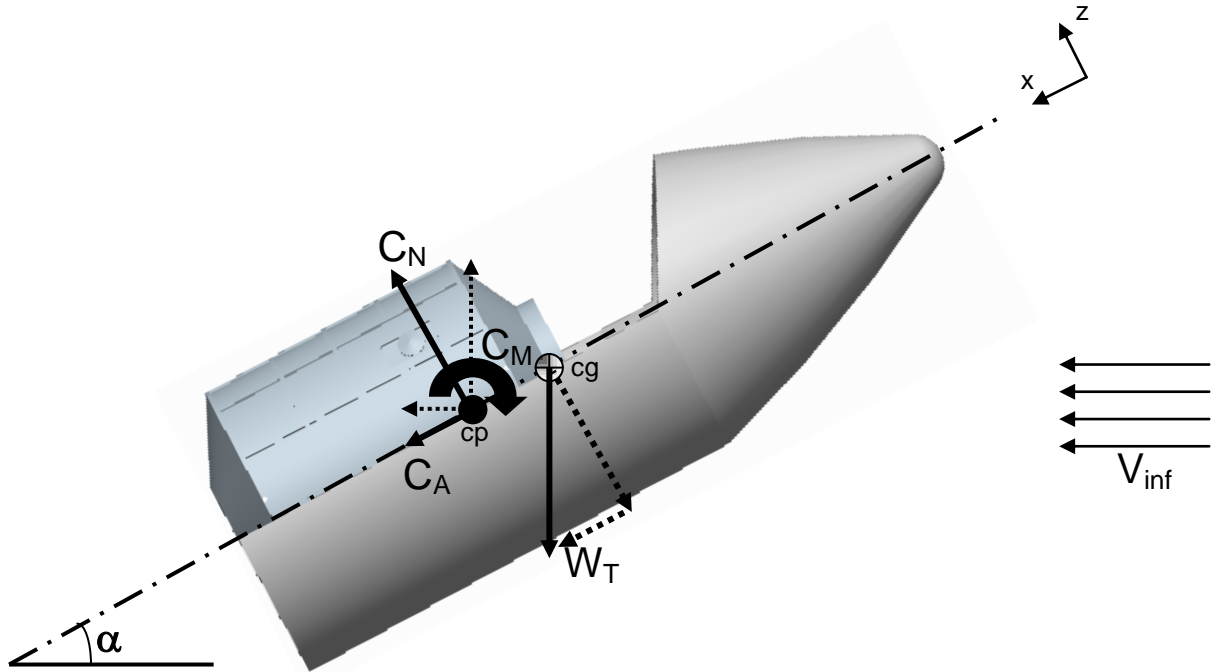


Figure 23 Ellipsed Stability Analysis Assumptions

Missile DATCOM measured from the C_M at Mean Reference Center (MRC), which was from the nose of the vehicle (X_0). The C_M at MRC was then converted into the C_M about the reentry vehicle's cg. The AOA varied between 0 and 60 degrees and C_M about the cg was calculated as a function of Mach number (for 1.5, 3, 5, 10, 20 & 25). The following figures (Figure 24-26) identify each reentry vehicle's stability with respect to the reentry cg and AOA versus Mach numbers. The negative slope value for each configuration shows the stable AOA for that specified Mach number. All vehicle configurations were analyzed up to a +/- 60 degree AOA. To simplify the aerodynamic analysis, the upper fairing area cutout was ignored and a symmetric aeroshell shape was assumed for the three vehicle configurations. [7,16]

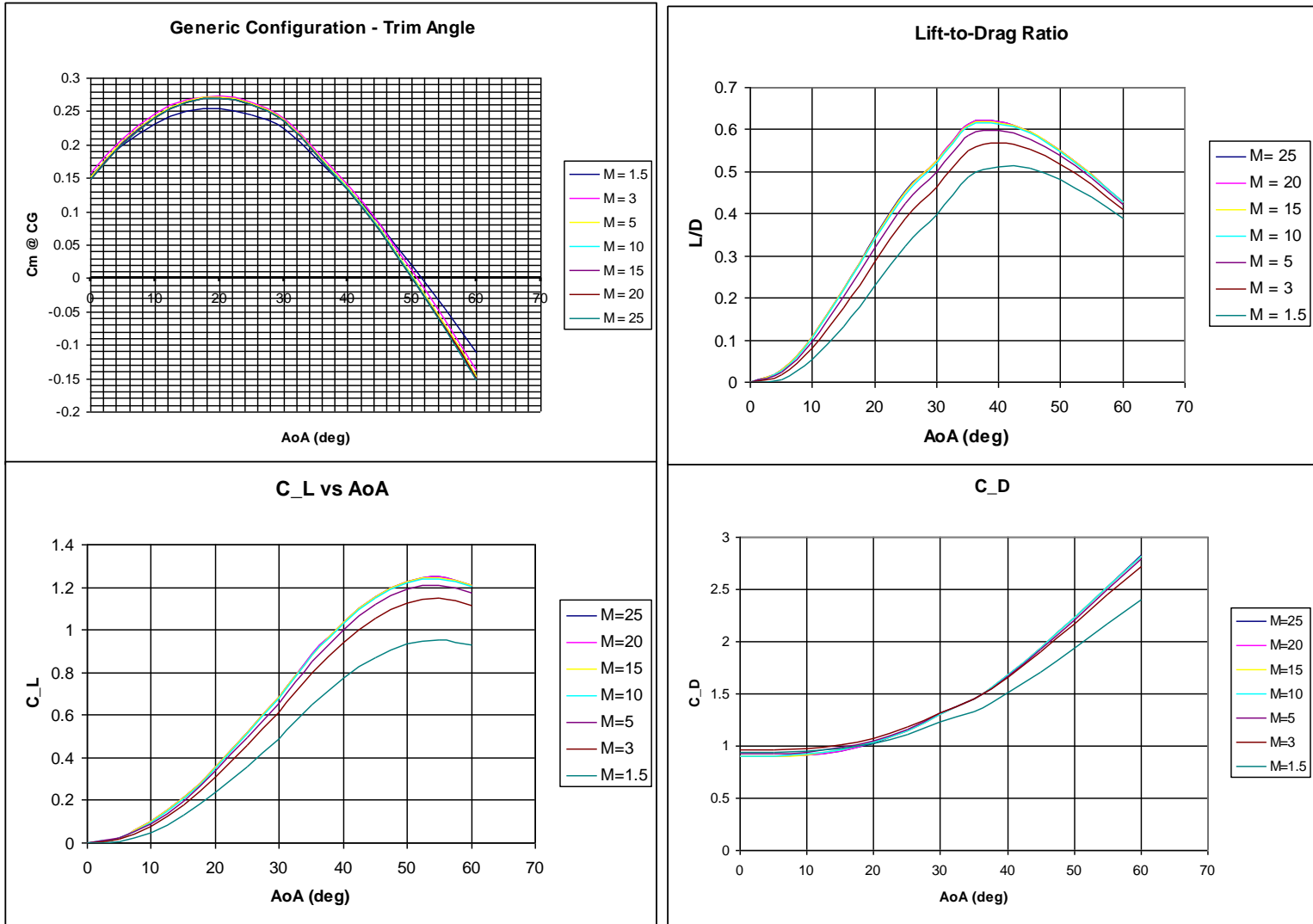


Figure 24 Force and Moment Coefficients for Generic Configuration

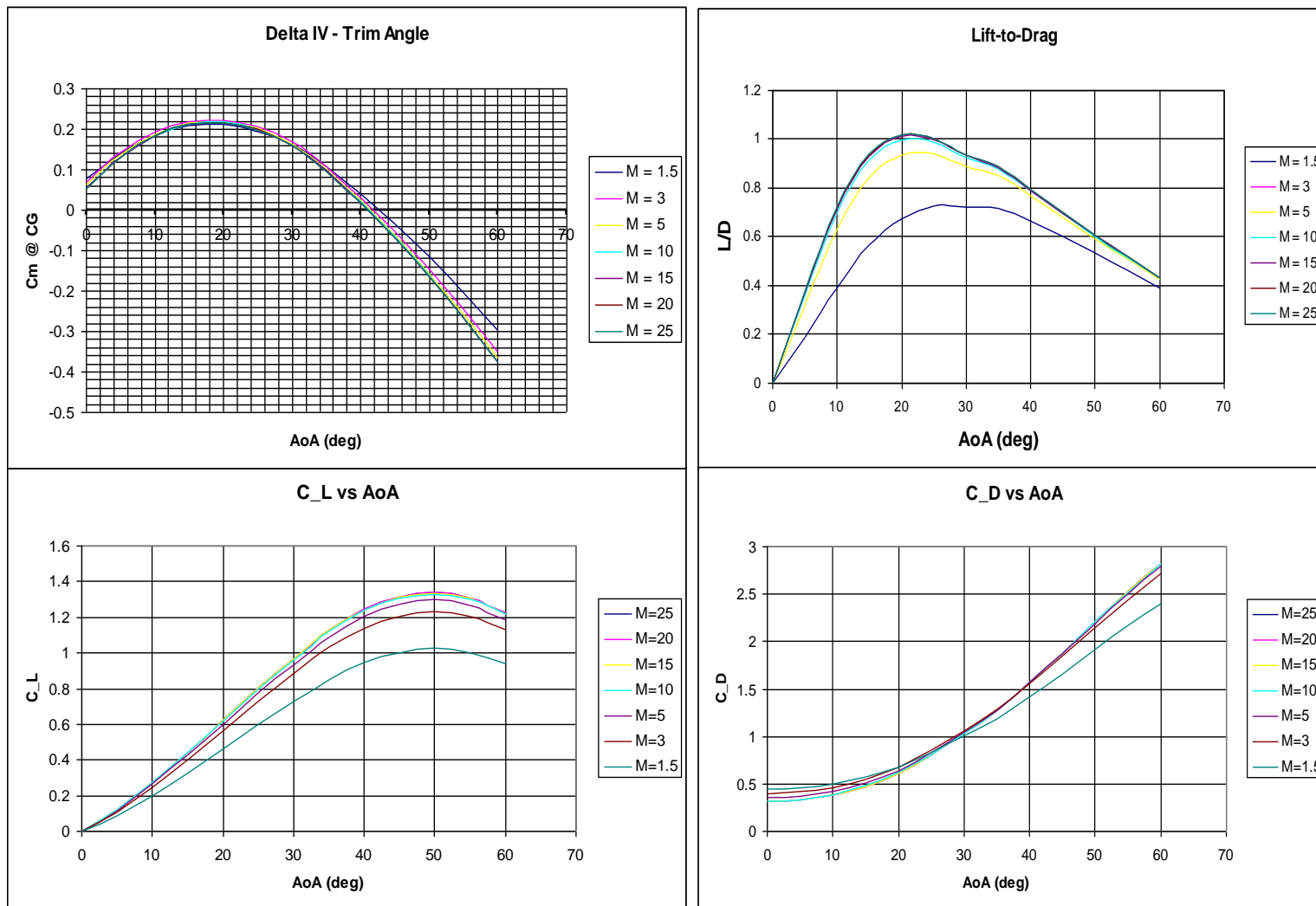


Figure 25 Force and Moment Coefficients for Delta IV Configuration

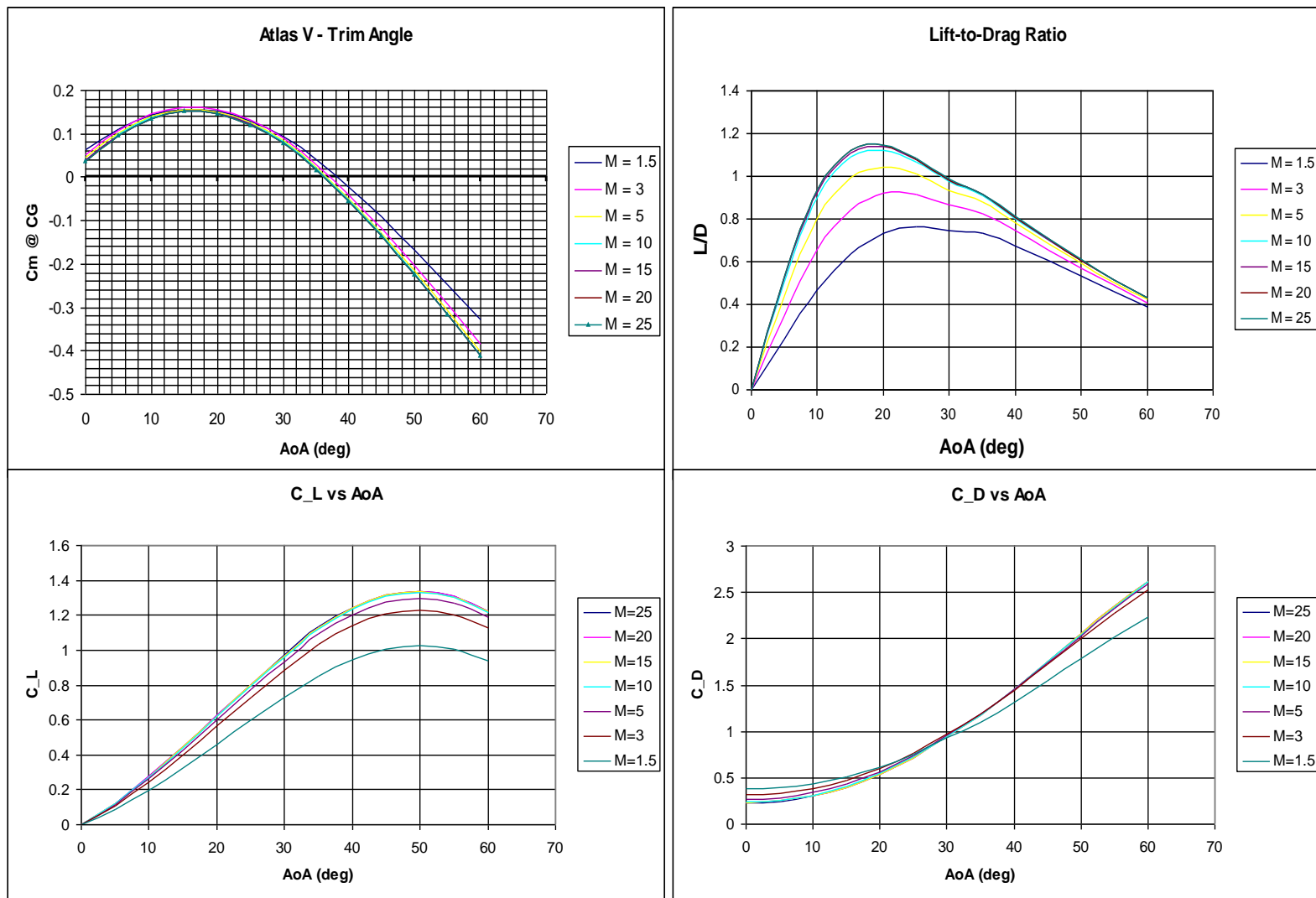


Figure 26 Force and Moment Coefficients for Atlas V Configuration

The trim AOA was obtained from aerodynamic analysis based on a configuration's cg. Table 7 identifies the trim AOA for the three reentry vehicle configurations from hypersonic through low supersonic reentry velocities. Reference appendix section A3 for all the aerodynamic data generated from Missile DATCOM for the three vehicle configurations, which provides a full range of available Mach numbers verses AOA from 0 to 60 degrees (in increments of 5 degrees).

Table 7 Trim Angle of Attack

Configuration	Mach No.	Trim AOA	L/D
Generic	1.5	50	0.4822
	25	52	0.5485
Delta IV	1.5	41	0.6671
	25	43	0.7475
Atlas V	1.5	35	0.7312
	25	38	0.9581

It was determined through the mass properties configuration layout and during the stability analysis, that the [COTS]² vehicle could not be fully loaded at the station for its return flight to Earth. A fully loaded MPLM during reentry would pull the vehicle's cg to far aft and not allow the vehicle to maintain its desired trim alpha during reentry. By only loading half the MPLM, the [COTS]² vehicle could maintain its desired trim alpha and fly a stable reentry.

CHAPTER 4

METHODOLOGY FOR TRAJECTORY ANALYSIS AND RESULTS

The following sections describe the trajectory analysis performed on the three reentry vehicle configurations and the results of their described reentry types. The basic difference between the three reentry types is velocity. Thus, the higher the vehicle's orbit prior to beginning reentry, the greater the reentry velocities.

All reentries described are considered direct entry. The aeroheating environment associated with direct entry dictates the type and size of the thermal protection system (TPS) that must be used for an entry vehicle. Peak heat rate generally determines the range of possible TPS materials, while the integrated heat load determines the thickness and mass of the TPS. Heat rate and integrated heat load calculations were performed with the engineering analysis techniques that address stagnation point convective heat load.

Section 4-1 Program to Optimize Simulated Trajectories

Atmospheric entry trajectories for the candidate vehicles returning from the ISS to Earth were modeled by numerically simulating the equations of motion. This was done using the to Optimize Simulation Trajectories (POST), a computer code developed by the Martin Marietta Corporation in the 1970's as a Space Shuttle trajectory optimization program. [2] Since that time, the program has been

significantly improved with additional capabilities added in the areas of vehicle modeling and trajectory simulation for a number of different mission types, as seen in Table 8. The program can be run in both a UNIX and also a PC based environment that consists of an input deck, program files, and various output files. The input deck controls all the user-specified parameters, to include aerodynamics, atmospheric conditions, integration methods and many others.

For the analysis, the three-degree-of-freedom (3DOF) version of POST was used. There is also a six-degree-of-freedom (6DOF) version of POST; however the rotational components were neglected in this initial research, leaving only the translation components of the 3DOF version. POST models the vehicle as a point mass and gives the capability to optimize and target for a given set of defined end conditions. [1,2]

Table 8 Typical Applications of POST [1,2]

Type of Mission	Type of Vehicle	Optimization Variable	Typical Constraints	
			Equality	Inequality
Ascent to Near-Earth Orbit	Titan, Space Shuttle, Single Stage to Orbit (VTO and HTO)	Payload, Weight at Burnout, Propellant, Burntime, Ideal Velocity	Radius, Flight Path Angle, Velocity	Dynamic Pressure, Accelerations
Ascent to Synchronous Equatorial Orbit	Titan, Space Shuttle/Upper Stage	Payload, Propellant	Apogee, Perigee, Inclination	Dynamic Pressure, Angle of Attack, Pitch Rate
Ascent Abort	Space Shuttle	Abort Interval	Landing Site Latitude and Longitude	Dynamic Pressure, Acceleration
ICBM Ballistic Missile	Titan, Minuteman, Peacekeeper	Payload, Misc Distance	Latitude, Longitude, Downrange, Crossrange	Reentry Flight Path Angle, Acceleration
Reentry	Space Shuttle, X-24C, Single Stage to Orbit	Heat Rate, Total Heat, Crossrange	Latitude, Longitude, Downrange, Crossrange	Heat Rate, Acceleration
ICBM Orbital Maneuvers	Titan, Transtage, Centaur, IUS, Solar Electrical Propulsion	Payload, Propellant, Ideal Velocity, Burntime	Latitude, Semimajor Axis, Eccentricity, Inclination, Argument of Perigee, Period	Reentry Attitude Angle, Perigee Altitude
Aircraft Performance	X-24B and C, Subsonic Jet Cruise, Hypersonic Aircraft	Mach, Cruise Time, Payload	Downrange, Crossrange, Dynamic Pressure, Mach, Altitude	Dynamic Pressure, Max Altitude, Dynamic Pressure

Section 4-1.1 Input Deck

An input deck must first be constructed in order to start working with POST. For a given trajectory problem, an input deck is created to simulate the desired trajectory. The input deck includes initial conditions, aerodynamic data for the vehicle, vehicle geometry, the atmospheric model and the planetary model. The aerodynamic data from the Missile DATCOM code was used in the POST input decks to provide the appropriate L/D per Mach number for each vehicle configuration. The input decks are then run by the POST source code, which is written in FORTRAN [1,2].

Examples of POST input decks can be found in appendix A1.

Section 4-2 Reentry Simulations

The ICM performs a deorbit burn to set the resupply vehicle on its return trajectory and initial entry velocity (as defined per sections 3-4.1 – 3-4.3). Prior to entry interface, the ICM separates from the resupply vehicle and returns for either berthing to the ISS or a defined parking orbit. The resupply vehicle uses its own internal RCS to maintain reentry orientation and required attitude throughout entry. The reentry simulation is from 124.9 km (400k ft) to 6 km (20k ft).

Section 4-2.1 Low Earth Orbit Reentry

The primary analysis of the reentry vehicle is based on the vehicle returning from the ISS. The ISS is maintained at a nearly circular orbit with a minimum mean altitude of 278 km and a maximum of 460 km. The station has an average orbital decay of 2 km per month but the nominal station altitude is 340 km. The nominal station orbital altitude was used for the purposes of this study and equates to an entry velocity of 7.8 km/sec.

Section 4-2.2 Geosynchronous Earth Orbit Reentry

Additional analysis of the reentry vehicle is based on the vehicle returning from geosynchronous orbit. A geostationary orbit (GEO) is a geosynchronous orbit directly above the Earth's equator (0° latitude), with orbital eccentricity of zero. From the ground, a geostationary object appears motionless in the sky and is therefore the orbit of most interest to operators of artificial satellites (including communication and

television satellites). Due to the constant 0° latitude, satellite locations may differ by longitude only. The GEO altitude is approximately 35,786 km. Return from GEO results in an atmospheric entry velocity of 10.3 km/sec.

Section 4-2.3 *Lunar Return Reentry*

Final analysis of the reentry vehicle is based on the vehicle returning from lunar orbit. The moon has a perigee of 363,104 km and an apogee of 405,696 km. The worst case scenario was used, which was the apogee plus the radius of the moon and 200 km for a typical lunar orbit altitude (i.e. 60 nm used by Apollo), thus giving 407,544 km. Return from the moon results in an atmospheric entry velocity of 11.1 km/sec [12].

Section 4-3 **Entry Corridor**

The entry corridor is defined by the difference between the undershoot boundary and the overshoot boundary angles. It is the three-dimensional narrow region in space that a re-entering vehicle must fly through to successfully return to the earth's surface. If the vehicle strays above the corridor, it may skip out of the atmosphere. If it strays below the corridor, it may hit the earth's surface or be subjected to excessive deceleration loads or heating and burn up. Entry corridors are affected by values of lift-to-drag ratios and imposed g-limits. The ellipsled configuration is a higher lift-to-drag ratio which creates a wider entry corridor than a capsule.

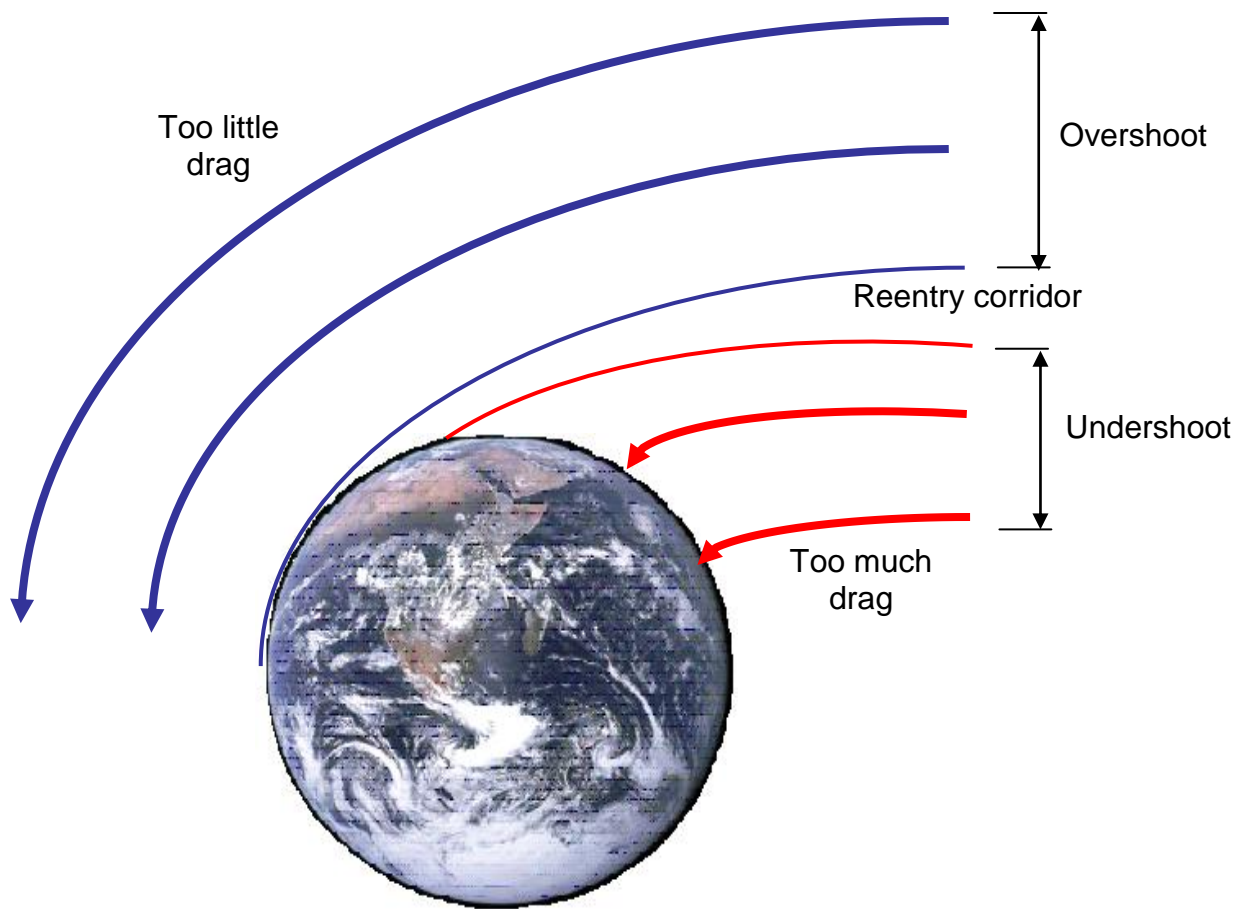


Figure 27 Reentry Corridor

Section 4-3.1 Undershoot Boundary

The undershoot trajectories require that the entry vehicle holds a zero degree bank and thus maintains full lift up. The only constraint placed on the undershoot trajectories during this research was that of the maximum 5-g peak deceleration requirements. The 5-g limit was selected to demonstrate the [COTS]² vehicle could meet the requirement for human returns. The undershoot trajectory is the steep trajectory that can be flown without violating the deceleration constraint.

Section 4-3.2 *Overshoot Boundary*

The overshoot trajectories required the entry vehicle to hold a bank angle of 180 degrees, thus providing a full lift down. The only constraint that applied to the overshoot trajectories was that the entry vehicle did not skip out of the atmosphere. The overshoot trajectory is the shallowest possible entry that can be flown within the entry corridor.

Section 4-3.3 *Entry Trajectory*

The entry trajectory is defined by the difference between the undershoot and overshoot boundaries. However, the nominal trajectory will be what path the vehicle typically would plan to fly for a direct entry to the Earth's surface. This trajectory is governed by the g-limit constraints imposed to avoid excessive deceleration and structural loading. It also allows for meeting the requirement for a crewed return.

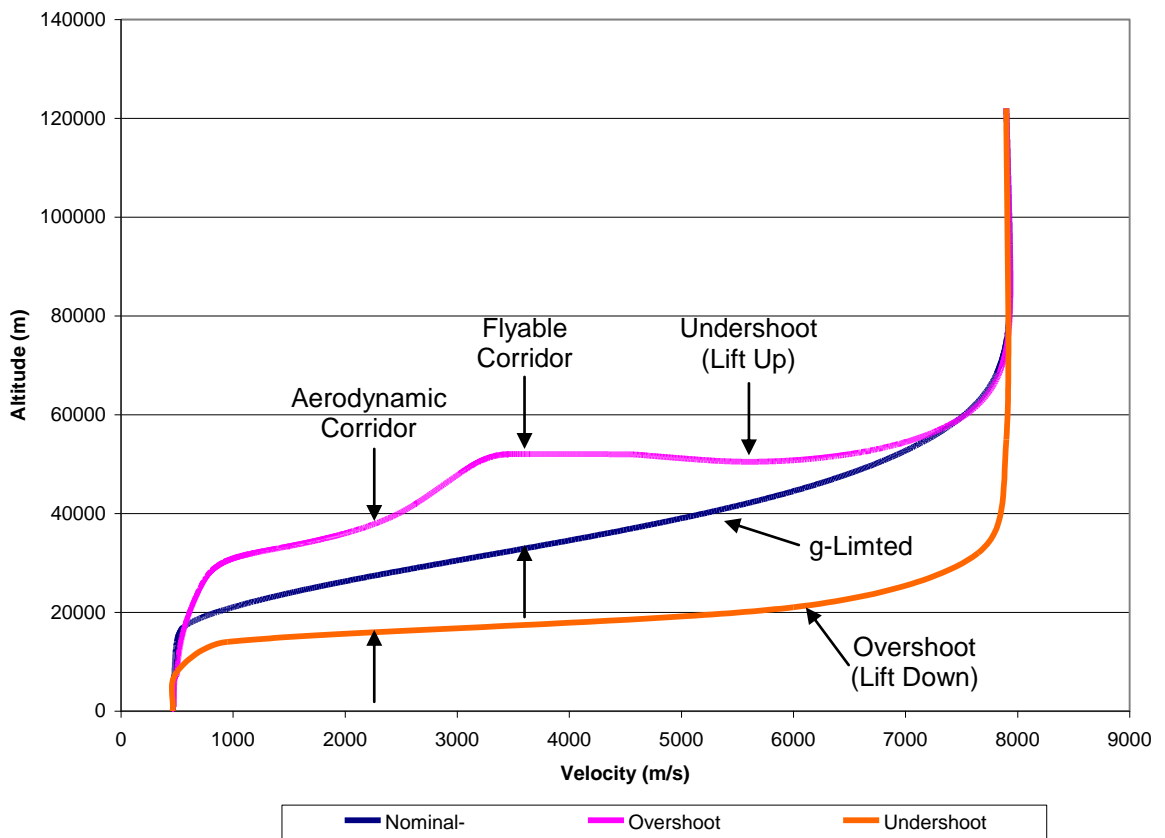


Figure 28 Entry Trajectory from LEO [8]

Section 4-3.4 Entry Corridor Width

The data obtained from the entry analysis has been translated into graphical form in Figure 29 which shows the entry angles (γ) verses entry velocity for both the undershoot and overshoot boundaries.

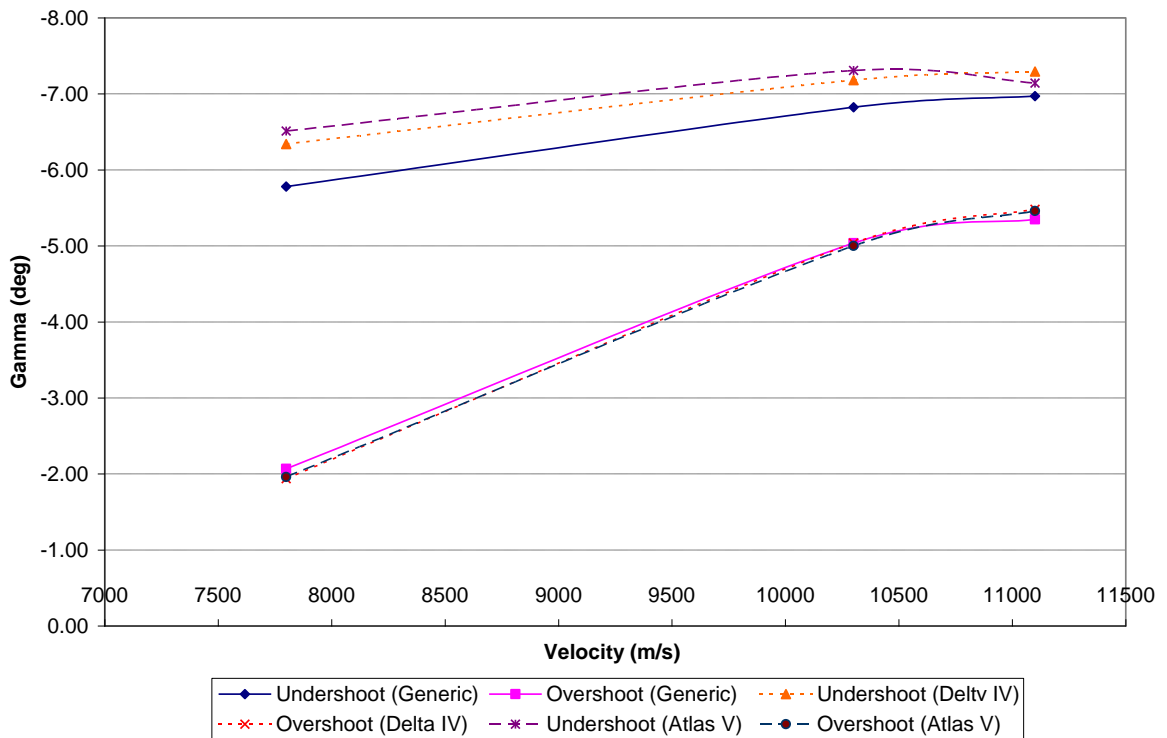


Figure 29 Entry Corridors per Vehicle Configurations

As mention previously, the area between the undershoot and overshoot boundaries is know as the entry corridor. Figure 30 details the entry corridor width as a function of entry velocity for the three ellipsled configurations as determined in this study. Figure 29 shows that the entry corridor with ranges from a maximum of 4.551 degrees at an entry velocity of 7.8 km/s for the Atlas V configuration to a minimum of 1.620 degrees occurring an entry velocity of 11.1 km/s for the Generic configuration. This is comparable to the Apollo lunar return corridor width of approximately 2 degrees [34].

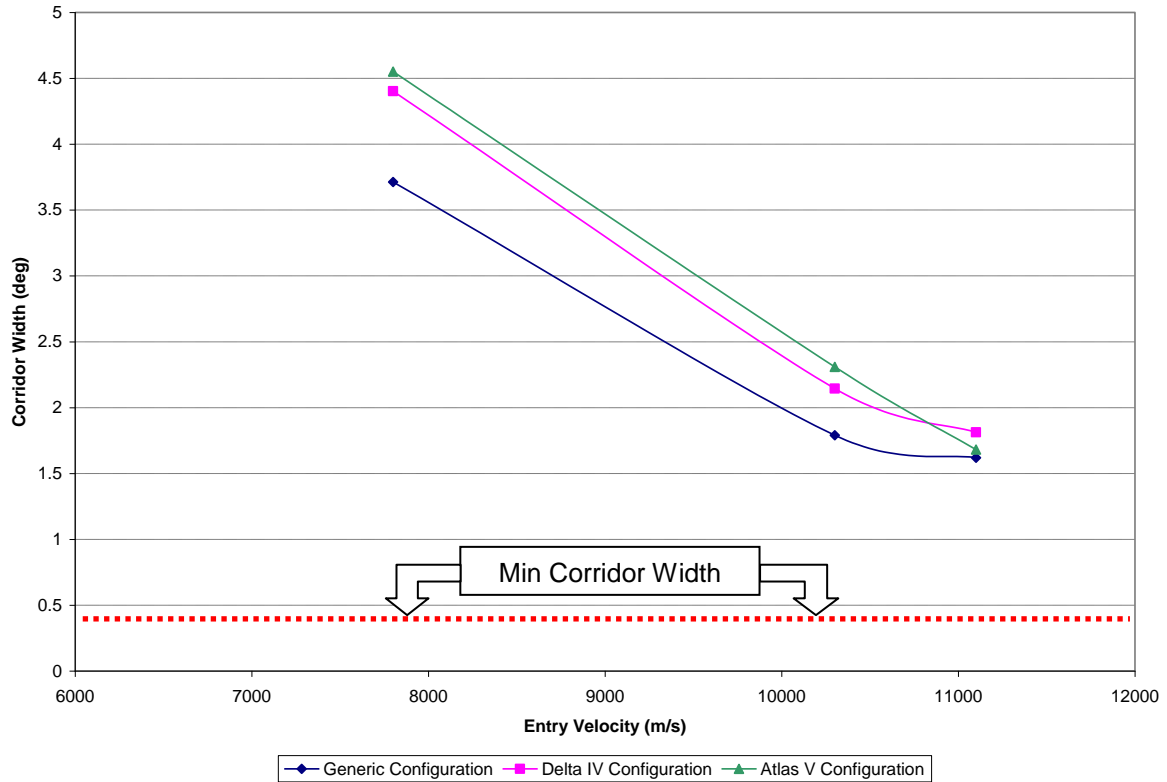


Figure 30 Entry Corridor Width per Vehicle Configuration

While a larger corridor is desirable to insure that the navigation systems can safely target the nominal trajectory, previous interplanetary robotic missions returning to Earth at even higher entry velocities have demonstrated high accuracy navigation techniques that reduced the required corridor width below that assumed previously. Stardust and Genesis sample return capsules with less than 0.1 L/D ratios, were able to target a corridor width of 0.16 degrees. Based off previous studies, a minimum corridor width of 0.4 degrees with a 0.1 L/D ratio provides sufficient control authority for up to lunar return velocities [8]. The following table helps summarize the results identified in the previous entry corridor figures.

Table 9 Summary of Entry Corridor Analysis

entry velocity (m/s)	Generic			Delta IV			Atlas V		
	Gamma (deg)		Entry Corridor Width	Gamma (deg)		Entry Corridor Width	Gamma (deg)		Entry Corridor Width
	under shoot	over shoot		under shoot	over shoot		under shoot	over shoot	
7800	-5.78	-2.067	3.713	-6.34	-1.937	4.403	-6.51	-1.959	4.551
10300	-6.825	-5.035	1.79	-7.18	-5.035	2.145	-7.309	-5.0	2.309
11100	-6.97	-5.35	1.62	-7.295	-5.482	1.813	-7.142	-5.46	1.682

Section 4-4 Heating Rate Analysis

The heat rate determines the type of Thermal Protection System (TPS) and the heat load determines the TPS thickness and amount of insulation required to protect the vehicles' structure. The ballistic coefficient can be reduced by increasing the angle of attack, thus increasing the drag profile and reducing the heating rate. The nose radius also plays a factor in determining the peak heating at the stagnation point, with a larger nose radius resulting in a less severe convective heating environment. For the entry velocities at or below 11 km/sec, which are most of those analyzed for this study, convection plays the dominant role in the total heating rate experienced by the vehicles. However for higher entry velocities (greater than 11 km/sec), radiative heating effects become significant and sometimes become the dominant form of heating. Only the stagnation point heating was analyzed; no centerline or off-centerline heating effects were considered in this analysis. In addition, an estimate of the total integrated heat load at the stagnation point was made. The heat load is the area under the heat rate verses time curve.

Section 4-4.1 Convective Heating Rates

To analyze the effects of convective heating on the three reentry vehicle configurations, a POST aeroheating rate option flag was used in the input deck. POST has a built-in subroutine to calculate laminar, convective heating rates at the stagnation point of the vehicles using the Chapman heating rate equation:

$$q'' = \frac{17600}{\sqrt{r_n}} \left(\frac{\rho}{\rho_{SL}} \right)^{\frac{1}{2}} \left(\frac{V_A}{26000} \right)^{3.15} (10^{-4})$$

where: q'' = laminar convective stagnation point heating rate (W/cm²)

r_n = nose radius of the vehicle or body (m)

ρ = local atmospheric density (kg/m³)

ρ_{SL} = sea level atmospheric density (kg/m³)

V_A = atmospheric relative velocity (m/s)

POST calculated the Chapman heating rates in the output along with the other trajectory parameters such as altitude, time, velocity, etc [1]. The maximum heating rates occur during the undershoot trajectory. Thus, only the undershoot heating rates have been plotted in Figure 31. The heating results presented will focus on LEO returns since the ISS resupply is the primary purpose of the [COTS]² vehicle.

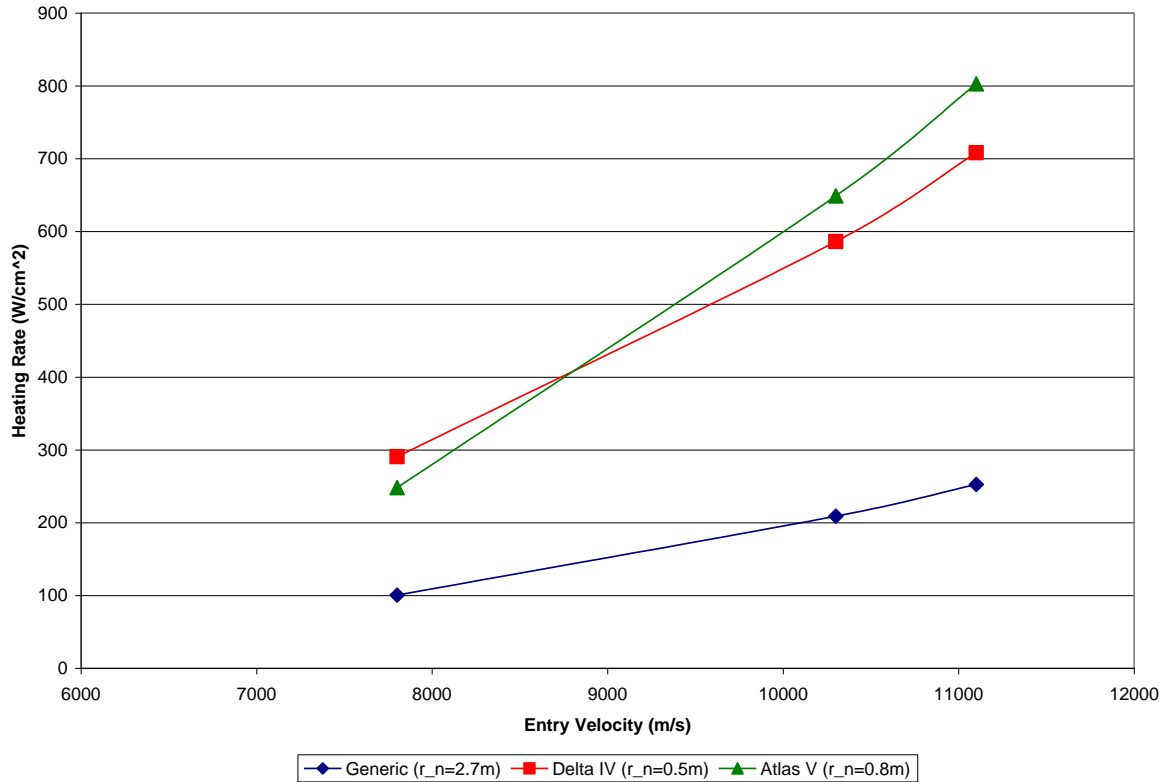


Figure 31 (Max Undershoot) Stagnation Point Results per Vehicle Configurations

The heating rate analysis reveals that even for the higher velocity lunar entries, there are different types of TPS materials that can meet the [COTS]² vehicle configuration and various mission requirements. Table 10 lists a few types of TPS material, that have been used previously on reentry vehicles but there are more in existence and under development.

Table 10 Candidate TPS Materials [32]

TPS Materials	Density (g/cm ³)	Maximum Allowable Heating Rate q _{max} (W/cm ²)	Maximum Allowable Surface Temperature (K)
Avco 5026-39 (Apollo)	0.512	432	3,033
Phenolic nylon	1.201	432-1,109	3,033-3,839
Carbon phenolic	1.458	>1,109	>3,839

Section 4-4.2 Total Heating Rates

The total heating rates are typically found by adding the radiative and convective heating. Since the highest entry velocity analyzed was from a lunar return, there is less radiative and more convective heating. The Apollo lunar entries had approximately 30% radiative heating of the total heating for the vehicle [3], thus cannot be ignored. However, for an entry from LEO the radiative heat transfer is almost negligible and the total heating rate is dominated by the convective heating. For the purposes of this study, only convective heating analysis was performed on the [COTS]² vehicles.

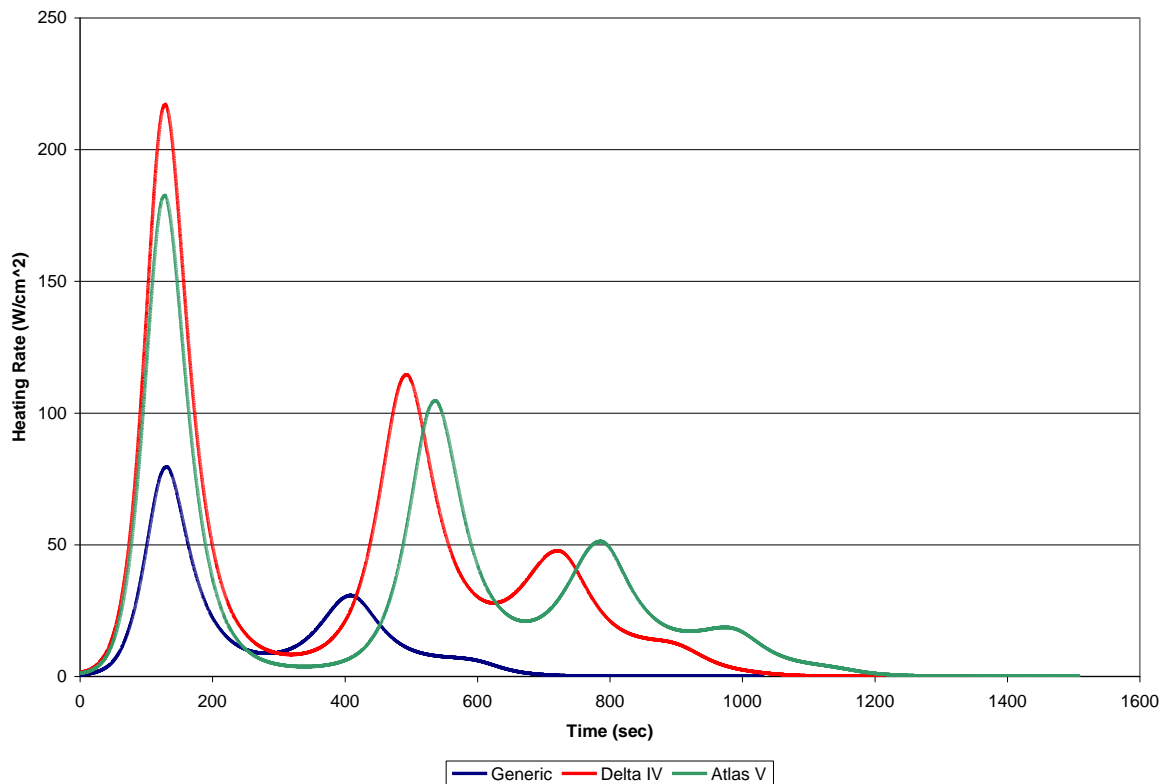


Figure 32 Stagnation Point Convective Heating Rate per Vehicle Configurations for Nominal Case (LEO Entry Velocity)

Section 4-4.3 Integrated Heating Loads

The integrated heat load encountered by the reentry vehicles was determined by integrating the heating rate data over the course of the trajectory. The heat load is the area under the heating rate curve, thus the integral of the heating rate or the total energy delivered per unit surface area. Referencing both figures 32 and 33, one can see that the generic configuration has much lower heating rates than the other two vehicles. This is due to the larger nose radii of the generic configuration and its function within the Chapman heating equation. The nominal LEO return trajectory was used for the heating analysis shown in both Figures 32 and 33.

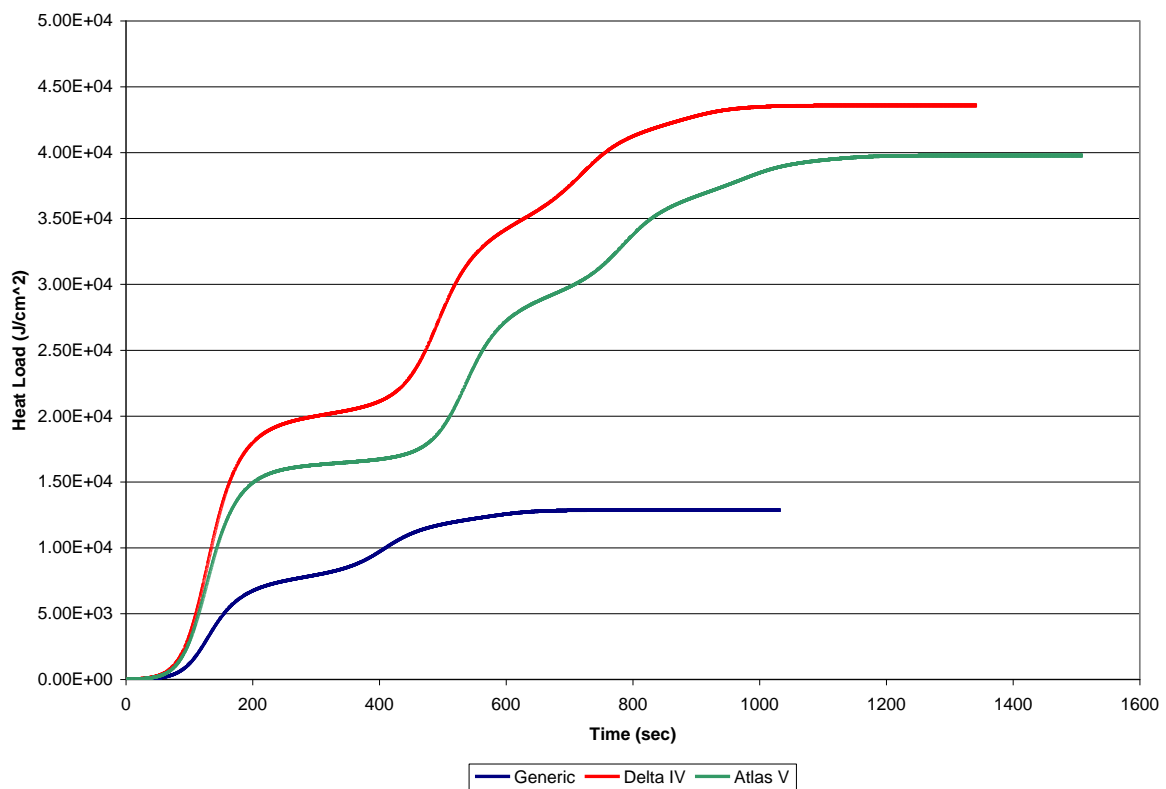


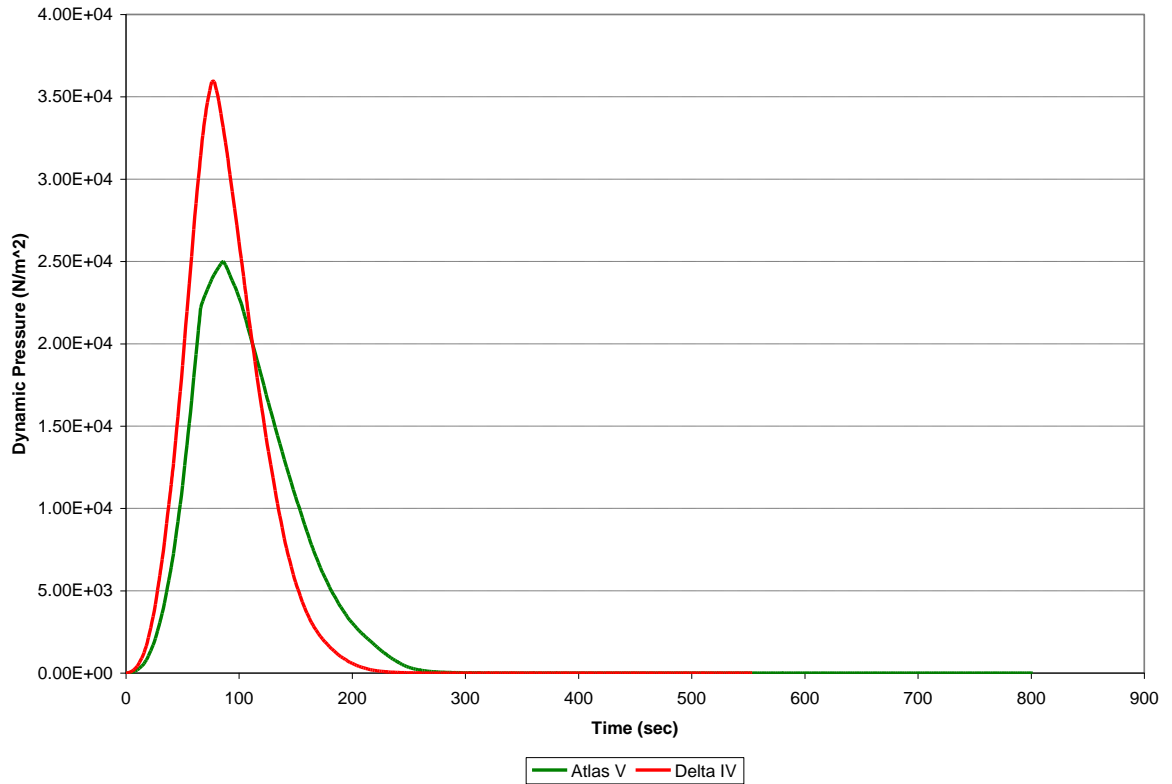
Figure 33 Integrated Heat Load per Vehicle Configurations for Nominal Case (LEO Entry Velocity)

Section 4-5 Dynamic Pressures

The dynamic pressure is a driver in the selection of the TPS for the resupply vehicle. The TPS has to be able to withstand the dynamic pressure the fairing (i.e. ellipsled) experiences during the ascent to orbit and later the dynamic pressure associated with reentry.

Section 4-5.1 Ascent

The maximum dynamic pressure, referred to as max q, is typically experienced during the early phase of flight for a launch vehicle. This is due to the atmospheric density being greater at lower altitudes on the Earth. The Payload Planner's Guide for the Delta IV [19] and the Mission Planner's Guide for the Atlas V [18] were used to provide vehicle configuration and performance data to create POST input decks. The input decks are for calculating the launch vehicle's detailed ascent performance data. The results from the POST analysis correlated the data found in the user guides. For the purposes of this study, only the Delta IV and Atlas V launch vehicle ascent profiles will be analyzed. Since the dynamic pressure for ascent is 37-58% greater than that for entry, it is the design driver for the fairing/ellipsled TPS selection.



*No data available for the Generic configuration since not an actual launch vehicle fairing shape.

Figure 34 Launch Vehicle's Dynamic Pressure Ascent Profiles [18,19]

Section 4-5.2 Reentry

The dynamic pressure from reentry is less than that from ascent. As seen previously with the heating analysis, the nominal trajectory data for a LEO entry was used in the following dynamic pressure profiles.

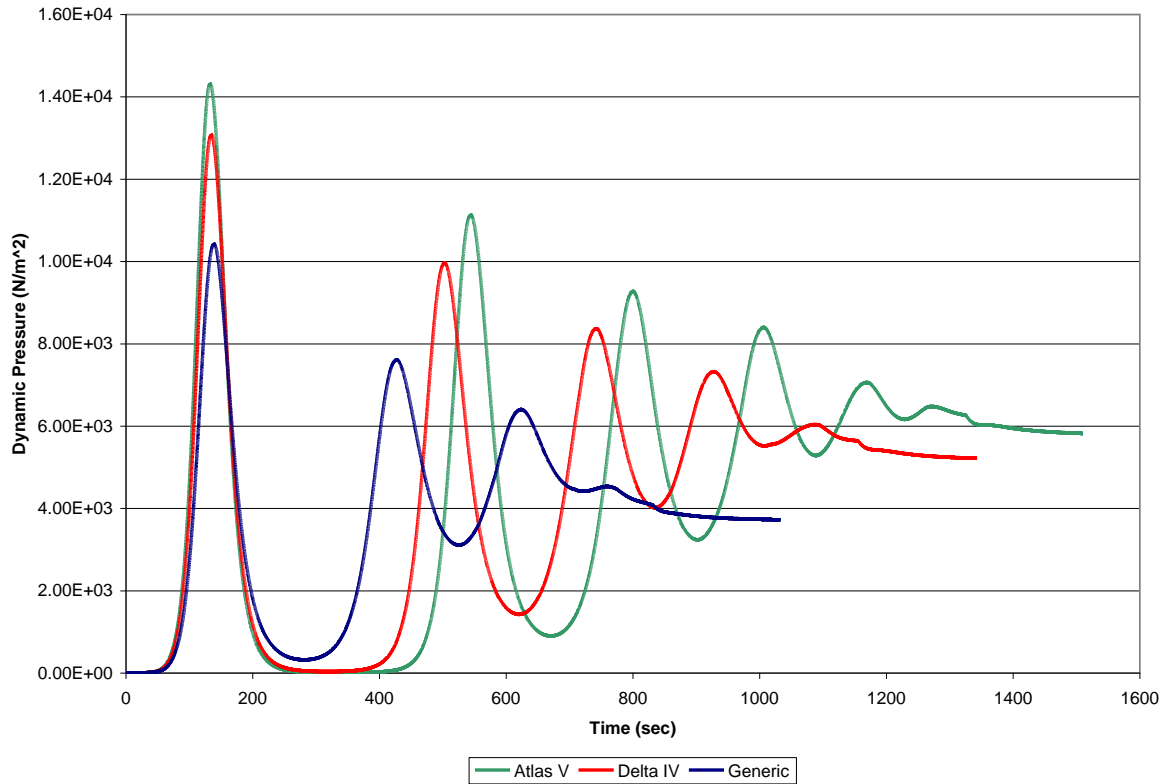


Figure 35 Dynamic Pressure during Reentry per Configurations for Nominal Case (LEO Entry Velocity)

Section 4-6 Deceleration Limit

The deceleration limit was based on the MPLM quasi-static load factors for the entry and landing phase of the space shuttle [31]. A 5 Earth-g constraint was used, which aligns with various studies performed on crewed ellipsoidal type design reference missions for Earth returns from Mars [5] as well as with Soviet experience with the Soyuz entry vehicle returning crews from extended-duration mission on Mir [34]. No limit is placed on duration of high-magnitude deceleration. Figure 36 shows the deceleration versus altitude profiles for the three vehicle configurations for a hypersonic direct entry.

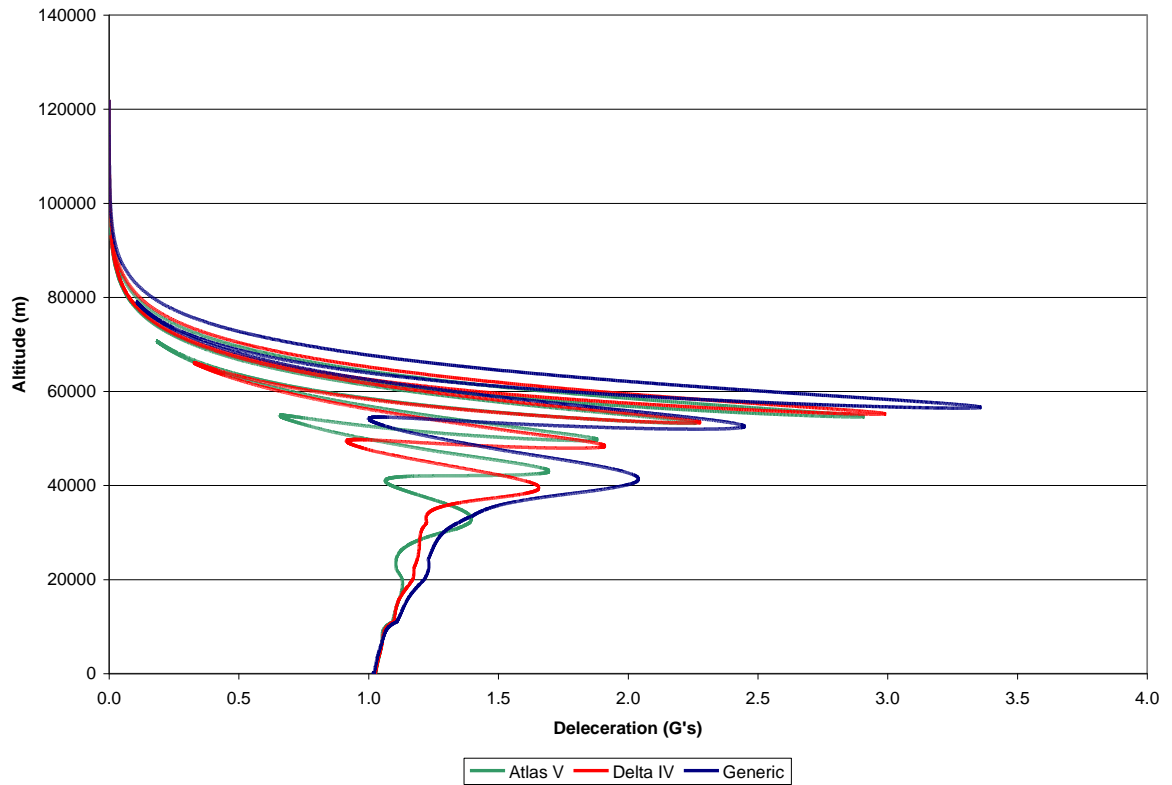


Figure 36 Deceleration vs Altitude per Vehicle Configuration for Nominal Case (LEO Entry Velocity)

Section 4-6.1 Ballistic Coefficient

In addition to factors like deceleration limits, other parameters may affect the width of the entry corridor. The parameter known as the ballistic coefficient is an example of this. The ballistic coefficient is defined in the following equation as:

$$\beta = \frac{m}{(C_d S_{ref})}$$

where: m = mass of vehicle (kg)
 C_d = coefficient of drag (unitless)
 S_{ref} = reference area of vehicle (m^2)

The relationship means that as ballistic coefficient goes up, deceleration goes down and vice versa. The ballistic coefficient reflects how far into the atmosphere a body must pass to decelerate a given amount. The ballistic coefficients, using the standard vehicle properties and aerodynamics, were calculated to be:

$$\beta_{Generic} = 362.3 \text{ kg/m}^2$$

$$\beta_{Delta IV} = 570.7 \text{ kg/m}^2$$

$$\beta_{Atlas V} = 682.5 \text{ kg/m}^2$$

The variation of the ballistic coefficients for the three configurations probably account for a great deal of the difference in performance as far as g-load, peak dynamic pressure, peak heating, etc. Reference appendix section A5 to see the nominal trajectories used to generate the various analysis figures.

CHAPTER 5

CONCLUSIONS AND RECOMMENDATIONS

Section 5-1 Conclusion

The analysis and research performed in this study helps verify the feasibility of the COTS² resupply vehicle concept. It was determined from the stability analysis that the MPLM could not be fully loaded for the ellipsled reentry vehicle to be able to maintain a desired trim alpha during reentry. Through analysis it was determined that only loading half the MPLM (opposite the docking side) with return cargo, would allow the reentry vehicle to be stable. Even with the pressurized module only half full, the COTS² vehicle still can return approximately 7,000 kg (4,000 kg pressurized & 2,500 kg unpressurized) cargo from the station.

The following table also identifies the advantages of the [COTS]² system to those of the current and future resupply vehicle systems for the ISS. This study identifies that the [COTS]² system has a lot more capabilities than the current and future systems under development.

Table 11 ISS Logistics Vehicle Delivery Capability [21-25]

	Progress M1 [21]	HTV [23]	ATV [22]	Dragon [24]	Cygnus [25]	COTS ²
Propellant (maximum)	1,950 kg	None	4,860 kg	None	None	*5,170 kg
Cargo, overall (maximum)	2,230 kg	6,000 kg	7,385 kg	6,000 kg	2,300 kg	11,500 kg
Cargo, pressurized (maximum)	1,800 kg dry cargo 6.6 m ³	6,000 kg 20m ³	5,500 kg dry cargo (TBD)	3,000 kg 7-10 m ³	2,300 kg 18.7 m ³	9,000 kg
Cargo, unpressurized (maximum)	0	1,500 kg	0	3,000 kg 14 m ³	2,300 kg 18.1 m ³	2,500 kg
Water (maximum)	300 kg	300 kg (TBD)	840 kg	(TBD)	(TBD)	200–400 kg
Gas (maximum)	40 kg	(TBD)	100 kg	(TBD)	(TBD)	30 kg
Reboost Control	Yes	No	Yes	No	No	Yes
Down Mass: Recoverable	None	None	None	3,000 kg	1,200 kg (Proposed)	7,000 kg
Down Mass: Non-recoverable	1,000 kg typical 1,600 kg max 6.6 m ³ max	6,000 kg 20 m ³	5,500 kg maximum dry cargo 840 kg max fluid 20.6 m ³ max	3,000 kg 14 m ³	2,300 kg 18.7 m ³	0 kg *All mass is recovered.
Maximum Number of Flights per year	7-12 flights total	2 flights	2 flights	(TBD)	2-8 flights	5-7 flights
Minimum Number of days between flights	30 days	180 days	180 days	5 months	(TBD)	60 -90 days MPLM depend
Maximum On-orbit docked duration	180 days	180 days (TBR)	180 days	2 years	(TBD)	14 days Based on MPLM only (TBR)

* Referring to the propellant in the ICM, which could be use to re-boost the ISS.

The author believes the [COTS]² resupply vehicle concept presented in this study could reduce cost and development time and offer a more robust system for resupplying the ISS. By utilizing already available COTS hardware, including some that have spaceflight heritage, the technical challenges of developing, building and testing a brand new design could be reduced. This vehicle system concept uses a majority of existing hardware, but in a different configuration than its initial design intent. By gaining a development head-start on the current ISS resupply competition, [COTS]² has the opportunity to set the standard by offering the only system with cargo return capability which is critical for the ISS maximize its capability as a world class international research facility.

Section 5-2 Recommendations for Future Work

The objective for future work would be to develop a higher fidelity design of the [COTS]² resupply vehicle concept by designing around the MPLM system requirements (i.e. ICDs and Specs) and evaluating against the specific EELV planner's guides to ensure the system meets requirements. Some specific areas of interest that need further development, design and analysis are as follows:

- Systems (subsystem integration and requirements verification)
- Mechanical (mass properties and system configuration)
- Structures (STS-to-EELV structure and mass optimization)
- Propulsion (reentry RCS sizing and performance analysis)

- Orbital mechanics (delta-V budget and performance analysis)
- Power systems (determine best power source to meet MPLM system requirements; solar, battery, fuel cell, etc.)
- Thermal controls (meet MPLM system & material requirements)
- Environmental systems (meet MPLM system requirements)

LIST OF REFERENCES

LIST OF REFERENCES

- 1) Brauer, G.L., D.E. Cornick, D.W. Olson, F.M. Peterson, and R. Stevenson, "Program to Optimize Simulated Trajectories (POST) Formulation Manual," Martin Marietta, Denver, CO September 1990
- 2) Powell, R.W., S.A. Strepe, P.N. Desai, and R.D. Braun, "Program to Optimize Simulated Trajectories (POST) Utilization Manual," NASA Langley Research Center, Hampton, VA, September 1996
- 3) Anderson, John D., Jr., *Hypersonic and High Temperature Gas Dynamics*. McGraw-Hill, New York, 1989.
- 4) Bate, Roger R., Donald D. Mueller, and Jerry E. White, *Fundamental of Astrodynamics*. Dover Publications, New York, 1971.
- 5) Schneider, W. and Simonsen, L., "Mars TransHab Aerobrake Design Study Team," taken from week long study conducted by various NASA engineers, November 21, 1997
- 6) Regan, Frank J. and Anandkrishnan, *Dynamics of Atmospheric Re-Entry*, AIAA Educational Series, Washington D.C., 1993
- 7) Hirschel, E.H., *Basics of Aerothermodynamics*, AIAA Educational Series, Washington D.C., 1991
- 8) Putnam, Z.R., Braun, R.D., Rohrschneider, R.R. and Dec, J.A., "Entry System Options for Human Return from the Moon and Mars", *Journal of Spacecraft and Rockets*, Vol. 44, No. 1, Jan-Feb 2007
- 9) Taylor, A.P. and Delurgio, P.R., "An Overview of the Landing System for the K-1 Launch Vehicle, Parachutes and Airbags", AIAA paper, 97-1515
- 10) University of Tennessee Senior Design Team, "An Investigation of Crew Return Vehicle Configurations for a Manned Mars Mission", taken from the UTK Senior AE Design Class Final Team Report, May, 1998
- 11) Blake, William B., "MISSILE DATCOM User's Manual – 1997 FORTRAN 90 Revision", Air Force Research Laboratory, Wright-Patterson Air Force Base, Ohio, February, 1998
- 12) Orloff, R.W. and Harland, D.M., *Apollo, The Definitive Sourcebook*, Springer-Praxis, 2006
- 13) Ewing, E.G., Bixby, H.W., Knacke, T.W., "Recovery Systems Design Guide", Irvin Industries Incorporated, Gardena, CA, December 1978

- 14) Sellers, J.J., *Understanding Space An Introduction to Astronautics*, Space Technology Sciences, McGraw-Hill, 2000, 1994
- 15) Hirschel, E. H., Weiland, C., *Selected Aerothermodynamics Design Problems of Hypersonic Flight Vehicle*, AIAA Educational Series, Washington D.C., 2009
- 16) Gallais, Patrick., *Atmospheric Re-Entry Vehicle Mechanics*, AIAA Educational Series, Washington D.C., 2007
- 17) NASA, Space Shuttle with MPLM,
http://www.nasa.gov/mission_pages/station/structure/elements/mplm.html
- 18) Lockheed Martin Payload Planner's Guide
- 19) Boeing Company Payload Planner's Guide
- 20) K-1 Vehicle Payload User's Guide: March 2007 Vol. 1
- 21) Russia, Progress Spacecraft, http://en.wikipedia.org/wiki/Progress_spacecraft
- 22) ESA, ATV, http://en.wikipedia.org/wiki/Automated_Transfer_Vehicle
- 23) JAXA, HTV, http://en.wikipedia.org/wiki/H-II_Transfer_Vehicle
- 24) SpaceX, Dragon, <http://www.spacex.com/dragon.php>
- 25) Orbital Sciences Corp, Cygnus,
http://www.orbital.com/NewsInfo/Publications/Cygnus_fact.pdf
- 26) RpK –Rocketplane Kistler, <http://www.rocketplanekistler.com/>
- 27) Airborne Systems (formally Irving Aerospace), www.airborne-sys.com/
- 28) Naval Research Laboratory (NRL) white paper, “NRL’s Solution for the De-orbit of the Hubble Space Telescope”, Nov. 25, 2003
- 29) Towsley, R., Chappie, S., Kelm, B., & Wojnar, R., “ICM EELV Launch Feasibility Study, NRL code 8200, Feb. 5, 2003
- 30) Lamit, L.G., *Introduction to Pro/ENGINEER Wildfire 2.0*, Schroff Development Corp. (SDC) Publications, 2004
- 31) Shuttle Orbiter/CargoStandard Interfaces, ICD 2-19001

- 32) NASA Ames Thermal Protection Materials and System Branch, TPSX Database Internet
Site: <http://asm.arc.nasa.gov>
- 33) Parker, P., “Apollo Command Module Earth Entry”
- 34) Hall, R.D., Shayler, D.J., *SOYUZ: A Universal Spacecraft*, Springer Praxis Publishing,
2003

APPENDIX

c gravity model

c

```
npc(16)=0, / oblate planet
j2 = 1.0826393e-3,
j3 = -2.53215307e-6,
j4 = -1.61098761e-6,
j5 = -2.35785649e-7,
j6 = 5.43169846e-7,
j7 = -3.32376398e-7,
j8 = -1.77210399e-7,

omega=7.29212e-05, / rotation rate
mu=3.986009e+14, / gravitational constant
re=6378141.991, / equatorial radius
rp=6356757.132, / polar radius
```

c

c vehicle geometry parameters

c

```
wgtsg=181485, / force, N=mass(18500)*Earthg(9.81),
sref=22.89, / reference area (m2)
rn=2.7, / nose radius (m)
lref=14.0, / reference length (m)
```

c

c guidance initialization

c

```
iguid(1)=0, / aero angles: alpha, beta, bank
iguid(2)=0, / same steering opt all angles
iguid(3)=1, / const poly term = input value
alppc(1)=52.0, / initial alpha
betpc(1)=0.0, / initial beta
bnkpc(1)=0.0, / initial bank (0=undershoot & 180=overshoot)
```

c

\$

I\$tblmlt \$

I\$tab

```
table='denkt',0,1.0,$
```

I\$tab table='cdt',1,'mach',7,1,1,1,

```
1.5, 1.9357,
```

```
3.0, 2.1707,
```

```
5.0, 2.2113,
```

```
10.0, 2.2257,
```

```
15.0, 2.2283,
```

```
20.0, 2.2292,
```

```
25.0, 2.2295,
```

\$end

```
$
I$tblmt $
I$tab
  table='denkt',0,1.0,$
I$tab table='clt',1,'mach',7,1,1,1,
  1.5, 0.9333,
  3.0, 1.1258,
  5.0, 1.1896,
  10.0, 1.2209,
  15.0, 1.2269,
  20.0, 1.229,
  25.0, 1.23,
endphs=1,
$
I$gendat
event=100,citr='gdalt',value=0.0,
endphs=1,endprb=1,endjob=1,
$
```

The following is an input deck set up so that the user must find the **overshoot** boundary “manually”. That is, the user must (manually – by hand) alter the entry angle until the shallowest angle is found that allows the entry vehicle to not skip out. (“c” or “/” Indicates comments that POST does not actually use)

```

cccccccccccccccccccccccccccccccccccc
c   Chad Davis                c
c   Generic EllipSled         c
c   Overshoot Boundary        c
cccccccccccccccccccccccccccccccccccc
I$search
    srchm=0,                    / no targeting
    ioflag=3,                   / SI units
$
I$gendat
    title='Earth Return from Orbit',
    prnt(1)= 'time','veli','gdalt','asmg','gammal','dens',
              'crrng','dwnrng',
    event=1,                    / current event number
    fesn=100,                   / final event number
    npc(1)=3,                   / Keplerian conic calc flag
    npc(2)=1,                   / Runge Kutta integration
    dt=1.0,                    / integration step size
    pinc=1,                     / print interval
    prnca=1,                    / ascii plotting interval
    prnc=1,                     / binary plotting interval
c
c state vector
c
    npc(3)=2,                   / velocity spherical coordinates
    gammal=-0.15,              / initial flight path angle
    azveli=90.0,               / inertial azimuth angle
    veli=7800.0,               / inertial velocity
    npc(4)=2,                   / position spherical coordinates
    gdalt=124900.0,            / initial geodetic altitude
    long=0.0,                  / initial longitude
    gclat=0.0,                 / initial geocentric latitude
    npc(12)=1,                 / calculate downrange, crossrange
c
c atmospheric parameters
c
    npc(5)=5,                   / 1976 US stand atm model
    npc(8)=2,                   / aero coefficient flag

```

```

c
c gravity model
c
  npc(16)=0,           / oblate planet
    j2 = 1.0826393e-3,
    j3 = -2.53215307e-6,
    j4 = -1.61098761e-6,
    j5 = -2.35785649e-7,
    j6 = 5.43169846e-7,
    j7 = -3.32376398e-7,
    j8 = -1.77210399e-7,

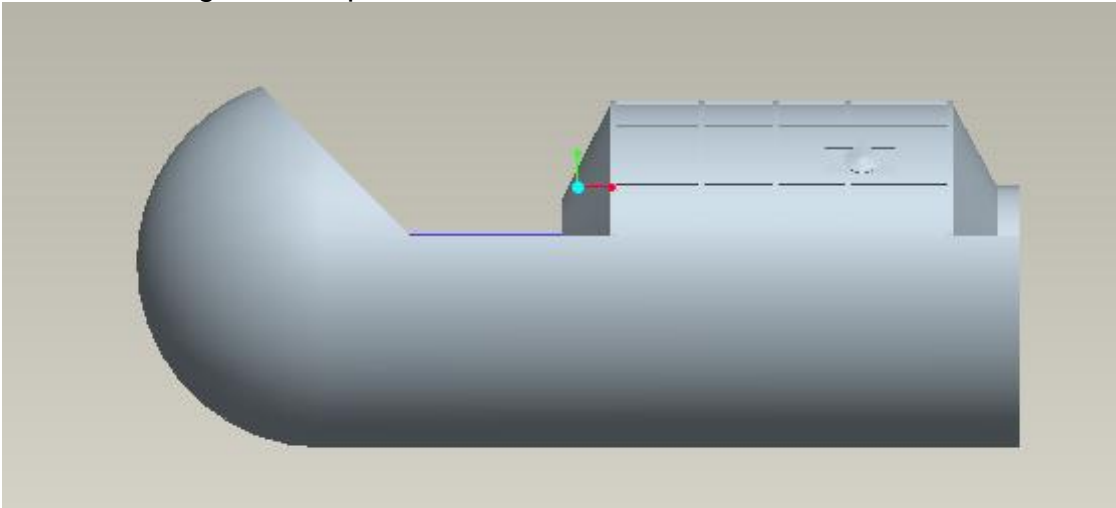
    omega=7.29212e-05,      / rotation rate
    mu=3.986009e+14,       / gravitational constant
    re=6378141.991,       / equatorial radius
    rp=6356757.132,       / polar radius
c
c vehicle geometry parameters
c
  wgtsg=181485,           / force, N=mass(18500)*Earthg(9.81),
  sref=22.89,            / reference area (m2)
  rn=2.7,                / nose radius (m)
  lref=14.0,             / reference length (m)
c
c guidance initialization
c
  iguid(1)=0,            / aero angles: alpha, beta, bank
  iguid(2)=0,            / same steering opt all angles
  iguid(3)=1,            / const poly term = input value
  alppc(1)=52.0,         / initial alpha
  betpc(1)=0.0,          / initial beta
  bnkpc(1)=180.0,        / initial bank (0=undershoot & 180=overshoot)
c
$
I$tblmt $
I$tab
  table='denkt',0,1.0,$
I$tab table='cdt',1,'mach',7,1,1,1,
  1.5, 1.9357,
  3.0, 2.1707,
  5.0, 2.2113,
  10.0, 2.2257,
  15.0, 2.2283,
  20.0, 2.2292,
  25.0, 2.2295,

```

```
$end
$
I$tblmt $
I$tab
  table='denkt',0,1.0,$
I$tab table='clt',1,'mach',7,1,1,1,
  1.5, 0.9333,
  3.0, 1.1258,
  5.0, 1.1896,
  10.0, 1.2209,
  15.0, 1.2269,
  20.0, 1.229,
  25.0, 1.23,
endphs=1,
$
I$gendat
event=100,citr='gdalt',value=0.0,
endphs=1,endprb=1,endjob=1,
$
```

A2 - Missile DatCom input decks

Generic Configuration input deck



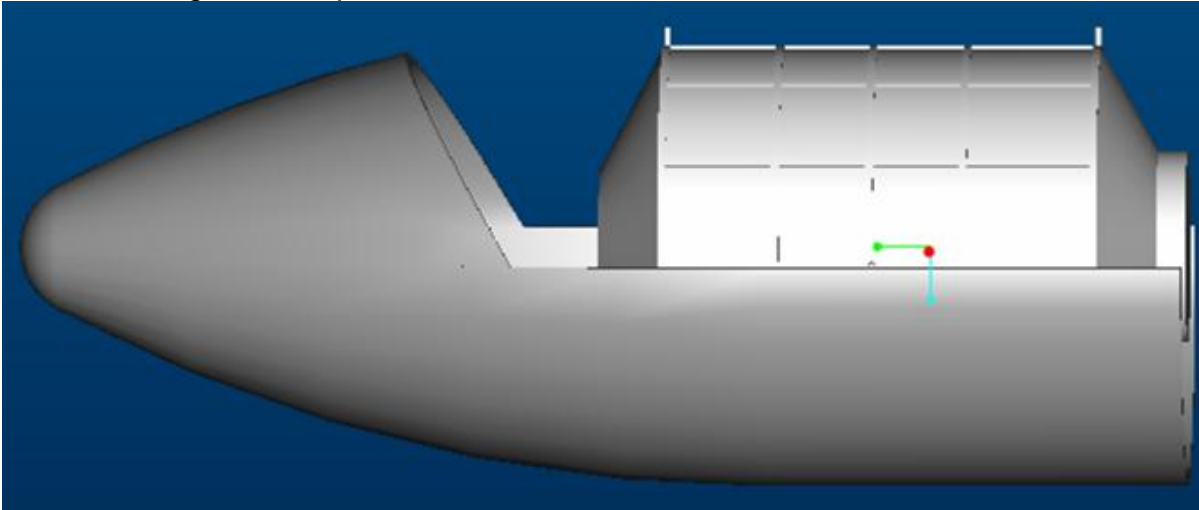
```
CASEID GENERIC
$FLTCON  NALPHA   = 13.0,
          ALPHA   = 0.0,  5.0, 10.0, 15.0, 20.0, 25.0, 30.0, 35.0,
          ALPHA(9) = 40.0, 45.0, 50.0, 55.0, 60.0,
          NMACH   = 7.0,
          MACH    = 1.5, 3.0, 5.0, 10.0, 15.0,
          MACH(6) = 20.0, 25.0,
          ALT     = 0.0, 0.0, 0.0, 0.0, 0.0,
          ALT(6)  = 0.0, 0.0,

$END
$REFQ   XCG      = 335.83,
        ZCG      = -35.0,
        LREF     = 212.6,
        SREF     = 35499.02,

$END
$AXIBOD X0       = 0.0,
        BNOSE    = 106.3,
        LNOSE    = 105.3,
        DNOSE    = 212.6,
        LCENTR   = 445.881,
        DCENTR   = 212.6,
        DEXIT    = 0.0,

$END
DIM IN
DERIV RAD
PLOT
HYPER
PRESSURES
PRINT GEOM BODY
NEXT CASE
```

Atlas V Configuration input deck



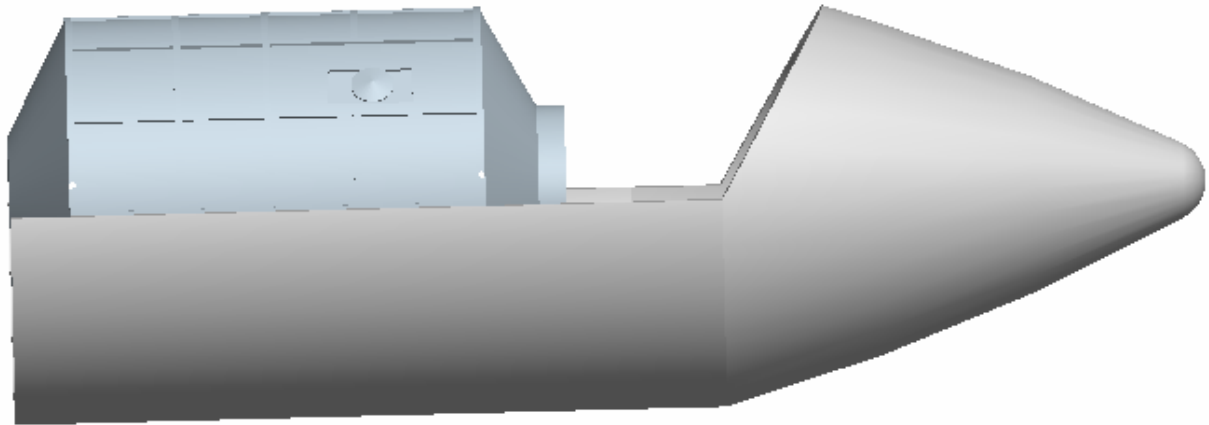
```
CASEID ATLAS V
$FLTCON  NALPHA  = 13.0,
          ALPHA  = 0.0,  5.0, 10.0, 15.0, 20.0, 25.0, 30.0, 35.0,
          ALPHA(9) = 40.0, 45.0, 50.0, 55.0, 60.0,
          NMACH  = 7.0,
          MACH   = 1.5, 3.0, 5.0, 10.0, 15.0,
          MACH(6) = 20.0, 25.0,
          ALT    = 0.0, 0.0, 0.0, 0.0, 0.0,
          ALT(6) = 0.0, 0.0,

$END
$REFQ   XCG      = 335.83,
        ZCG      = -35.0,
        LREF     = 213.602,
        SREF     = 35834.43,

$END
$AXIBOD X0       = 0.0,
        BNOSE    = 31.496,
        LNOSE    = 335.748,
        DNOSE    = 213.602,
        LCENTR   = 215.433,
        DCENTR   = 213.602,
        DEXIT    = 0.0,

$END
DIM IN
DERIV RAD
PLOT
HYPER
PRESSURES
PRINT GEOM BODY
NEXT CASE
```


Delta IV Configuration input deck



```
CASEID DELTA IV
$FLTCON  NALPHA    = 13.0,
          ALPHA    = 0.0,  5.0, 10.0, 15.0, 20.0, 25.0, 30.0, 35.0,
          ALPHA(9) = 40.0, 45.0, 50.0, 55.0, 60.0,
          NMACH    = 7.0,
          MACH     = 1.5, 3.0, 5.0, 10.0, 15.0,
          MACH(6)  = 20.0, 25.0,
          ALT      = 0.0, 0.0, 0.0, 0.0, 0.0,
          ALT(6)   = 0.0, 0.0,

$END
$REFQ    XCG      = 335.83,
          ZCG      = -35.0,
          LREF     = 202.008,
          SREF     = 32049.93,

$END
$AXIBOD  X0       = 0.0,
          BNOSE    = 19.685,
          LNOSE    = 250.084,
          DNOSE    = 202.008,
          LCENTR   = 301.097,
          DCENTR   = 202.008,
          DEXIT    = 0.0,

$END
DIM IN
DERIV RAD
PLOT
HYPER
PRESSURES
PRINT GEOM BODY
NEXT CASE
```

A3 - Aerodynamic data from Missile DatCom Generic Configuration

M	AoA	CN	Cm @ MRC	CA	CL	CD	Cm @ CG
1.5	0	0	0.1549	0.941	0	0.941	0.1549
1.5	5	0.0874	0.227	0.9374	0.0053	0.9415	0.19997013
1.5	10	0.2143	0.2981	0.9268	0.0501	0.9499	0.23182425
1.5	15	0.3776	0.3666	0.9093	0.1294	0.976	0.24982107
1.5	20	0.5732	0.4315	0.8852	0.2359	1.0278	0.2542286
1.5	25	0.7958	0.4913	0.8548	0.36	1.1111	0.24518594
1.5	30	1.0393	0.545	0.8188	0.4907	1.2288	0.22357961
1.5	35	1.2971	0.5819	0.7187	0.6503	1.3327	0.18075078
1.5	40	1.5619	0.6182	0.659	0.7729	1.5087	0.13515708
1.5	45	1.8263	0.6459	0.5954	0.8703	1.7124	0.08108709
1.5	50	2.0828	0.6647	0.5294	0.9333	1.9357	0.0205603
1.5	55	2.3241	0.6745	0.462	0.9546	2.1688	-0.0442656
1.5	60	2.5434	0.6752	0.3946	0.93	2.4	-0.1113877
3	0	0	0.1582	0.961	0	0.961	0.1582
3	5	0.1001	0.2409	0.9574	0.0163	0.9625	0.20994245
3	10	0.2455	0.3225	0.9466	0.0774	0.9749	0.24657514
3	15	0.4327	0.4015	0.9289	0.1776	1.0092	0.2676805
3	20	0.6568	0.4763	0.9045	0.3078	1.0746	0.27317394
3	25	0.9119	0.5456	0.8739	0.4571	1.1774	0.26358013
3	30	1.1909	0.6079	0.8376	0.6126	1.3208	0.23959485
3	35	1.4863	0.6511	0.7286	0.7996	1.4493	0.19143761
3	40	1.7897	0.6938	0.6665	0.9425	1.661	0.14030623
3	45	2.0926	0.7267	0.6008	1.0549	1.9045	0.07952949
3	50	2.3865	0.7496	0.5328	1.1258	2.1707	0.01153615
3	55	2.6631	0.7621	0.4639	1.1474	2.4475	-0.0615069
3	60	2.9143	0.7644	0.3953	1.1148	2.7216	-0.1368946
5	0	0	0.1528	0.9281	0	0.9281	0.1528
5	5	0.1031	0.238	0.9247	0.0222	0.9301	0.20611465
5	10	0.2529	0.3223	0.9143	0.0903	0.9444	0.24408657
5	15	0.4458	0.4038	0.8973	0.1984	0.9821	0.26592912
5	20	0.6767	0.4812	0.8739	0.337	1.0526	0.27191954
5	25	0.9394	0.5529	0.8445	0.4945	1.1624	0.26237531
5	30	1.2269	0.6175	0.8097	0.6577	1.3147	0.23806127
5	35	1.5312	0.6625	0.7005	0.8525	1.4521	0.18895155
5	40	1.8438	0.7071	0.64	1.001	1.6754	0.13687493
5	45	2.1559	0.7416	0.576	1.1171	1.9317	0.07485294
5	50	2.4586	0.7658	0.5101	1.1896	2.2113	0.00543805
5	55	2.7435	0.7794	0.4434	1.2104	2.5017	-0.0690719
5	60	3.0024	0.7825	0.3773	1.1744	2.7888	-0.1460409
10	0	0	0.1491	0.9057	0	0.9057	0.1491
10	5	0.1044	0.2355	0.9024	0.0254	0.908	0.20321261
10	10	0.2562	0.3208	0.8923	0.0973	0.9232	0.24156599
10	15	0.4514	0.4035	0.8758	0.2094	0.9628	0.26389722
10	20	0.6852	0.482	0.8531	0.3521	1.036	0.27009078

M	AoA	CN	Cm @ MRC	CA	CL	CD	Cm @ CG
10	25	0.9513	0.5548	0.8246	0.5137	1.1494	0.26059504
10	30	1.2424	0.6206	0.7908	0.6806	1.3061	0.23636764
10	35	1.5506	0.6664	0.6819	0.879	1.448	0.18685179
10	40	1.8671	0.7118	0.6226	1.0301	1.6771	0.13436903
10	45	2.1831	0.7472	0.5599	1.1478	1.9397	0.0720409
10	50	2.4898	0.772	0.4954	1.2209	2.2257	0.00198895
10	55	2.7783	0.7862	0.4303	1.241	2.5227	-0.0730344
10	60	3.0404	0.7898	0.3659	1.2033	2.8161	-0.150493
15	0	0	0.1483	0.901	0	0.901	0.1483
15	5	0.1047	0.2349	0.8977	0.026	0.9034	0.20251983
15	10	0.2567	0.3205	0.8877	0.0987	0.9188	0.24111136
15	15	0.4525	0.4034	0.8713	0.2116	0.9587	0.26345703
15	20	0.6868	0.4821	0.8487	0.3551	1.0325	0.26969595
15	25	0.9535	0.5551	0.8204	0.5175	1.1466	0.26021465
15	30	1.2453	0.6211	0.7869	0.685	1.3042	0.23597077
15	35	1.5542	0.6671	0.6781	0.8841	1.447	0.18643843
15	40	1.8715	0.7126	0.619	1.0357	1.6772	0.13380825
15	45	2.1882	0.7482	0.5567	1.1537	1.941	0.07146364
15	50	2.4956	0.7732	0.4925	1.2269	2.2283	0.0013952
15	55	2.7848	0.7875	0.4277	1.2469	2.5265	-0.0737446
15	60	3.0475	0.7911	0.3637	1.2088	2.8211	-0.1513888
20	0	0	0.148	0.8993	0	0.8993	0.148
20	5	0.1048	0.2347	0.8959	0.0263	0.9016	0.2022889
20	10	0.257	0.3203	0.886	0.0992	0.9171	0.24081858
20	15	0.4529	0.4033	0.8696	0.2124	0.9572	0.26323333
20	20	0.6874	0.4821	0.8471	0.3562	1.0311	0.2695104
20	25	0.9543	0.5552	0.8189	0.5188	1.1455	0.26006724
20	30	1.2464	0.6212	0.7854	0.6867	1.3034	0.23573057
20	35	1.5555	0.6673	0.6767	0.886	1.4465	0.18623638
20	40	1.873	0.7129	0.6177	1.0377	1.6771	0.13364436
20	45	2.19	0.7485	0.5555	1.1558	1.9414	0.07120696
20	50	2.4976	0.7735	0.4914	1.229	2.2292	0.00107667
20	55	2.787	0.7879	0.4268	1.249	2.5278	-0.074025
20	60	3.05	0.7916	0.3629	1.2107	2.8228	-0.151662
25	0	0	0.1479	0.8984	0	0.8984	0.1479
25	5	0.1048	0.2346	0.895	0.0264	0.9008	0.2021889
25	10	0.2571	0.3202	0.8851	0.0995	0.9163	0.24068765
25	15	0.453	0.4033	0.8688	0.2127	0.9564	0.2632024
25	20	0.6876	0.4821	0.8463	0.3567	1.0304	0.26944854
25	25	0.9547	0.5553	0.8181	0.5195	1.1449	0.26004353
25	30	1.2468	0.6213	0.7847	0.6874	1.303	0.23570687
25	35	1.556	0.6674	0.676	0.8869	1.4463	0.18618175
25	40	1.8737	0.7131	0.6171	1.0387	1.6771	0.13362787
25	45	2.1909	0.7486	0.5549	1.1568	1.9415	0.07102862
25	50	2.4986	0.7737	0.4909	1.23	2.2295	0.0009674
25	55	2.7881	0.7881	0.4263	1.25	2.5284	-0.0741652
25	60	3.0512	0.7918	0.3625	1.2117	2.8236	-0.1518331

Atlas V Configuration

M	AoA	CN	Cm @ MRC	CA	CL	CD	Cm @ CG
1.5	0	0	0.0627	0.3827	0	0.3827	0.0627
1.5	5	0.1272	0.1511	0.3855	0.0931	0.3952	0.11194587
1.5	10	0.2752	0.2283	0.3938	0.2027	0.4356	0.14358918
1.5	15	0.4443	0.2933	0.4065	0.324	0.5076	0.15653759
1.5	20	0.6335	0.3461	0.4223	0.4509	0.6135	0.1510989
1.5	25	0.8406	0.3878	0.4394	0.5762	0.7535	0.12905032
1.5	30	1.0623	0.4195	0.4562	0.6919	0.9262	0.09250763
1.5	35	1.2934	0.4372	0.441	0.8066	1.1031	0.03907147
1.5	40	1.5277	0.4486	0.4406	0.8871	1.3195	-0.0216497
1.5	45	1.7583	0.4502	0.4338	0.9365	1.55	-0.0910319
1.5	50	1.9783	0.4422	0.4201	0.9498	1.7855	-0.1667513
1.5	55	2.1812	0.4247	0.3992	0.9241	2.0157	-0.2467071
1.5	60	2.361	0.3983	0.3709	0.8593	2.2302	-0.3284523
3	0	0	0.0528	0.3224	0	0.3224	0.0528
3	5	0.1457	0.1542	0.3261	0.1167	0.3376	0.10935129
3	10	0.3154	0.2429	0.3369	0.2521	0.3866	0.145815
3	15	0.5091	0.3177	0.3538	0.4002	0.4735	0.16099114
3	20	0.7259	0.3788	0.3751	0.5538	0.6007	0.15535675
3	25	0.9632	0.4272	0.3988	0.7044	0.7685	0.13071214
3	30	1.2172	0.4644	0.4228	0.8427	0.9748	0.08972701
3	35	1.4821	0.4855	0.4111	0.9782	1.1868	0.02928669
3	40	1.7505	0.4996	0.4169	1.073	1.4446	-0.039231
3	45	2.0147	0.5026	0.4162	1.1303	1.7189	-0.1175558
3	50	2.2668	0.4947	0.4081	1.1444	1.9988	-0.2030561
3	55	2.4994	0.476	0.3923	1.1122	2.2724	-0.293354
3	60	2.7053	0.4472	0.3685	1.0336	2.5271	-0.3855332
5	0	0	0.0444	0.2708	0	0.2708	0.0444
5	5	0.1501	0.1489	0.2749	0.1256	0.287	0.1026969
5	10	0.3249	0.2403	0.2868	0.2702	0.3389	0.14029075
5	15	0.5245	0.3176	0.3054	0.4276	0.4307	0.15615079
5	20	0.7478	0.3808	0.329	0.5902	0.5649	0.15061559
5	25	0.9923	0.4311	0.3556	0.7491	0.7417	0.12565471
5	30	1.254	0.4698	0.3829	0.8945	0.9586	0.0837994
5	35	1.5269	0.492	0.3738	1.0363	1.182	0.02199656
5	40	1.8034	0.5071	0.3832	1.1352	1.4528	-0.0480144
5	45	2.0756	0.5109	0.3862	1.1946	1.7407	-0.1280018
5	50	2.3353	0.5033	0.3819	1.2086	2.0344	-0.2155415
5	55	2.5749	0.4848	0.3698	1.174	2.3214	-0.3077941
5	60	2.7871	0.4558	0.3498	1.0906	2.5886	-0.4021125
10	0	0	0.0394	0.2407	0	0.2407	0.0394
10	5	0.152	0.1453	0.2449	0.1301	0.2573	0.09851205
10	10	0.329	0.238	0.2574	0.2793	0.3106	0.13672871
10	15	0.5311	0.3163	0.2769	0.4414	0.4049	0.1528192
10	20	0.7573	0.3805	0.3018	0.6084	0.5426	0.14739134
10	25	1.0049	0.4316	0.3299	0.7713	0.7237	0.12227623

M	AoA	CN	Cm @ MRC	CA	CL	CD	Cm @ CG
10	30	1.2699	0.471	0.3591	0.9202	0.9459	0.08010513
10	35	1.5462	0.4938	0.3515	1.065	1.1748	0.01785572
10	40	1.8262	0.5094	0.3629	1.1657	1.4519	-0.0527326
10	45	2.1019	0.5135	0.3679	1.2261	1.7464	-0.1334973
10	50	2.3649	0.5063	0.3658	1.2399	2.0468	-0.2216528
10	55	2.6075	0.4879	0.356	1.204	2.3401	-0.3147288
10	60	2.8224	0.4589	0.3382	1.1183	2.6134	-0.4098784
15	0	0	0.0384	0.2346	0	0.2346	0.0384
15	5	0.1524	0.1445	0.2389	0.131	0.2513	0.09758892
15	10	0.3298	0.2375	0.2515	0.2811	0.3049	0.13598246
15	15	0.5324	0.316	0.2712	0.4441	0.3997	0.15211904
15	20	0.7591	0.3804	0.2963	0.6119	0.5381	0.14673728
15	25	1.0073	0.4316	0.3248	0.7756	0.72	0.12153748
15	30	1.2728	0.4712	0.3543	0.9252	0.9432	0.07941247
15	35	1.5498	0.4941	0.347	1.0705	1.1732	0.01704758
15	40	1.8305	0.5098	0.3588	1.1716	1.4515	-0.0536562
15	45	2.1068	0.514	0.3643	1.2321	1.7473	-0.1345056
15	50	2.3704	0.5068	0.3627	1.2459	2.049	-0.2228458
15	55	2.6136	0.4884	0.3533	1.2097	2.3436	-0.3161065
15	60	2.829	0.4595	0.3359	1.1236	2.6179	-0.41131
20	0	0	0.0381	0.2324	0	0.2324	0.0381
20	5	0.1525	0.1443	0.2367	0.1313	0.2491	0.09735814
20	10	0.3301	0.2373	0.2493	0.2818	0.3028	0.13569011
20	15	0.5328	0.3159	0.2691	0.445	0.3978	0.15189592
20	20	0.7597	0.3803	0.2943	0.6132	0.5364	0.14645259
20	25	1.0081	0.4316	0.3229	0.7772	0.7187	0.12129122
20	30	1.2739	0.4712	0.3525	0.9269	0.9422	0.07907387
20	35	1.5511	0.4942	0.3454	1.0724	1.1726	0.01674742
20	40	1.832	0.5099	0.3574	1.1737	1.4513	-0.0540179
20	45	2.1085	0.5142	0.363	1.2342	1.7476	-0.1348289
20	50	2.3724	0.507	0.3615	1.248	2.0497	-0.2232614
20	55	2.6157	0.4886	0.3523	1.2117	2.3447	-0.3165529
20	60	2.8313	0.4597	0.3351	1.1254	2.6195	-0.4118179
25	0	0	0.0379	0.2313	0	0.2313	0.0379
25	5	0.1526	0.1441	0.2356	0.1314	0.248	0.09712736
25	10	0.3302	0.2372	0.2483	0.2821	0.3018	0.13555933
25	15	0.533	0.3159	0.2681	0.4455	0.3969	0.15183435
25	20	0.76	0.3803	0.2933	0.6138	0.5356	0.14636024
25	25	1.0085	0.4316	0.322	0.7779	0.718	0.1211681
25	30	1.2744	0.4712	0.3517	0.9278	0.9417	0.07891997
25	35	1.5516	0.4942	0.3446	1.0734	1.1723	0.01659352
25	40	1.8327	0.51	0.3566	1.1747	1.4512	-0.0541334
25	45	2.1093	0.5142	0.3624	1.2353	1.7477	-0.1350752
25	50	2.3733	0.507	0.3609	1.249	2.05	-0.2235385
25	55	2.6167	0.4887	0.3518	1.2127	2.3453	-0.3167607
25	60	2.8324	0.4598	0.3347	1.1263	2.6203	-0.4120565

Delta IV Configuration

M	AoA	CN	Cm @ MRC	CA	CL	CD	Cm @ CG
1.5	0	0	0.0784	0.4523	0	0.4523	0.0784
1.5	5	0.1257	0.1827	0.4544	0.0856	0.4636	0.14178689
1.5	10	0.28	0.2765	0.4604	0.1958	0.502	0.185365
1.5	15	0.4609	0.3586	0.4697	0.3236	0.573	0.20858527
1.5	20	0.6657	0.4282	0.4814	0.4609	0.6801	0.21152653
1.5	25	0.8905	0.4851	0.4943	0.5982	0.8243	0.19525814
1.5	30	1.1308	0.5293	0.5069	0.7259	1.0044	0.16124477
1.5	35	1.381	0.5555	0.4834	0.854	1.1881	0.10600914
1.5	40	1.635	0.5736	0.4779	0.9453	1.4171	0.04143667
1.5	45	1.8859	0.58	0.4658	1.0042	1.6629	-0.0338268
1.5	50	2.1266	0.575	0.4465	1.025	1.9161	-0.1171704
1.5	55	2.35	0.5589	0.4197	1.0041	2.1658	-0.2059831
1.5	60	2.5495	0.5321	0.3856	0.9408	2.4007	-0.2977168
3	0	0	0.0696	0.4016	0	0.4016	0.0696
3	5	0.1441	0.1892	0.4044	0.1083	0.4154	0.14229802
3	10	0.3208	0.297	0.4127	0.2443	0.4621	0.19258532
3	15	0.5281	0.3914	0.4257	0.4	0.5479	0.21951287
3	20	0.7628	0.4717	0.4423	0.5655	0.6765	0.22342221
3	25	1.0204	0.5376	0.4611	0.7299	0.8492	0.205478
3	30	1.2957	0.5891	0.4805	0.8819	1.064	0.16737277
3	35	1.5824	0.6201	0.4592	1.0329	1.2838	0.10505703
3	40	1.8734	0.6419	0.4594	1.1398	1.5562	0.03214172
3	45	2.161	0.6506	0.4526	1.208	1.8481	-0.0527669
3	50	2.4368	0.6461	0.4381	1.2308	2.1483	-0.1470349
3	55	2.6928	0.6291	0.4156	1.2041	2.4441	-0.2473584
3	60	2.9213	0.5999	0.3851	1.1271	2.7225	-0.350931
5	0	0	0.061	0.3521	0	0.3521	0.061
5	5	0.1484	0.1843	0.3552	0.1169	0.3668	0.13599845
5	10	0.3305	0.2954	0.3645	0.2622	0.4164	0.18782815
5	15	0.5441	0.3929	0.3791	0.4274	0.507	0.21580516
5	20	0.7858	0.476	0.398	0.6023	0.6428	0.22023612
5	25	1.0513	0.5442	0.4195	0.7755	0.8245	0.20202061
5	30	1.3349	0.5978	0.442	0.935	1.0503	0.16331387
5	35	1.6303	0.6302	0.4232	1.0927	1.2817	0.09956644
5	40	1.9301	0.6533	0.4268	1.2042	1.5675	0.02508688
5	45	2.2263	0.6628	0.4235	1.2748	1.8737	-0.0618209
5	50	2.5104	0.659	0.4125	1.2976	2.1883	-0.1580904
5	55	2.7742	0.6421	0.3937	1.2687	2.4983	-0.2608526
5	60	3.0096	0.6128	0.3669	1.1871	2.7898	-0.3667711
10	0	0	0.0559	0.3226	0	0.3226	0.0559
10	5	0.1503	0.1808	0.326	0.1213	0.3378	0.13188003
10	10	0.3347	0.2934	0.3358	0.2713	0.3888	0.18446112
10	15	0.551	0.3923	0.3513	0.4413	0.4819	0.21295933
10	20	0.7958	0.4765	0.3713	0.6208	0.6211	0.2174813
10	25	1.0646	0.5458	0.3944	0.7981	0.8073	0.19929169

M	AoA	CN	Cm @ MRC	CA	CL	CD	Cm @ CG
10	30	1.3518	0.6003	0.4187	0.9614	1.0385	0.16031322
10	35	1.6509	0.6334	0.4012	1.1222	1.2756	0.0960615
10	40	1.9545	0.6572	0.4068	1.2358	1.5679	0.02104512
10	45	2.2545	0.6672	0.4056	1.3074	1.8809	-0.0665995
10	50	2.5422	0.6637	0.3968	1.3302	2.2025	-0.1637407
10	55	2.8093	0.647	0.38	1.3	2.5192	-0.267377
10	60	3.0477	0.6178	0.3554	1.216	2.8171	-0.374172
15	0	0	0.0549	0.3167	0	0.3167	0.0549
15	5	0.1507	0.18	0.32	0.1222	0.332	0.13094984
15	10	0.3355	0.2929	0.33	0.2731	0.3832	0.18370074
15	15	0.5523	0.3921	0.3457	0.444	0.4768	0.2123362
15	20	0.7976	0.4765	0.366	0.6244	0.6167	0.21689543
15	25	1.0671	0.546	0.3893	0.8025	0.8038	0.19867799
15	30	1.355	0.6007	0.4139	0.9664	1.036	0.15967167
15	35	1.6548	0.634	0.3969	1.1279	1.2742	0.09539212
15	40	1.9591	0.6578	0.4028	1.2418	1.5678	0.0201479
15	45	2.2597	0.6679	0.402	1.3136	1.8821	-0.067592
15	50	2.5481	0.6645	0.3936	1.3364	2.205	-0.1648611
15	55	2.8158	0.6479	0.3774	1.306	2.523	-0.2685927
15	60	3.0548	0.6187	0.3532	1.2215	2.8222	-0.3755829
20	0	0	0.0545	0.3144	0	0.3144	0.0545
20	5	0.1508	0.1798	0.3178	0.1225	0.3298	0.13071729
20	10	0.3358	0.2928	0.3278	0.2737	0.3811	0.18350309
20	15	0.5527	0.392	0.3436	0.445	0.4749	0.21210601
20	20	0.7983	0.4765	0.364	0.6257	0.615	0.21666759
20	25	1.0679	0.5461	0.3874	0.8041	0.8025	0.1985176
20	30	1.3561	0.6009	0.4122	0.9683	1.035	0.15951364
20	35	1.6561	0.6341	0.3952	1.1299	1.2737	0.095069
20	40	1.9607	0.6581	0.4013	1.244	1.5677	0.01992713
20	45	2.2616	0.6682	0.4007	1.3159	1.8825	-0.0679105
20	50	2.5502	0.6648	0.3925	1.3386	2.2059	-0.1652446
20	55	2.8181	0.6482	0.3764	1.3081	2.5244	-0.2690413
20	60	3.0573	0.619	0.3524	1.2235	2.8239	-0.3760966
25	0	0	0.0543	0.3133	0	0.3133	0.0543
25	5	0.1508	0.1796	0.3168	0.1226	0.3287	0.13051729
25	10	0.3359	0.2927	0.3267	0.274	0.3801	0.18337054
25	15	0.5529	0.3919	0.3426	0.4454	0.474	0.21194091
25	20	0.7986	0.4765	0.363	0.6263	0.6142	0.21656995
25	25	1.0683	0.5461	0.3865	0.8049	0.8018	0.19838741
25	30	1.3566	0.6009	0.4113	0.9691	1.0345	0.1593509
25	35	1.6567	0.6342	0.3944	1.1309	1.2734	0.09497371
25	40	1.9614	0.6582	0.4006	1.245	1.5676	0.01979929
25	45	2.2624	0.6683	0.4	1.3169	1.8826	-0.0680708
25	50	2.5512	0.6649	0.3919	1.3396	2.2062	-0.1654701
25	55	2.8192	0.6483	0.3759	1.3091	2.525	-0.2692993
25	60	3.0585	0.6192	0.352	1.2244	2.8247	-0.3762872

A4 - PARACHUTE CALCULATION DETAILS

Direct copy from the Recovery Systems Design Guide (AFFDL-TR-78-151), Irvin Industries Inc. [13]

Conical Ribbon. The constructed shape of this canopy is obtained in the same manner as that described for solid cloth conical parachutes. Gores, like the flat circular ribbon design, are composed of a grid of horizontal ribbons spaced and retained at close intervals by narrow vertical tapes. Radial tapes which extend from the vent to the skirt are sewn together in the joining of adjacent gores.

The conical ribbon parachute shows higher drag than the flat circular ribbon just as the solid cloth conical parachute does over the solid flat parachute of equal area. Data for several specific conical ribbon parachute and load configurations are listed below.

Varied Porosity. Unlike other parachutes of the conical ribbon classification, the gore of the 14.2 ft diameter drogue parachute in the table below is constructed with geometric porosity varied in three levels, increasing from vent to skirt, e.g., the upper one-third of the gore uses closer spacing and the lower one-third, a wider ribbon spacing than the center section. With this parachute, a drag coefficient, $C_{D0} = 0.64$, was obtained in wind tunnel tests without loss of stability. However, the opening load factor increased (see Table 2.2).

$$h_s = \left[\frac{S_g}{N \tan \beta/2} \right] \%$$

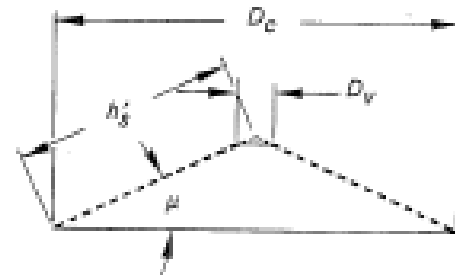
$$e_s = 2 h_s \tan \beta/2$$

$$\beta = 2 \sin^{-1} \left[\left(\sin \frac{180^\circ}{N} \right) \cos \mu \right]$$

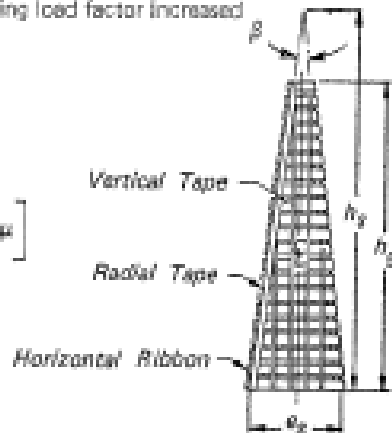
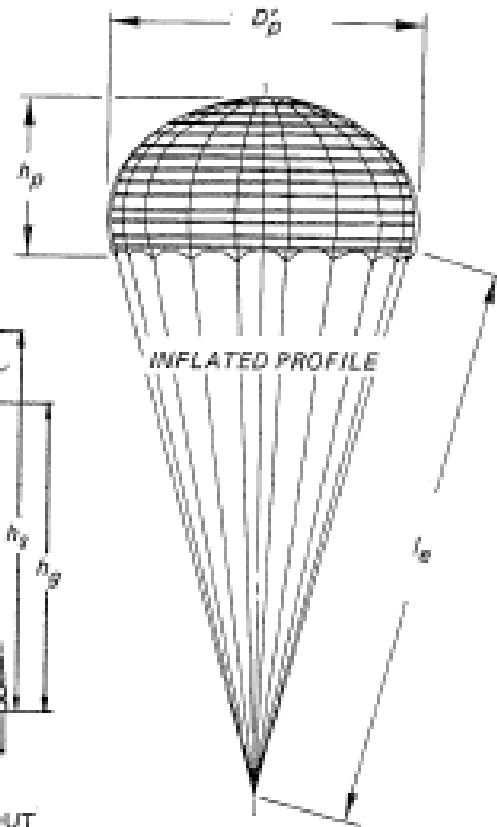
Generally:

$$S_v < 0.01 S_g$$

$$\frac{l_e}{D_0} = 1.00 \text{ to } 2.0$$



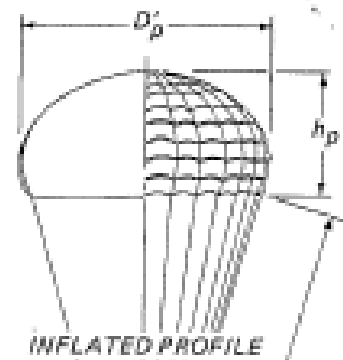
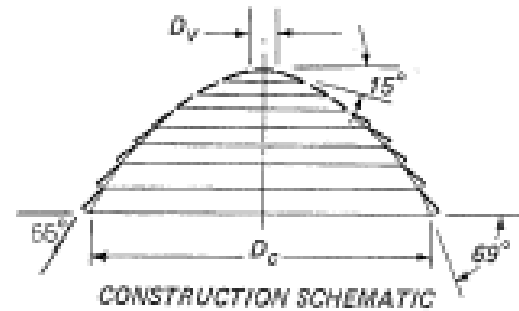
CONSTRUCTION SCHEMATIC



GORE LAYOUT

Size D_0 , ft	Conc Angle μ	Ribbon (Nylon) lbs	No. of Gores N	Geom. Porosity λ_g , %	Line Str. (Nylon) lbs	Line Length $l_e \cdot C_{D0}$	Parachute Weight lbs	Payload	Payload Weight lbs	Max. Deploy. Cond.	Rate of Descent fps	Special Cond.	Ref.
16.5	25°	300	20	26.5	2000	2.0	25.2	Apollo	13,000	204 psf	310	Drogue	27
115	20°	1000 400	96	16	6000	1.7	1400	Booster	164,000	200 psf	85	Cluster of 3	
17.0	20°	3000 2000	24	25	10000	1.0	76	Ordnance	716	800 lbs	71		
14.2	20°	2000 1500 1000	32	10/14/17	6000	2.0	75	B-1 Capsule	8700	1.6M 1600 psf		Drogue	213

Ringsail. This parachute design is complex and develops a unique shape from the combination of a curved basic profile and fullness at the leading edge of annular cloth rings. The constructed profile is a circular arc, tangent to a 15° cone at the apex and tangent to a 55° cone at the skirt edge. Earlier designs, including a personnel type known as Skysail and the Mercury main parachute, were based on a quarterspherical profile. The ringsail canopy is constructed of wide concentric cloth strips, spaced apart in the upper crown with slots like the ringlot, but adjacent over the remainder of the canopy, obtaining geometric porosity through crescent-shaped slots resulting from the cloth dimension between radials being longer for the leading edge of each sail than the trailing edge of the sail below it. Geometric features including sail fullness, (f_1 = trailing edge and f_2 = leading edge fullness), are illustrated on this page. The determination of geometric porosity of crescent shaped slots is a complex process [see Reference 217]. Data for several specific parachute and load configurations are listed below. The Apollo main parachute is a modification of the standard ringsail design, having 75 percent of the fifth (of 12) ring removed.



$$N = 0.78 D_c \text{ to } 0.88 D_c$$

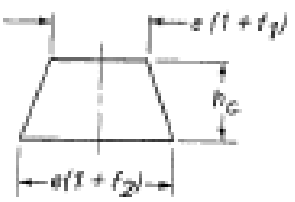
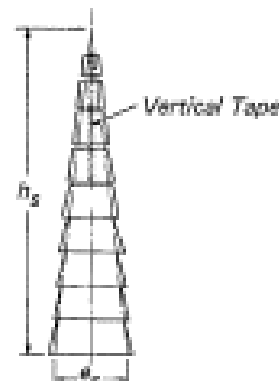
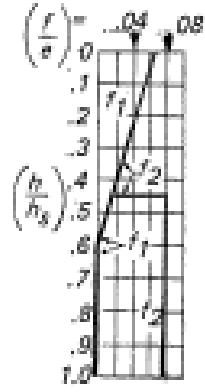
$$e_s = 6.44 (h_p/N) \sin 54^\circ$$

$$h_s = 0.519 D_c$$















$$\frac{l_s}{D_c} = 0.97 \text{ to } 1.45$$

$$\frac{h_p}{D_p} \approx 0.41$$

$$h_c = \text{width of cloth} = 24 \text{ to } 36 \text{ inches}$$



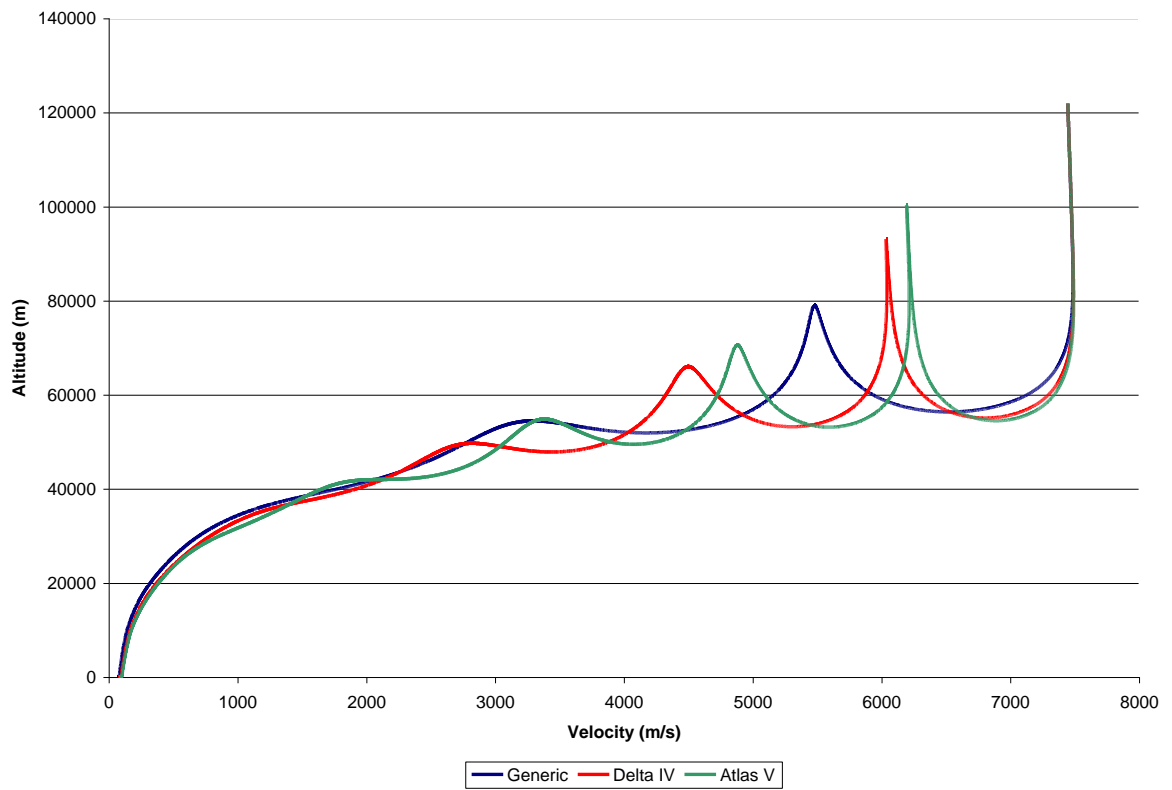
Size D_c , ft	Canopy (nylon) oz/yd ²	Geom. Porosity λ_g	No. of Gores N	Line Str. (nylon) lbs	Line Length l_s/D_c	Parachute Weight lbs	Application	Suspended Load lbs	Max. Deploy. Velocity	Rate of Descent fps	Comment	Ref.
29.6	1.1 2.25	14	24	550	.98	11.0	Personnel	250	275 kts	18.0	Skysail	217
63.1	1.1 2.25	7.1	48	550	.97	70.0	Mercury	2340	150 kts	32	Rafted	
85.6	1.1 2.25	12.0	68	650	1.45	145	Apollo	13,000	183 kts	31.4	Cluster of 3, Rafted	
189.5	1.1 2.25 3.5		156	650	1.18	557	Research	20,560	153 kts	26.0	Rafted	217

Type	Constructed Shape		$\frac{D_c}{D_o}$	Inflated Shape $\frac{D_p}{D_o}$	Drag Coef. C_{D_o} Range	Opening Load Factor C_X (Inf. Mass)	Average Angle of Oscillation	General Application
	Plan	Profile						
Flat Ribbon			1.00	.67	.46 to .50	~1.05	0° to ±3°	Drogue, Descent, Deceleration
Conical Ribbon			.95 to .97	.70	.50 to .55	~1.05	0° to ±3°	Descent, Deceleration
Conical Ribbon (Varied Porosity)			.87	.70	.55 to .65	1.05 to 1.30	0° to ±3°	Drogue, Descent, Deceleration
Ribbon (Hemisfile)			.62	.62	.30* to .46	1.00 to 1.30	±2°	Supersonic Drogue
Ringslot			1.00	.67 to .70	.56 to .65	~1.05	0° to ±5°	Extraction, Deceleration
Ringsail			1.18	.69	.75 to .80	~1.10	±5° to ±10°	Descent
Disc-Gap-Band			.73	.65	.52 to .58	~1.30	±10° to ±15°	Descent

*Supersonic

A5 – TRAJECTORIES USED IN ANALYSIS

The following are the nominal trajectories for the three vehicle configurations:



VITA

Chad Davis was born in Kingsport, Tennessee. He joined the United States Marine Corps Reserves after graduating Volunteer High School in Church Hill, Tennessee. Following completion of his active duty training and activation due to Operation Desert Shield/Storm, he began his undergraduate studies at the University of Tennessee. He graduated in 1998 with a Bachelor of Science in Engineering Sciences with a Minor in Aerospace Engineering. During his senior year, he was selected for pilot training by the Tennessee Air National Guard. Prior to his class start date for pilot training, he accepted a position at Pratt & Whitney as a Project Engineer on the space shuttle main engine (SSME) system. During this time, he supported the development, certification and ultimately production of the High Pressure Fuel Turbopumps (HPFTP). Following his first year at Pratt & Whitney, he took military leave and began Joint Specialized Undergraduate Pilot Training (JSUPT) at Vance Air Force Base, Oklahoma. He graduated JSUPT and went to advance flight training at Altus Air Force Base, Oklahoma to be trained in the KC-135R Stratotanker. Upon completion of flight training, he returned to Pratt & Whitney as a reserve flyer and continued working SSME systems, to include the first overhaul of the High Pressure Oxygen Turbopump (HPOTP) and supported work on the RL-10 upper stage for the Titan IV and future Atlas V programs. It was during this time he decided to start the pursuit of a graduate degree in aerospace engineering.

He later accepted a position at Orbital Sciences Corp as the Propulsion Lead on the Orbital Space Plane. Unfortunately NASA cancelled the program and he was asked to support a DARPA sponsored technology demonstrator microsat program called MiTEEx. Following the successful launch of the MiTEEx spacecraft, NASA announced the award of their Crew Exploration Vehicle (CEV) contract to Lockheed Martin which Orbital was a teammate. Orbital was subcontracted to design and build the Launch Abort System (LAS) for the CEV (later officially named Orion by NASA) and he was asked to be the Flight Test / Operations Lead. During this period of time, he transferred to the Pennsylvania Air National Guard. He took military leave from Orbital and attended advanced flight training at Little Rock Air Force Base, Arkansas to fly the C-130J Super Herc, then the EC-130J Commando Solo III & EC-130J Super J at home station. Upon completion of training, he returned to a reserve flying status and back to work at Orbital. Over the course of the ongoing Orion LAS program, he was promoted to Production / Operation Manager. He was called to active duty again to perform a tour of duty in Afghanistan supporting Operation Enduring Freedom. Following his deployment and the successful flight test of the LAS, he accepted a position in Houston, Texas supporting the Constellation Program as the Launch, Ascent & Abort Phase Engineer. He currently still resides in Houston supporting various NASA programs for Orbital Sciences.

It is his hope that upon review and acceptance of this thesis will complete the graduation requirements and he will receive his Master of Science in Aerospace Engineering in the Summer of 2011.